Università degli Studi di Firenze

Dipartimento di Scienze Biomediche Sperimentali e Cliniche

Scuola di Dottorato di Ricerca in Scienze Biomediche

curriculum Oncologia Sperimentale e Clinica

XXVII Ciclo

(MED/04)

Tesi di Dottorato di Ricerca

THE RECEPTOR FOR UROKINASE-PLASMINOGEN ACTIVATOR (uPAR) CONTROLS PLASTICITY OF CANCER CELL MOVEMENT IN MESENCHYMAL AND AMOEBOID MIGRATION STYLE

Candidato: **Dr. Cristina Luciani**

Coordinatore del Dottorato:
Prof. Persio Dello Sbarba

Tutor:
Prof. Mario Del Rosso

TABLE OF CONTENTS

Alle donne della mia famiglia

Abstract

The receptor for the urokinase plasminogen activator (uPAR) is up-regulated in malignant tumors. Historically the function of uPAR in cancer cell invasion is strictly related to its property to promote uPA-dependent proteolysis of extracellular matrix and to open a path to malignant cells. These features are typical of mesenchymal motility. Here we show that the full-length form of uPAR is required when prostate and melanoma cancer cells convert their migration style from the "path generating" mesenchymal to the "path finding" amoeboid one, thus conferring a plasticity to tumor cell invasiveness across three-dimensional matrices. Indeed, in response to a protease inhibitors-rich milieu, prostate and melanoma cells activated an amoeboid invasion program connoted by retraction of cell protrusions, RhoA-mediated rounding of the cell body, formation of a cortical ring of actin and a reduction of Rac-1 activation. While the mesenchymal movement was reduced upon silencing of uPAR expression, the amoeboid one was almost completely abolished, in parallel with a deregulation of small Rho-GTPases activity. In melanoma and prostate cancer cells we have shown uPAR colocalization with β1/β3 integrins and actin cytoskeleton, as well integrins-actin co-localization under both mesenchymal and amoeboid conditions. Such co-localizations were lost upon treatment of cells with a peptide that inhibits uPAR-integrin interactions. Similarly to uPAR silencing, the peptide reduced mesenchymal invasion and almost abolished the amoeboid one. These results indicate that full-length uPAR bridges the mesenchymal and amoeboid style of movement by an inward-oriented activity based on its property to promote integrin-actin interactions and the following cytoskeleton assembly.

CHAPTER 1:
INTRODUCTION

1.1 TUMOR PROGRESSION

Stepwise progression of human cancer has been clinically recognized. Several types of pre-malignant lesion, such as dysplasia and hyperplasia, can be detected in diverse organs prior to appearance of fully malignant invasive tumors. The pre-malignant lesions are caused either by genetic alterations which induce monoclonal expansion of the cells, or by environmental factors, such as viral infection, which induce polyclonal expansion of the cells. Subsequently, accumulation of genetic alteration occurs in one (or a few) of the premalignant cells, and the cells convert into malignant ones of clonal origin and produce primary tumor. However, at the early stage of primary tumor expansion, the cells are not invasive and metastatic. Then, new clones with invasiviness and metastatic ability appear as a result of further accumulation of genetic alterations in the cells. Thus, fully malignant cells are invasive and metastatic; however, only a restricted fraction of the cells in a primary tumor are considered to be highly metastatic.

Namely, cells in a primary tumor are phenotypically and biologically heterogeneous, and such heterogeneity is caused by the difference in the genes altered in each cancer cell [1]. Therefore, highly metastatic cells often acquire alterations in more genes than non-metastatic cells, and various genes are differentially expressed between metastatic and non-metastatic cells. Such cells selectively produce a metastatic tumor in a distant organ; thus, cells in the metatstatic tumor are considered to carry all the genetic alterations necessary to maintain malignant phenotypes of cancer cells, including invasiviness and metastatic ability. [1] (fig.1)

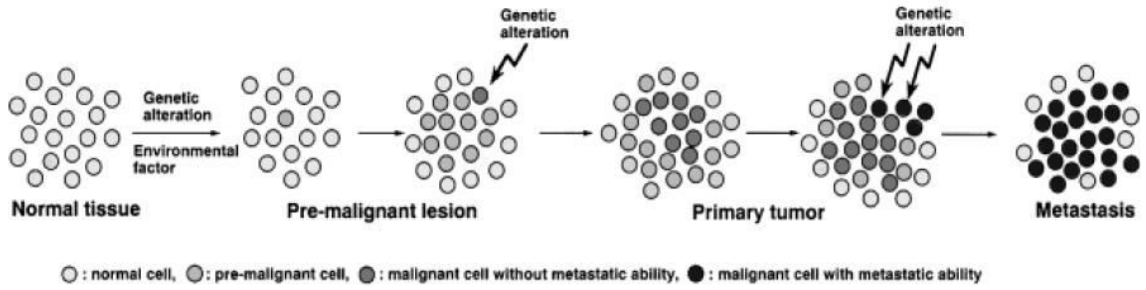

Figure 1. Stepwise malignant progression of human cancer in association with accumulation of genetic alterations in cells.

In a primary tumor are often contained sub-populations of metastatic and non-metastatic cancer cells because various genes are differentially expressed between these sub-populations.

Among the genes differentially expressed between metastatic and non-metastatic cells, several genes have the effect of inducing or suppressing metastasis. [1]

One of the genetic alterations occurring significantly higher than in primary tumors in metastatic cells is Loss of Heterozygosity (LOH). These mutations suggest that some tumor suppressor genes are involved in acquisition of metastatic potential in cancer cells. In particular, frequent LOH on chromosome 14q has been consistently observed in metastatic and advanced colorectal carcinomas in the studies of three different groups [2,3], suggesting that chromosome 14q harbors a metastasis suppressor gene for colorectal carcinoma.

To understand how cancer cells acquire metastatic potentials, it is necessary to clarify the causative genetic alterations for metastatic transformation of normal cells and resulting epigenetic alterations unique to cancer cells with metastatic ability [4]. We now know that a number of oncogenes and tumor suppressor genes are genetically altered in cancer cells and that those alterations accumulate during tumor progression. Thus, it goes without saying that alterations of those genes are causative events for multistage carcinogenesis, although we still do not know all genes are responsible for the acquisition of invasiveness and metastatic potential in cancer cells.

Genetic alterations are not the only pro-metastatic event, actually is also known that the tumor microenvironment can promote the metastatic cascade and that intercellular communication is necessary for this to occur.

Tumor microenvironment, or stromal compartment, is biologically heterogeneous, consisting of various cell types, such as fibroblasts, endothelial cells, and immune cells, along with growth factors and cytokines, and numerous extracellular matrix (ECM) components. Paracrine signals from these factors released by the tumor activate signaling and gene expression in the neighboring cells and vice versa, ultimately setting up a cycle of reinforcement and continued signal propagation. This interactions between the cancer cells and this stromal compartment are required for invasion, angiogenesis, and metastasis of cancer cells to ectopic sites [5-7].

In a recent study authors demonstrate that exosomes, which are small membranous vesicles secreted by most cell types into the extracellular environment, promote angiogenesis, invasion, and proliferation in recipient cells to support tumor growth and a prometastatic phenotype [8].

The development of metastases implicates the migration of cancer cells from the primary tumor to distant organs and this is the most devastating aspect of cancer, since most deaths

from cancer are due to metastasis. In this study we investigate the migration mechanisms involved during cancer progression.

1.2 CELL MIGRATION

Cell migration is a complex and heterogeneous process performed by all nucleated cell types. Some cells migrate only in the context of a defined substrate, such as epithelial cells moving along a basement membrane but not through interstitial tissues, whereas other cell types, including leukocytes or cancer cells, are versatile, as they interact with and migrate within virtually any substrate present in the body.

In tridimensional extracellular matrix (ECM) migration is a multistep process involving changes in the cytoskeleton, cell-substrate adhesions and the extracellular matrix components. Cell migration in three-dimensional ECM can be schematized into five separate steps [9]:

1. lamellipodium extension at the leading edge
2. formation of new focal adhesions complexes
3. secretion of surface proteases to ECM contacts and
focalized proteolysis
4. cell body contraction by actomyosin complexes
5. tail detachment

Lamellipodium extension at the leading edge involves actin polymerization, and it is known that lamellipodia consist of branched or unbranced filament networks formed through the actin-nucleating activity of the actin-related proteins 2/3 (Arp2/3) protein complex. Rac stimulates new actin polymerization, acting on Arp2/3 complex, which binds to a family of proteins called nucleating promoting factors [10;11] and initiates the formation of new actin filaments on the sides of existing filaments to form a branching actin network . The Arp2/3 complex is activated by Rac through its target insulin receptor tyrosine kinase substrate p53 (IRSp53) [12]. Rac interacts with IRSp53, which in turn interacts through an Src-homologous domain 3 (SH3) domain with a member of the WASP family, which then binds to and activates the Arp2/3 complex. Rac is required for lamellipodium extension induced by growth factors, cytokines and extracellular matrix components [13]. Rac activation by both tyrosine kinases and G-protein-coupled receptors is dependent on phosphoinositol3-kinase (PI3K)

activity, and inhibitors of PI3K block Rac activation. During lamellipodia extension phosphoinositol phosphates (PIPs) also bind and activate Guanine nucleotide exchange factors (GEFs) that regulate the activity of Rac that bind the Arp2/3 complex. A number of myosins, the main motor protein in eukaryotic non-muscle cells, have been implicated in cell migration [14]. Myosin light chain (MLC) phosphorylation is enhanced in the lamellipodial region of cells, which suggests a role for myosins in lamellipodium extension. Rac can affect the phosphorylation of both myosin heavy chain (MHC) and MLC via activation of its downstream kinase p21 activated-kinase (PAK) [15].

Formation of new focal adhesions complexes is localized in the lamellipodia of most migrating cells. Upon the attachment of the extending lamellipodium to the extracellular matrix, integrins come into contact with ECM ligands and cluster in the cell membrane interacting with the focal adhesion kinase (FAK), α-actinin and talin. All these proteins can bind adaptor proteins through SH2, SH3 or proline rich domains to recruit actin binding proteins (vinculin, paxillin and a-actinin) as well as regulatory molecules PI3K to focal complexes. Rac is required for focal complex assembly and cell adhesion to the extracellular matrix itself activates Rac [16,17].

Secretion of surface proteases to ECM contacts and focalized proteolysis is crucial for cells to migrate in a three-dimensional matrix and, even on a two-dimensional matrix proteases production can be important for migration. There are some indications that Rho GTPases could play a role in regulating the release and/or activation of secreted proteases. For example, Rac is required for shear stress-induced matrix metalloproteinase 9 (MMP9) expression in chondrocytes, and activated Rac can induce expression of the MMP1 in fibroblasts [18,19]. Constitutive expression of activated Rac induces activation of Jun N-terminal kinase (JNK), which phosphorylates and activates the transcription factor Jun. Jun is a component of the activator protein 1 (AP-1) transcription factor complex and regulates transcription of many genes, including MMP genes [20]. Furthermore, in HT1080 cells, Rac1 mediates MMP2 activation and membrane type matrix metalloproteinase (MT1-MMP) expression/processing during the encounter between invading tumor cells and type I collagen rich stroma, thereby facilitating collagenolysis and cell invasion [21].

Cell body contraction is dependent on actin filaments and myosin II interaction. Stress-fiber assembly and contraction, which are controlled by myosin II, are predominantly induced by the small G-protein Rho and its important downstream effector, the Rho-associated serine/threonine kinase (ROCK) [22]. Rho acts via ROCKs to affect MLC phosphorylation, both by inhibiting MLC phosphatase and by phosphorylating MLC. It is likely that ROCKs

and MLCK act together to regulate different aspects of cell contractility, because ROCK appears to be required for MLC phosphorylation associated with actin filaments in the cell body, whereas MLCK is required at the cell periphery. This allows the cell to separately control cortical actin dynamics from contractions in inner regions [23].

Tail detachment occurs when cell-substrate linkages is preferentially disrupt in the back of the cell, whereas the leading edge remains attached to the ECM and further elongates. At the trailing edge, focal complex disassembly occurs through several mechanisms dependent on the type of cell and strength of adhesion to the extracellular matrix. In slowly moving cells tail detachment appears to depend on the action of the protease calpain, which cleaves focal complex components like talin and cytoplasmic tail of β1 and β3 integrins at the rear of cells. A reduction in Rho activity could inhibit tail detachment, through decreased actomyosin contractility [24,25].

For most cells, including epithelial, stromal, and neuronal cells, migration phases are confined to morphogenesis and end with terminal differentiation toward intact tissue to become reactivated only for tissue regeneration or during specific phases of neoplastic progression such as metastatic dissemination or angiogenesis. Furthermore cells can move within tissues collectively or as single cells.

In collective migration, cells maintain their cell–cell junctions and move as multicellular connected strands or chords into tissues; the leading edge of a moving cell group is formed by one or several cells that utilize actin-mediated ruffles and integrin-dependent traction to perform steps 1–4 of the migration sequence. In cell cultures, collective migrating cancer cells develop preferential integrin and protease (MT1-MMP, MMP-2) engagement in a subset of cells at the leading edge [26].

The junctions within invading collective cells are stabilized by cadherins, members of the immunoglobulin superfamily (e.g. NCAM or activated leukocyte adhesion molecule) [27-29] and gap-junctional cell–cell communication [30,31].

The rear of the leading cell(s) maintain the adhesive interaction with other cells, so the retraction of the trailing edge has an important modification: as it glides along the ECM structure, neighboring cells are dragged forward along the established migration track by means of cell–cell adhesion [32,33]. While the leading cells generate actin- and integrin-mediated traction, a linear cortical actin network extends along cell–cell junctions into deeper regions of the collective, suggesting that cortical actin plays a role in sustaining collective integrity [34-36]. By contrast, non-neoplastic developing glandular ducts and blood vessels contain polarized cells that form an inner lumen andnewly produce a surrounding basement

membrane [37]. Sprouting blood vessels, unlike other groups of cells undergoing collective migration, use cadherins to recruit pericytes as a second cell type; these pericytes then participate in the *de novo* synthesis of an encircling basement membrane [38].

While collective movement has been associated with tumor cell entry into the open lymphatic vessels, the movement of individual cells is required for cancer cells to sneak across basement membranes, to enter the bloodstream and disseminate to distant organs [39]. The invasion strategy of single tumor cells develops according to at least two distinct modes of migration: the so-called elongated-mesenchymal mode and rounded-amoeboid mode.

Mesenchymal migration

Cells that use mesenchymal migration accomplish the complete five-step migration sequence [39]. In 3D tissues, mesenchymal cells adopt a spindle-shaped, fibroblast-like morphology, as characteristic for fibroblasts, myoblasts, single endothelial cells or sarcoma cells [40;41]. The elongated morphology is dependent on integrin-mediated adhesion dynamics and the presence of high traction forces on both cell poles [42]. Blocking of integrins in spindle-shaped tumor cells by antibody or small-molecule inhibitors causes cell retraction, acquisition of spherical shape and impaired migration rates [43].

Concomitant to integrin and actin focalization at substrate-binding sites, mesenchymal cells recruit surface proteases to digest and remodel ECM [44]. b1 and b3 integrins, MT-MMPs and other proteases then colocalize at contact regions to ECM fibers, proteolytically cleave ECM molecules near to the cell surface, and generate structural matrix defects along cell migration tracks [44;45]. Focal contact formation and turnover occur in the timescale of 10–120 minutes, resulting in relatively slow migration velocities (0.1–2 mm/min) in 3D models [46-49]. If other cells follow along the newly generated matrix defect, a moving cell chain evolves and is guided by matrix strands (contact guidance).

In migrating mesenchymal cells, Rac and Cdc42 generate pseudopod and lamellipod dynamics at outward edges, favoring a rapid and dynamic type of b1 integrin engagement towards 2D and 3D substrata. Interfering with Rac and Cdc42 activity perturbs cell extension and polarized force generation, thereby severely impairing migration [50]. Rho, on the other hand, stabilizes initial integrin–substrate linkages, increases focal contact size and strength, and further thickens actin filaments through several mechanisms [51;52]. In mesenchymal or adhesive cells interacting with 2Dsubstrata, active Rho leads to increased adhesiveness, stress

fiber formation,and retardation of migration speed [51;52]; for cell migration within 3D substrata, the functions of Rho with regard to cell shape and adhesion dynamics appear to be more complex (see below). Together, the coordination and synergy between polarized cytoskeletal dynamics at the leading edge, as mediated by Rac and Cdc42, and the somewhat opposing effect of Rho-mediated adhesionstrengthening and cell contractility is thought to play a key role in adhesion-dependent cell migration and related dynamics in cell morphology [50-52] (fig. 2).

Amoeboid migration

Arguably the most primitive and in some ways the most effective form of cell migration is amoeboid movement, which mimics features of the single cell behavior of the amoeba Dictyostelium discoideum. Dictyostelium is an ellipsoid cell that has fast deformability (within seconds) and translocates via rapidly alternating cycles of morphological expansion and contraction.

In higher eukaryotes, amoeboid movement is carried out by hematopoietic stem cells, leukocytes and certain tumor cells [53-55]. These cells use a fast 'crawling' type of movement that is driven by short-lived and relatively weak interactions with the substrate. Integrins mediated adhesion is completely or partially dispensable for cell migration within connective tissue, both in vitro and in vivo. Amoeboid migrating cells are highly deformable and, because of their lack of stable focal contacts, move at high velocities (2–30 mm/min) [46]. Shape change is generated by cortical filamentous actin, which mediates cell dynamics as well as providing stiffness to the cell body, but mature focal contacts and stress fibers are lacking [56;57].

In amoeboid migration cells use protease independent physical mechanisms to overcome matrix barriers, including adaptation of the cell shape to preformed matrix structures (contact guidance), extension of lateral footholds ('elbowing') [58] and squeezing through narrow spaces constriction rings) [57]. Such shape-driven migration allows cells to glide through or circumnavigate, rather than degrade, ECM barriers [59]. The ellipsoid cell shape in amoeboid migration requires actin polymerization along the plasma membrane to stiffen and contract the cell cortex.

These cortical actin dynamics are critically controlled by the small GTPase RhoA and its effector ROCK to generate cortical tension, stiffness and the maintenance of roundish cell morphology [60;61]. In contrast to the five-step migration paradigm, focal contacts and

focalization of proteolysis are thus eliminated in amoeboid movement, whereas fast and non-focalized receptor assemblies at cell–matrix interactions are retained. (fig. 2)

Among environmental conditions, an interesting paper has highlighted the role of matrix-bound plasminogen inhibitor type-1 (PAI-1) in supporting amoeboid movement and cell blebbing of human colorectal cancer cells via RhoA/ROCK1 signaling [62].

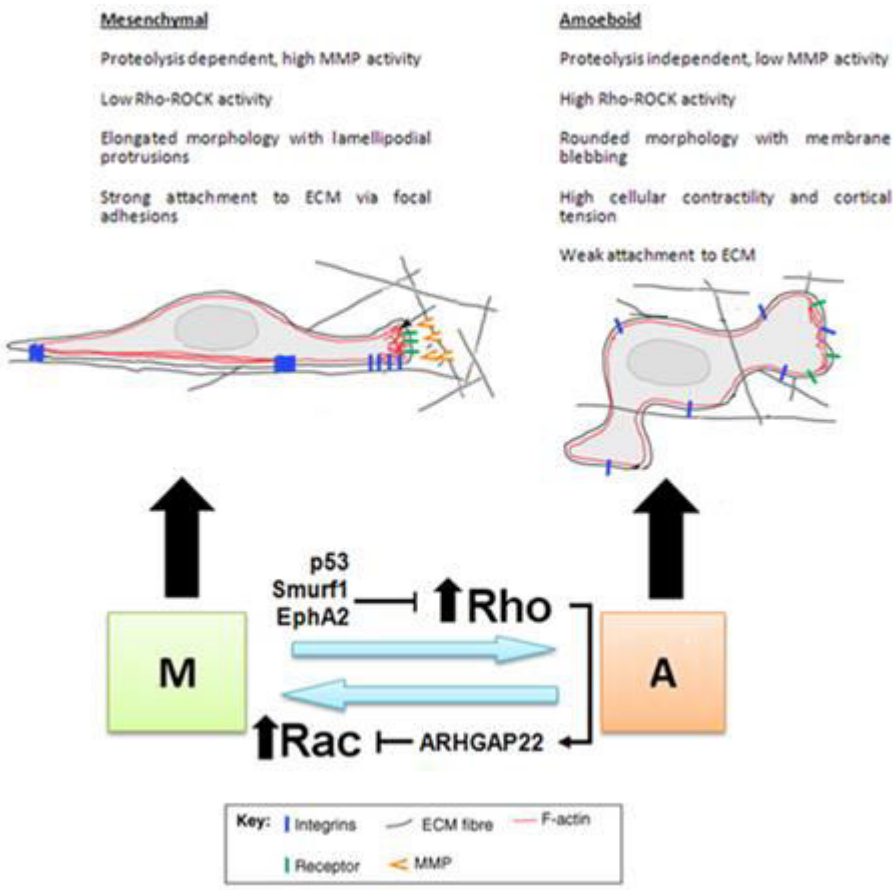

Figure 2. Mesenchymal, metalloproteinase-dependent mode and amoeboid mode. Migrating tumor cells can shift between the two type of motility. This shift appears to be high dependent on an inverse relationship between Rho and Rac activity.

Mesenchymal–amoeboid transition (MAT)

Mesenchymal movement can convert towards amoeboid migration. Known mechanisms leading to mesenchymal–amoeboid transition (MAT) are the abrogation of pericellular proteolysis using protease inhibitors, the strengthening of RHO/ROCK signal pathways, and the weakening of integrin–ECM interactions by antagonists.

Mesenchymally migrating tumor cells such as HT1080 fibrosarcoma and MDA-MB-231 mammary carcinoma cells cease their proteolytic migration after the addition of protease

inhibitors that target MMPs, ADAMs, cathepsins and serine/threonine proteases [44]. Instead of widening the pericellular space and cleaving ECM fibers, the cells then switch to amoeboid behavior involving vigorous shape change and the ability to squeeze through narrow regions, thereby rescuing their migration independently of pericellular proteolysis [44].

Consistent with an amoeboid phenotype, both β1 integrin distribution and filamenous actin adopt a diffuse cortical pattern, reminiscent of migrating lymphocytes [59]. MAT after inhibition of surface proteases was confirmed in vivo for tumor cells injected into the mouse dermis [44]. A similar phenotypic change was obtained in fibroblasts populating excisional wounds in rats treated with the broad-spectrum MMP inhibitor, GM6001. Despite MMP inhibition, these fibroblasts retain the capacity to infiltrate the fibrin-rich wound matrix; however they now exhibit roundish amoeboid morphology coupled to a strongly reduced capacity to remodel the wound and generate scar contraction.

How protease inhibitors interfere with the regulation of integrin and cytoskeletal dynamics and thereby reprogram mesenchymal cells towards amoeboid movement remains unknown.

Similar transition from mesenchymal to amoeboid movement occurs in HT1080 cells that penetrate thick 3D matrigel layers after constitutive activation of the Rho effector kinase ROCK [63]. ROCK acts by increasing myosin-II-mediated actin filament stabilization and contraction [64;65]. Active Rho A is required for diffuse cortical actin polymerization and cell retraction in dividing cells [66] and overexpression of constitutively active ROCK causes cortical contraction and cell rounding in originally mesenchymal cell lines, such as 3T3 fibroblasts and HT1080 cells [63,67]. Active ROCK not only causes HT1080 cells to loose their mesenchymal characteristics and convert to a roundish, contracted shape: driven by small filopodia and blebbing-type cell protrusions that contain cortical actin, the cells convert to a protease-independent migration type, reminiscent of amoeboid movement [63]. Because ROCK activation generates cortical actin and cell rounding in some cells [61,63,68], yet stabilizes stress fibers and causes cell spreading, flattening, and migratory cell arrest in other cell types [64], it appears that additional endogenous or environmental cofactors determine if cell–substrate adhesions are stabilized or weakened by Rho/ROCK-mediated signals.

Reducing attachment forces without interfering with cell contractility prompts cell rounding and transition towards amoeboid movement. In 3D collagen substrate, such approaches include the following: selection for low endogenous β1 integrin expression by FACS sorting; titrating β1-integrin-mediated adhesion downwards by blocking antibody; interfering with the cytoplasmic β1 integrin domain by a dominant-negative peptidomimetic; and abrogating integrin expression by knockout strategies. All these procedures uniformly generate a

roundish yet dynamic cell shape, an even surface distribution of (residual) β1 integrins, and a non-focalized cortical layer of filamentous actin, supporting amoeboid migration in 3D collagen lattices. Together, these findings indicate that cells can use a spectrum of migration modes ranging from adhesive to nonadhesive and from proteolytic to protease-independent [59].

GTPases in cancer cell migration

As previously described the main GTPases involved in migration belong to the Ras superfamily. They are small (21-25 kDa) molecules that share structural homology and become activated only when bound to GTP. The best-characterized molecules are Rho, which controls the stress fibers and focal adhesion formation, and Rac and Cdc42, which regulate membrane ruffling, and filopodium formation, respectively. A structural feature that distinguishes the Rho proteins from other small GTPases is the so-called Rho insert domain located between a β-strand and an α-helix within the small GTPase domain [69-71]. Typically Rho proteins are 190-250 residues long and consist only of the GTPase domain and short terminal C-terminal extensions. Within their GTPase domains, they share approximately 30% amino acid identity with the Ras proteins and 40-95% identity within the family. All members contain the sequence motifs characteristic of all GTP-binding proteins, bind to GDP and GTP with high affinity. In addition, the majority of members undergo C-terminal post-translational modification by isoprenoid lipids. Together with other C-terminal modifications or sequences, isoprenoid addition facilitates their subcellular location and association with specific membranes or organelles. These lipid modifications are mainly palmitoylation or prenylation, being farnesylation and geranyl-geranylation the most frequent post-translation modifications [72].

Rho GTPases work as sensitive molecular switches existing either in an inactive, GDP-bound form or an active GTP-bound form. They are endowed with GTP hydrolytic activity, mainly involved in cytoskeleton rearrangements and cell motility, but also involved in cell proliferation, transformation and differentiation [70]. Among other members, we will focus our attention on the Rac and Rho subfamilies, as they are the main effectors of cell motility.

The exchange of GDP to GTP and thus the activation of Rho GTPases is catalyzed by guanine nucleotide exchange factors (GEFs), which act downstream of numerous growth factor receptors, integrins, cytokine receptors, and cadherins. Rho GTPases are key integrating

molecules from different extracellular signals, as they can be activated by different GEFs. In turn, GTP-bound active GTPases can interact with a plethora of different effectors which mediate the different cellular functions of this family of proteins. Rho GTPase effectors are a large group of proteins and include actin nucleation promoting molecules, adaptors, as well as kinases. Two factors concur to determine specific Rho GTPase function: tissue specificity of GTPase effectors and distinct intracellular localizations of closely related Rho GTPases, due to different lipid modifications [69].

The GEF family is really large, consisting of over 70 proteins mainly belonging to the Dbl or the Dock families [73;74]. Lipid modification of Rho and Rac GTPases are also strategic for subcellular compartmentalization, allowing interaction with membrane-localised GEFs upon masking of isoprenoids by GDI. The hydrolysis of GTP and contact with GAPs allows a new association of the GTPases with GDI and return to the cytosol [75]. In addition, Rho GTPases can also be regulated by phosphorylation. RhoA has been reported to be phosphorylated by protein kinase A and G (PKA and PKG) at serine at position 188, without any modification of its interaction with GEFs, but increasing its interaction with GDI and leading to extraction of RhoA from plasmamembrane [76]. Inactivation of Rho GTPases is due to an intrinsic GTPase activity, which hydrolyses GTP to GDP. However, this activity is very weak and needs to be up-regulated by GTPase activating enzymes (GAPs). Of note, Rnd1-3 [77] and RhoH [78;79] are not regulated via GAPs, due to their inability to hydrolyse GTP, and are therefore regulated through gene expression and protein degradation.

An additional negative control is achieved through Rho guanine nucleotide dissociation inhibitors (GDIs). They bind Rho GTPases and prevent their activation by means of blocking interaction of the GTPbound form with effectors, sequestering GDP-bound Rho proteins in the cytoplasm away from the GDP-GTP cycle, as well as by hanging membrane compartment to GTPases [80].

Beside the GEF family, the GAP group is also huge: more or less 100 members have been found in the human genome, but their regulation are even less clear than those of the GEFs. Indeed, external to their GEF or GAP domains, these proteins strongly diverge in structure and secondary functions [74;81].

The Rac-related subfamily includes Rac1 (and its splice variant Rac1b), Rac2 and Rac3 [72]. Several Rac related proteins, sharing more than 80% identity, they stimulate the formation of lamellipodia and membrane ruffles, presumably through interaction with the WAVE complex. The splice variant Rac1b contains an additional C-terminal 19-residue insert and is constitutively active due to an increased intrinsic guanine nucleotide exchange rate, decreased

intrinsic GTPase activity, its inability to interact with Rho GDI and enhanced association with the plasma membrane [82;83]. In addition, Rac1 can also be regulated by phosphorylation by Akt on Ser71, thereby leading to inhibit the binding of GTP but not Rac1 GTPase activity [84]. Rac1 is ubiquitously expressed, whereas Rac2 is expressed only in hematopoietic cells, where it seems to have specialized functions [85]. Rac2 inactivation has been correlated with several neutrophilic, phagocytic and lymphocytic defects [86]. Indeed, Rac2 is mainly responsible for activation of NADPH oxidase and consequent generation of reactive oxygen species (ROS) in hematopoietic cells [87]. Finally Rac3, highly expressed in brain and upregulated upon serum stimulation of fibroblasts [88], is strongly localized to the membranes where it appears to be hyperactive [89]. Animals have 3 Rho isoforms, RhoA, Rho B, and Rho C, sharing 85% amino acid sequence identity [69; 74]. Despite their similarity, both modulators (GEFs and GAPs) and downstream effectors show favoured interaction with single Rho isoforms, and the three proteins play differential roles in cells. Rho A and Rho C play key roles in the regulation of actomyosin contractility and in cell locomotion, while Rho B, primarily located in endosomes, has been shown to regulate intracellular trafficking and cell survival [90]. Mostly, the functional differences are a consequence of divergence in their C-terminal 15 amino acids, where the highest level of difference is found.

1.3 THE uPA/uPAR SYSTEM

Generation of plasmin catalyzed by urokinase-type plasminogen activator (uPA) plays an important role in pericellular proteolysis during tissue remodeling and cell migration in many normal and pathological processes, such as trophoblast invasion, mammary gland involution, spermatocyte release, wound healing, psoriasis, and cancer cell invasion [91-93].

uPA is a serine protease of 45-55 kDa that exists in a proenzyme form (pro-UPA), which, upon activation, activates plasminogen to the active serine-protease plasmin. It has a specific membrane receptor: urokinase-type plasminogen activator receptor (uPAR).

Plasmin is a broad-specificity protease, which degrades several ECM components, such as fibronectin, laminin and collagen [94]. uPA triggers a proteolytic cascade that involves the activation of MMPs, which are responsible for collagen degradation. In addition, the ability of uPAR to localize and focalize the proteolytic activity of uPA on the cell surface is

extremely important for the invasive ability of tumor cells. The uPA/uPAR complex, besides its proteolytic function as a zymogen, also functions as a vitronectin receptor and it participates in normal and tumor cell motility processes such as and tumor cells migration and invasion [91;95].

uPAR is composed of three homologous domains (D1, D2, and D3) and is extensively glycosylated and attached to the cell membrane by a GPI (Glycosyl Phosphatidylinositol) anchor.

Due to its GPI-anchor attachment [96], uPAR is devoid of a cytoplasmic domain, a feature that renders uPAR incapable of signalling. This characteristic requires membrane partners enabling uPAR to deliver signals that propagate to the cell contractile apparatus. Most consistently uPAR has been found associated with integrins [92;93;97]. The integrin-uPAR interaction regulates several cellular responses, such as the EGF (Epidermal Growth Factor)-receptor-dependent proliferation of a tumor cell line by activating FAK (Focal Adhesion Kinase), GRB2 (Growth Factor Receptor-bound protein-2), and ERK (Extracellular signal Regulated Kinase)/MAPK (Mitogen Activated Protein Kinases) and downregulating p38 MAPK. uPA binding to uPAR activates several tyrosine kinases from the Src family (Fyn, Lck,HCK), which in turn activates SHC, PI3K (Phosphatidylinositol 3-Kinase)-Akt1 pathway and cell migration. It also stimulates the JAK (Janus kinase)-STAT (Signal Transducer and Activator Of Transcription) pathway, PKC-Epsilon (Protein Kinase-C), and CSNK2 (Casein Kinase-2) [98] (fig.3).

Receptor-bound uPA can be inhibited by PAI-1 (Plasminogen Activator Inhibitor-1) and PAI-2, and uPAR provides a mechanism for internalization of PAI1-inactivated uPA. The uPAR therefore plays an important role both in localizing and modulating cell surface plasminogen activation. uPA expression can also be up-regulated in tumor cells by GFs (Growth Factors), including HGF/SF (Hepatocyte Growth Factor/Scatter Factor), VEGF (Vascular Endothelial Growth Factor), EGF, IGF-I (Insulin-like Growth Factors-I) and IGF-II, bFGF (basic Fibroblast Growth Factor), LPA (Lysophosphatidic Acid), CSF1 (Colony Stimulating Factor-1), vasopressin, and thrombin, among others. Most of these exogenous signals, through their receptors, activate PLC (Phospholipase-C), PKC, Ras, Raf, MEK1 (MAPK/ERK Kinase-1) and ERK1/2 and also members of the Ras superfamily of small GTP-binding proteins.

uPA/plasmin-mediated proteolysis is critical for cellular migration and tissue remodeling in inflammation, tumor propagation, and metastasis. uPA is also essential for pericellular proteolysis and is localized to the leading edge of migrating cells.

The interactions between uPA and uPAR can facilitate cellular movement, which contribute to remodeling of the lung in ARDS or the interstitial lung diseases. This interaction at the cancer cell surface is critical event in the pathogenesis of neoplastic growth and metastasis, mediating tissue remodeling, tumor cell invasion, adhesion, and proliferation. In addition, the binding of uPA to uPAR mediates cell proliferation in several cell types, including non-malignant lung epithelial cells, lung carcinoma-derived cells, and mesothelioma cells [99].

uPAR is also highly expressed during tissue remodelling in the placenta and migrating keratinocytes in wounds. The receptor is, however, implicated in providing oval progenitor cells with a growth advantage during liver regeneration. Regulation of the uPA-uPAR system is therefore germane to the pathogenesis of disparate pathological conditions, including lung injury and neoplasia.

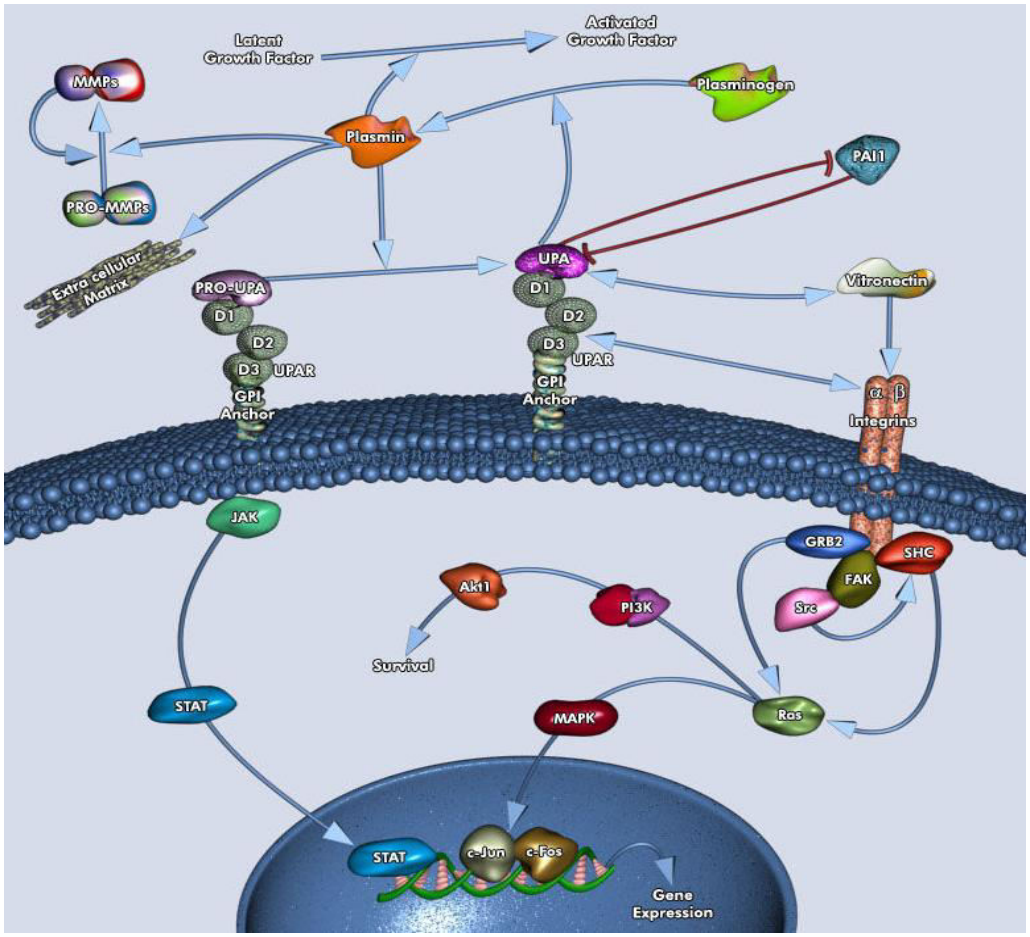

Figure 3. uPA/uPAR pathway. **:** uPAR binds uPA in its active and zymogen (pro-uPA) forms. uPA cleaves plasminogen, generating the active protease plasmin, which cleaves and activeates matrix metalloproteases (MMPs). Plasmin can also activate pro-uPA. Both plasmin and MMPs degrade many extracellular matrix (ECM).

uPAR is overexpressed across a variety of tumor cell lines and tissues, including breast, ovary, lung, pancreas, colon, kidney, liver, stomach, endometrium, bone and high endogenous level of uPAR was also found to be associated with cancer invasion and metastasis [100-102]. uPA also aids in anti-thrombolytic activities to remove blood clots and helps stimulate angiogenesis in tumor cells [103].

In gastric cancer lesions, uPAR expression has been observed in macrophages, endothelial cells and cancer cells located at the invasive front of the tumors [104,105]. Increased expression of uPAR antigen or mRNA in tissue extracts and blood from patients with gastric cancer have been associated with some clinico-pathological aspects of the disease including poor prognosis [106-109]. Interestingly, studies in bone marrow aspirates from curatively resected patients with gastric cancer show that those cases with uPAR-positive cancer cells disseminated into the bone marrow have worse prognosis than patients with disseminated uPAR-negative cancer cells [110,111].

Elevated expression of uPAR in tumors and particularly in cancer cells may be an indication of more aggressive gastric cancers. Therefore, uPAR expression in cancer cells may represent an important prognostic marker for patients with cancer, and may become an important target for cancer diagnosis and therapy.

Experimental evidences accumulated over the last 25 years connote the receptor for the uPAR as the prototype receptor regulating the mesenchymal style of cell movement by triggering pericellular proteolysis of invasive cells.

On these considerations, uPAR appears a good candidate molecule capable of modulating integrin function and to sustain the style of movement of a cell. Here we show that uPAR bridges the mesenchymal and amoeboid style of movement in a series of prostate carcinoma and melanoma cell lines, by its property to warrant the integrin-mediated connection between actin cytoskeleton and the cell membrane.

1.4 TUMOR ANGIOGENESIS

Tumor growth requires the induction of new capillary blood vessel, thus neoplastic cells beckon endothelial cells (ECs) in the primary cancer site [112].

In healthy adults, ECs remain quiescent for years. However, these cells can very rapidly start to proliferate and migrate to form new vessels in conditions of injury, inflammation, cancer,

or other pathologies. Vessel sprouting in mammals is a highly coordinated process, relying on a migratory (but non- or rarely proliferative) tip cell, and trailing proliferating stalk cells, elongating the sprout shaft.

In the figure 4 is shown a schematic pattern of angiogenesis, which involves signaling through VEGFR2, the receptor for the pro-angiogenic factor VEGF [113]. VEGFR2 signaling activates the expression of Dll4 on the surface of tip cells. Dll4 is a ligand for the Notch receptor expressed in neighboring stalk cells. Activation of Notch is a potent pro-stalk cell signal in part by downregulation of VEGFR2 and other VEGF coreceptors (like neuropilin-1) and upregulation of VEGF inhibitors (like the VEGF trap VEGFR1) in stalk cells. By activating Notch signaling in neighboring cells, a tip cell thus ensures that it is flanked by stalk cells [114]. In this feedback system, tip cells promote neighboring ECs to assume the stalk cell phenotype in an effect known as lateral inhibition.

An exciting discovery was that tip and stalk cells are not genetically predetermined, irreversible cell fates, but rather represent plastically changing, reversible EC phenotypes.

Tip cells do not remain at the tip for extended periods of time, but continuously shuffle as ECs compete for the position at the tip [116]. Indeed, cells are seen to overtake each other, with cells moving towards or away from the tip [115]. During this movement, cellular VEGFR1 and VEGFR2 levels are continuously readjusted to account for the changes in Dll4 expression in neighboring cells. Thus, the tip-stalk cell pattern is a dynamic shuffle among competitive ECs. Until recently, only genetic signals were known to specify the tip versus stalk cell identity, but recent evidence indicates that metabolism is also a key determinant of the EC subtype specification.

During maturation of newly formed vessels, EC secretion of PDGF-B and other signals attracts PDGFR-β expressing pericytes in order to stabilize and functionalize nascent vessels [117]. Mural cell coverage contributes to vessel maturation and induces ECs to once again become quiescent phalanx cells, a process relying on angiopoietin- 1/Tie2 signaling, the PHD2 oxygen sensor, junctional molecules (VE-cadherin, claudins, etc.), and other signals [118].

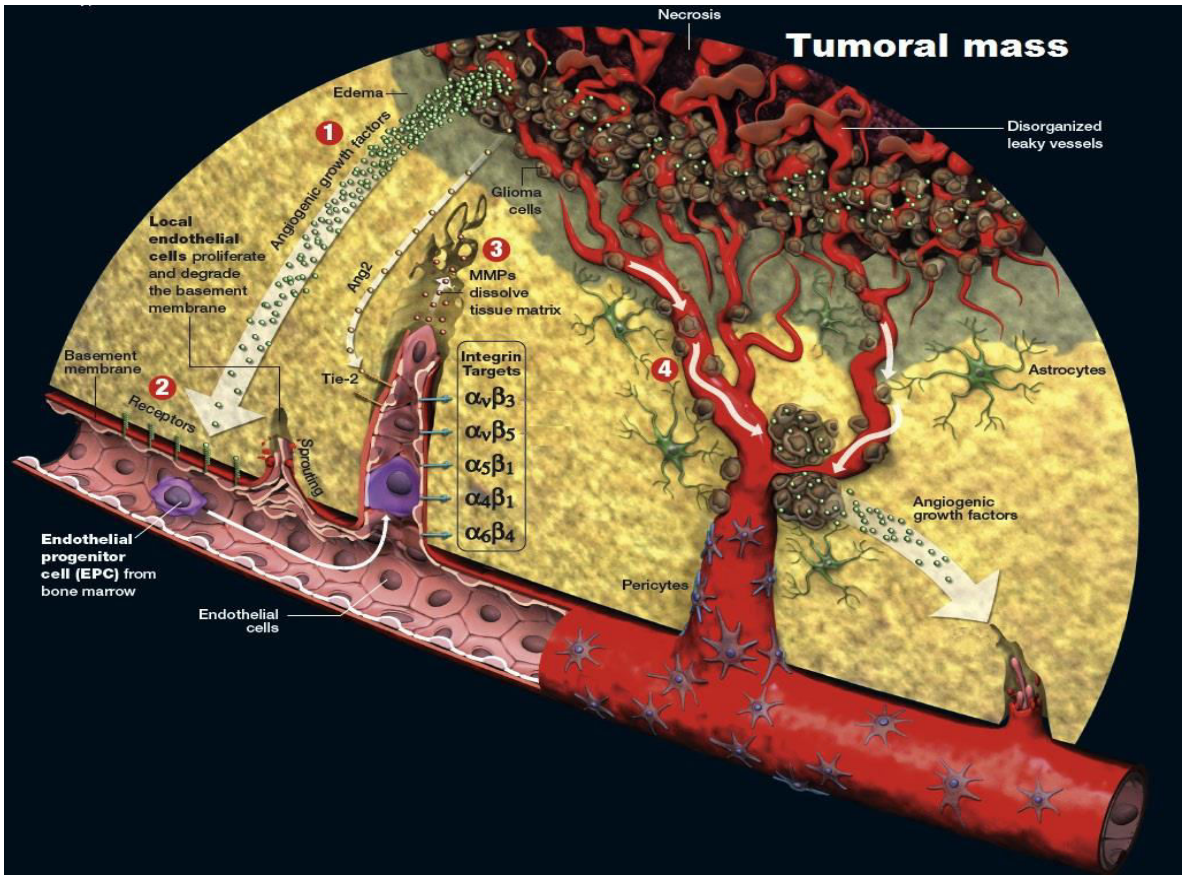

Figure 4. Cancer angiogenesis: 1) Cancer cells issues angiogenic growth factors (VEGF); 2) VEGF activates endothelial cells, which acquire the angiogenic phenotype; 3) Endothelial cells release metalloproteinases to dissolve the ECM and migrate to the cancer ; 4) Once molded new vessels within the tumor, some metastatic cells may enter the bloodstream to get to other organs.

Identification of an increase of endothelial progenitor cells (EPCs) or angioblasts in peripheral blood of cancer patients, has highlighted an alternative mechanism of tumor vessel formation based on EPCs recruitment from bone marrow [119].

Similarly to mature endothelial cells involved in the "classical" process of angiogenesis, EPCs are able to migrate and differentiate to form primitive tubes in Matrigel. Moreover, EPCs can form endothelial-like colonies *in vitro* and show a high proliferative rate, that is lacking in mature ECs [120]. However, it is not yet clear how to define the EPCs that really contribute to vessel formation and their exact role in the process [121]. In this part of the project we propose to use cells from human umbilical cord blood taking into consideration their capability to form a capillary network *in vitro* coupled with a high proliferation potential. Cancer cells are not the only cells which recruit EPCs, also fibroblasts cancer-associated (CAF) are able to engage EPCs to tumor site through the secretion of stromal cell-derived factor-1 (SDF-1), thereby promoting tumor vascularisation [123]. In order to move towards

tumors, to enter into tumor mass and to take a part in new vessel formation EPCs must cross the endothelial barrier and to move within the tumor microenvironment.

Preliminary data obtained in our laboratory show that EPCs are more prone than mature EC to shift from mesenchynal to amoeboid style of movement (MAT, mesenchymal to amoeboid transition).

Once in the tumor EPCs, besides taking part in tumor angiogenesis, synergize with CAFs to promote an epithelial to mesenchymal transition (EMT) and a MAT of cancer cells [116].

In the second part of the project we plan to investigate the role of uPAR in modulating EPC mesenchymal and amoeboid movement in order to control both types of EPCs movement styles by controlling uPAR.

Characterization of Endothelial Progenitor Cells

It was discovered that 3 markers characterize the functional early EPC: CD133, CD34, and the vascular endothelial growth factor receptor-2 (VEGFR-2), termed also kinase insert domain receptor (KDR) or Flk-1 [124,125]. CD133 (termed originally AC133), an early hematopoietic stem-cell marker, is a 120- kDa transmembrane polypeptide, expressed on hematopoietic stem and progenitor cells from human bone marrow, fetal liver, and peripheral blood [126].

We can distinguish two cellular populations:

- "Early EPCs" that we can find both in the bone marrow and immediately after their migration into the systemic circulation. These cells are positive, as we mentioned above, for CD133/CD34/VEGFR-2.
- "Late EPCs" that are present only in peripheral blood. These cells are positive for CD34/VEGFR-2/CD31/VE-cadherin and obviously lose CD133 and begin to express von Willebrand factor (vWF).

It seems that the loss of CD133 reflects the transformation of circulating EPCs into more mature endothelial-like cells. However, it is unclear at which time point the EPCs begin to lose CD133 during their transmigration from the bone marrow into the systemic circulation or later during their circulation. CD133, therefore, is not detectable on the surface of human umbilical vein ECs. Circulating EPCs express with different intensity a variety of markers, which are typical for the endothelial lineage. These markers include platelet endothelial cell

adhesion molecule-1 (CD31), CD146, VE-cadherin, von Willebrand factor, endothelial NO synthase, and, on stimulation, E-selectin.

Furthermore, an interesting observation contrasting the notion of CD34-positive EPC represents the work of Harraz et al.[127]. The authors suggest that CD34-negative angioblasts are a subset of CD14-positive monocytic cells and that these monocytes have the potential to transdifferentiate into ECs. Monocytes may also coexpress endothelial lineage markers and form cord-like structures *in vitro* under angiogenic conditions. Recent data demonstrate that human peripheral blood contains pluripotent stem cells, which are a subset of peripheral monocytes [128]. These cells can be induced by different growth factors or cytokines (eg, VEGF) to acquire different (eg, endothelial) phenotypes. This transdifferentiation potential of monocytic cells into cells with endothelial characteristics would suggest a possible common origin, respectively the existence of a bone marrow–located hemangioblasts.

The colonies of early EPCs were termed colony forming unit–endothelial cells (CFU-EC). These cells are able to ingest and kill microbes, a characteristic of macrophages but not of ECs. In fact, they are not able to form capillary-like structures *in vivo* but facilitate angiogenesis by paracrine secretions of different growth factors.

Subsequent studies it became clear that these colonies were in fact not endothelial cells, but consisted of a core of round, hematopoietic cells, including myeloid progenitor cells, monocytes and T lymphocytes, and spindle-shaped monocytes/macrophages that display some features of endothelial cells. Thus, as mentioned above, early-outgrowth cells can also support angiogenesis in an indirect manner by producing essential growth factors and cytokines, similar to monocytes.

The colonies of late EPCs are composed of true endothelial cells, endothelial colony forming cells (ECFCs) and have the classical endothelial cobblestone phenotype and display a wide range of vascular endothelial markers, but do not express CD45, CD14, or CD115, nor do they ingest bacteria (a monocyte/macrophage characteristic). In comparison with the early-outgrowth CFU-EC, late-outgrowth ECFC show exponential growth and a high proliferative capacity.

Furthermore, in contrast to CFU-EC, the late-outgrowth ECFC spontaneously form blood vessels that associate with the nearby vessels and become a part of the systemic circulation in mice. On the basis of these and other experiments, it has been suggested that the late-outgrowth ECFC are derived from circulating cells that best approximate the true “endothelial progenitor cell” definition of EPC [129-132].

The EPC can be isolated from bone marrow, peripheral blood and cordon blood. Human cord blood is the best alternative for isolating EPCs and the transplantation of cord blood–derived EPCs may participate in and effectively augment postnatal neovascularization *in vivo*. In fact, human umbilical cord blood has been shown to contain a large number of endothelial colony-forming cells compared to other sources [133]. In contrast to adult bone marrow–derived HSCs, cord blood progenitors have distinctive proliferative advantages, including the capacity to form a greater number of colonies, a higher cell-cycle rate, and a longer telomere [134-136]. All of these properties should favor the growth of the cord blood progenitors compared with adult peripheral blood or bone marrow progenitors. In addition, cord blood can be obtained non invasively, in contrast to invasive bone marrow isolation.

Cord blood contained cells with the ability to form colonies after 100 population doublings, which were termed high proliferative potential endothelial colony-forming cells (HPP-ECFC). The colonies themselves included cells expressing an array of EC surface proteins. The development of such assays, which evaluate the self-renewal and proliferative capacity of putative EPCs, will be very helpful in determining the phenotype of the EPC and its differentiation pathway.

Many investigators are currently detecting and quantifying circulating EPCs (CEPCs) using magnetic beads which have been coated with anti-endothelial antibodies, like CD146 antibodies (a cell surface marker).

CHAPTER 2:
PROJECT AIM

The fundamental abnormality resulting in the development of cancer is the continual unregulated proliferation of cancer cells. Rather than responding appropriately to the signals that control normal cell behavior, cancer cells grow and divide in an uncontrolled manner, invading normal tissues and organs and eventually spreading throughout the body. The generalized loss of growth control exhibited by cancer cells is the net result of accumulated abnormalities in multiple cell regulatory systems and is reflected in several aspects of cell behavior that distinguish cancer cells from their normal counterparts. The cells which constitute the tumor eventually undergo metaplasia, followed by dysplasia and then anaplasia, resulting in a malignant phenotype. This malignancy allows for invasion into the circulation, followed by invasion to a second site for tumorigenesis.

After the tumor cells come to rest at another site, they re-penetrate the vessel or walls and continue to multiply, eventually forming another clinically detectable tumor. This new tumor is known as a metastatic (or *secondary*) tumor. Metastasis is one of the main hallmarks of malignancy. Most neoplasms can metastasize, although in varying degrees (e.g., basal cell carcinoma rarely metastasize) [137].

The uPA/uPAR complex, besides its proteolytic activity, also functions as a vitronectin receptor and it participates in normal and tumor cell motility processes such as tumor cells migration and invasion, for this reason we have investigated the uPAR role in cancer cells migration to better understand the trigger mechanisms involved in metastasis process.

We first verified the role of uPAR in the mesenchymal movement. We measured uPAR by a quantitative Real-Time PCR and Western Blotting analysis in cell lines representative of two of the more aggressive human cancer: prostatic carcinoma and melanoma.

Once evaluated uPAR levels, we have verified the capability of our cancer cell lines to shift from mesenchymal to amoeboid migration. To study this aspect we have induced the amoeboid migration using a mixture of protease inhibitors and we have assayed the capability of treated cells to migrate across tridimensional Matrigel matrices (proteases-indipendent condition) compared with control cells.

As previously described amoeboid migrating cells have a roundish shape, which changes frequently thanks to actin polymerization controlled by high activation level of the small GTPase RhoA. Starting from this premise, we have searched amoeboid features in protease inhibitors treated cells using confocal microscope and quantifing active RhoA, to confirm the occurred transition from mesenchymal migration to amoeboid mode in our cell lines[138].

As it is known from literature, uPA-receptor regulates the mesenchymal style of cell movement by triggering pericellular proteolysis. Therefore we have evaluated if uPAR has a role in amoeboid migration treating cancer cells with antisense oligodeoxinucleotide, which blocks uPAR mRNA down-regulating uPAR expression.

uPA is able to cleave its cell surface receptor uPAR and this cleavage leads to the formation of cell surface truncated forms, devoid of the N-terminal domain 1 (D1).

To investigate the possible role(s) of the forms of cell surface glycophosphatidylinositol-anchored uPAR in amoeboid migration, we have performed invasivity assays and phenotypical analysis in uPAR-negative human embrional kidney 293 cells (no-uPAR), transfected with the cDNA of intact uPAR (D1D2D3-uPAR) or with cDNAs corresponding to the truncated forms of uPAR (D2D3-uPAR). These experiments have been performed in presence and absence of protease inhibitor mixture.

Due to its glycosyl-phosphatidyl-inositol (GPI)-anchor attachment [96], uPAR is devoid of a transmembrane domain, a feature that makes uPAR incapable of signalling. This characteristic requires membrane partners enabling uPAR to deliver signals that propagate to the cell contractile apparatus. Most consistently uPAR has been found associated with integrins [92,93,97]. Besides interaction with ECM ligands, integrins provide a molecular link that connects microenvironment to the cytoskeleton. Together with a long series of adaptor proteins integrins define molecular mechanical pathways in cells, which subsequently determine actin dynamics and cell movement [139]. Thus, a major pathway that controls in-ward integrin activity may define and distinguish cancer cell invasion strategies. On these considerations, we used a peptide known as M25 able to prevent uPAR-integrin interaction during focal adhesion complex formation.

The most important purpose in this study is to demonstrate that uPAR bridges the mesenchymal and amoeboid style of movement in a series of prostate carcinoma and melanoma cell lines, by its interaction with integrins.

Metastatic development is not the only cellular migration occurrence of cancer progression, infact also during tumor angiogenesis endothelial cells migrate to the tumor, recruited by cancer cells.

We decided to enrich this project with a second part focused on uPAR role cancer amoeboid angiogenesis in endothelial progenitor cells (EPC), because in cancer patients peripheral blood have been found high numbers of EPCs recruited from bone marrow [119].

Once isolated EPCs, we have proceeded with invasivity experiment to evaluate their migratory capability with and without proteases inhibition.

To induce the amoeboid-migration in EPCs we have tested, in addition to chemical protease inhibitor mixture, a physiologic protease inhibitor mix in this part of the project, with the aim to recreate a proteases-indipendent condition closer to tumoral microenvironment. We evaluated the main amoeboid migration parameters (cell morphology, Rho/Rac activation level) using confocal microscopy and activation assays of small GTPases involved in migration.

A future prospective is to treat EPC with anti-sense oligodeoxinucleotide to down-regulate uPAR expression, and understand if the receptor has a role in this migratory process. The anti-uPAR treatment of EPC has the possibility to block the entrance of EPCs into tumor mass and eliminate the EPC-dependent tumor progression.

CHAPTER 3:
MATERIALS AND METHODS

Cancer cell lines and culture conditions

Prostate cancer cell lines LNCaP and PC3 were purchased from ATCC (Manassas, VA, USA). LNCaP are androgen-sensitive human prostate adenocarcinoma cells, while PC3 cells, derived from a bone metastasis of a grade IV prostatic adenocarcinoma, are reported to be androgen receptor (AR)-negative. Pcb1 cell line, established from a bone metastasis of PC3, were provided by Professor Adriano Angelucci (L'Aquila, Italy). All prostate cancer cell lines were grown in RPMI-1640 culture medium (Euroclone, Milano, Italy) containing 2 mM glutamine, 100 UI/ml penicillin, 100 μg/ml streptomycin and supplemented with 10% fetal bovine serum (FBS; Euroclone). Melanoma cell lines MeWo and A375 were purchased from ATCC. A375 M6 cells, derived from a metastasis of A375, were provided by Professor Lido Calorini (Firenze, Italy). Melanoma cells were maintained in DMEM culture medium (Euroclone, Milano, Italy) containing 2 mM glutamine, 100 UI/ml penicillin, 100 μg/ml streptomycin and supplemented with 10% FBS (Euroclone). uPAR-negative human embrional kidney 293 (HEK-293) cells transfected with cDNA of intact uPAR (uPAR-D1D2D3), with cDNAs corresponding to the truncated form of uPAR (uPAR-D2D3) and with pcDNA3 empty vector (no-uPAR), were kindly provided by Professor Pia Ragno (Napoli, Italy). HEK-293 transfected cells were grown in DMEM culture medium (Euroclone, Milano, Italy) containing 2 mM glutamine, 100 UI/ml penicillin, 100 μg/ml streptomycin and supplemented with 10% fetal bovine serum (FBS; Euroclone).

Isolation and characterization of EPCs

Human umbilical cord blood (UCB) samples (volume > 50 mL) were collected in citrate phosphate dextrose solution from health newborns. We used cord blood units with a number of total nucleated cells < $1.3x10^9$ (threshold of suitability for the banking established by the Umbilical Cord Bank of Careggi, Florence, Italy) after maternal informed consent in accordance with the Declaration of Helsinki and in compliance with Italian legislation. Blood was diluted 1:1 with Hanks balanced salt solution (EuroClone) and was overlaid on an appropriate volume of density gradient separation medium (Lympholyte; Cedarlane). Cells were centrifuged for 30 minutes at room temperature at 740*g*. Mononuclear cells were recovered, washed 3 times with Hanks balanced salt solution and resuspended in complete EGM-2 medium (Lonza) supplemented with 10% FBS (Hyclone), 50 ng/mL VEGF (PeproTech) and 5 IU/mL heparin. Cells were seeded on gelatin-coated 6-well tissue culture plates at a density of $5x10^5$ cells/cm2 in a 5%CO2 humidified incubator at 37°C. On days 4 and 7, half of the medium was exchanged with fresh medium. Then the medium was changed

completely with EGM2–10% FBS every 3 days. EPC colonies appeared in cell cultures after 2-3 weeks and were identified as circumvented monolayers of cobblestone-like cells. The colonies were mechanically picked from the original plate and seeded on another gelatin-coated well with EGM2–10% FBS for expansion. These cells can be maintained in culture for 8-10 passages with the same culture medium of EC.

Flow cytometric analysis:

ECFCs were CD31+, KDR+, CD105+, ULEX+, vWF+, CD45-, CD34-. The characterization was based on flow cytometric analysis. ECFCs were analyzed for the expression of typical surface staminal, endothelial or monocyte-macrophage antigens by flow cytometry. To recognize surface antigens, it was necessary to use fluorochrome-labeled monoclonal antibodies. The fluorochrome that we used was phycoerytrin (PE-red) and fluorescein (FITC-green). Both are exited at wavelength of 488 nm (blue), so they can be used together for a very sensitive detection system in the double labeling. To characterize the cells obtained by the technique described above, first, washed cells were resuspended in flow cytometry buffer (CellWASH 0.1% sodium azide in PBS; BD Biosciences). Aliquots ($0.1x10^6$ cells/100 μL) were incubated with the following conjugated monoclonal antibodies: CD45-FITC, CD34-FITC, CD31-FITC (all from BD Biosciences PharMingen); CD105/R-phycoerythrin (Ancell); ULEXFITC (Vector Laboratories); phycoerythrin-labeled by Tetra-Tag phycoerythrin-labeling kit (StemCell Technologies) KDR (RELIATech), uPAR/R3 (BioPorto Diagnostic A/S), and vWF (BD Biosciences PharMingen). Nonspecific fluorescence and morphologic parameters of the cells were determined with isotype-matched mouse monoclonal antibodies (BD Biosciences PharMingen). All incubations were done for 20 minutes; and, after washing, cells were resuspended in 100 μL of CellWASH. 7-Aminoactinomycin (BD Biosciences PharMingen) was added to exclude dead cells from the analysis. Flow cytometric acquisition was performed by collecting 104 events on a FACSCalibur (BD Biosciences) instrument, and data were analyzed on DOT-PLOT biparametric diagrams using Cell Questpro OS X.1 software (BDBiosciences) on a Macintosh PC.

Capillary morphogenesis:

Capillary morphogenesis was performed in 13-mm tissue culture wells coated with Matrigel. Experimental conditions were the same used for invasion assay. ECFCs were plated ($60x10^3$/well) in complete EBM-2 medium 2% FCS and incubated at 37°C, 5% CO2. Plates were photographed at 6 hours and at 24 hours. Results were quantified by image analysis, giving the percentage of photographic field occupied by ECFC. Six to 9 photographic fields

from 3 plates were scanned for each point. Results were expressed as percentage field occupancy with respect to control taken as 100% ± SD.

Quantitative Real-Time PCR analysis

Total RNA was prepared using Nucleospin RNA II (Macherey-Nagel), agarose gel checked for integrity, and reverse transcribed with GoScript system (Promega) using random primers according to manufacturer's instructions. uPAR expression in all cancer cell lines and after anti-uPAR aODN treatment was determined by a quantitative Real-Time (RT)–PCR with an Applied Biosystem 7500 Fast Real Time PCR System (Applied Biosystems, Milano, Italy) and determined by the comparative C_t method using 18S ribosomal RNA as the normalization gene. Amplification was performed with the default PCR setting: 40 cycles of 95°C for 15 seconds and of 60°C for 60 seconds using SYBR Green–based detection (GoTaq qPCR Master Mix; Promega). Primers (IDT, Tema Ricerca, Italy) used for RT-PCR were as follows: -18S-rRNA: sense, 5'-CCAGTAAGTGCGGGTCATAAG-3' antisense, 5'-GCCTCACATAACCATCCAATC-3'; -uPAR: sense, 5'- GCCCAATCCTGGAGCTTGA-3; antisense, 5'- TCCCCTTGCAGCTGTAACACT-3'.

Semiquantitative reverse transcription– polymerase chain reaction (PCR) analysis

Total RNA preparation and reverse transcription were performed as described in the previous paragraph. The levels of messenger RNA for the integrin chains were determined by an internal-based semiquantitative RT-PCR. RT-PCR was performed for 35 cycles at 58°C in a thermocycler. The reaction products were analyzed by electrophoresis in 1% agarose gel containing ethidium bromide, followed by photography under ultraviolet illumination using Polaroid positive/ negative instant films. Primers sequences and cycling conditions are: uPAR primer sense 5'-AAAATGCTGTGTGCTGCTGACC-3' and antisense 5'-CCTGCCCTGAAGTCGTTAGTG-3'; GAPDH primer sense 5'-CCACCCATGGCAAATTCCATGGCA-3' and antisense 5'-TCTAGACGGCAGGTCAGGTCCACC-3'; their cycling profile is 94°C 1 minute, 56°C 1 minute, 72°C 1 minute.

Immunoprecipitation and Western blotting

Cells were lysed as were directly lysed in RIPA buffer. Five hundred micrograms of cell protein was transferred into an Eppendorf tip, and the relevant primary antibody (anti-integrin or antiuPAR) was added in 0.1% bovine serum albumin, followed by overnight incubation at

4°C. To each lysate, protein A agarose beads (Sigma, St. Louis, MO) were added for 3 hours at 4°C. The beads were collected by centrifugation at 14,000 revolutions per minute for 30 seconds, and the supernatant was stocked for further Western blotting. Aliquots of the pellets were processed, electrophoresed, and blotted as described previously [140]. After incubation with 5% skim milk in 20 mM Tris buffer, pH 7.4 (blocking solution), membranes were probed with a monoclonal antibody directed against uPAR (1:200) (American Diagnostica, Stamford, CT), overnight at 4°C. After incubation with horseradish peroxidase (HRP)–conjugated anti-mouse or anti-rabbit IgG (1:5,000) for 1 hour (Amersham Biosciences, Uppsala, Sweden), immune complexes were detected with the enhanced chemiluminescence (ECL) detection system (Amersham Biosciences). The membranes were exposed to autoradiographic films (Hyperfilm MP; Amersham Biosciences) for 1–30 minutes. After 30 minutes' incubation with stripping solution (62.5 mM Tris HCl, pH 6.8, containing 100 mM -mercaptoethanol and 2% sodium dodecyl sulfate), the membrane was washed for 5 minutes with 20 m*M* Tris buffer, pH 7.4, incubated for 30 minutes at room temperature with blocking solution, and reprobed with anti-integrin or anti-uPAR antibodies.

Invasion assay with Boyden chambers

Invasion was studied in Boyden chambers in which the upper and lower wells were separated by 8µm–pore size polycarbonate filters coated with Matrigel (BD Biosciences). In order to increase uPAR dependency of the invasion process, the Matrigel was enriched with human VN (Sigma-Aldrich, cat. V8379), to a final concentration of 300 µg/ml. To obtain a "thick" layer, we added 100 µl of Matrigel/cm_2 porous membrane. According to the manufacturer's instruction such an amount results into a 500 µm thick Matrigel layer, corresponding to about 25 folds the average diameter of circulating prostate and melanoma cells [141]. Cancer cells (25 x 10_3) were placed in the upper well of the Boyden chamber, and invasion was performed at 37 °C in 5% CO2 for 12 hours, a time consistent with the average speeds of cell migration under amoeboid and mesenchymal conditions in 500 µm thick gels [2]. To evaluate the uPAR-dependent invasion, some experiments were performed in the presence of anti-uPAR R3 antibody which blocks uPA/uPAR interaction (American Diagnostica) or after anti-uPAR aODN treatment. Invasion quantified as previously described [140].

Protease-indipendent invasion was evaluated by 3D-Boyden chamber assays with Matrigel coating in the presence of a protease inhibitor cocktail (Tab.1), a mixture of protease inhibitors with a broad specificity for serine, cysteine, aspartic and amino-peptidase, and MMPs [142]. To analyse the protease-indipendent invasion in EPC we have

accomplished invasiviness assay in presence of physiologic protease inhibitor cocktail (Tab. 2). Protease inhibitor cocktail was added to un-polymerized Matrigel solution on the upper surface of the porous filter. To induce the amoeboid phenotype, cells were treated for 2 hours with the protease inhibitor cocktail at the same concentrations used in the invasion assay.

INHIBITOR	PROTEASES	CONCENTRATION
AEBSF	**Serine Proteases**	**104 mM**
Aprotinin	**Serine proteases**	**80 µM**
Leupeptina	**Serine and Cysteine proteases**	**2 mM**
Bestatin	**Amino peptidasi**	**4 mM**
Pepstatin A	**Acid proteasi**	**1,5 mM**
E-64	**Cysteine proteases**	**1,4 mM**
Ilomastat	**Metallo-proteases**	**10 µM**

Table 1. Composition of protease inhibitor mixture and respective concentration.

INHIBITOR	PROTEASES	CONCENTRATION
α_2-antiplasmina	**Serine Proteases**	**5 µg/ml**
Cystatin	**Cysteine proteases**	**5 µM**
PAI 1	**uPA, tPA**	**10 ng/ml**
TIMP 1	**MMP**	**0,5 µg/ml**
TIMP 2	**MMP**	**0,5 µg/ml**
TIMP 3	**MMP**	**0,5 µg/ml**

Table 2. Composition of physiologic protease inhibitor mixture and respective concentration.

Cell Proliferation Assay and Trypan blue exclusion assay

The viability of cancer cell lines and EPCs was determined by a cell proliferation assay using WST-1 reagent (Roche). WST-1 is a water-soluble sulfonated tetrazolium salt that is cleaved by cellular succinate-dehydrogenases in living cells, yielding dark blue formazan. Damaged

or dead cells exhibit reduced or no dehydrogenase activity. Briefly, the cells were plated onto a 96-multiwell plate in quadruple. After 24, 48 and 72 hours WST-1 solution/culture medium (5 mmol/l, 1:9) was added to each well. Following 1-hour incubation at 37°C, absorbance at 450 nm (reference at 630 nm) was measured by a Multiskan JX microplate reader. Percentage of cell viability was calculated based on the absorbance measured relative to that of the untreated control cells maintained in culture medium alone. After proteases inhibitors mixes (chemical and physiologic) harvested EPCs were mixed with an equal volume of 0.4% trypan blue dye. For quantization of cell viability, blue and bright cells were counted, and viability was calculated as the percentage of live (bright) cells versus control set to 100%.

Collagen degradation assay

The collagen degradation assay was performed using a Matrigel layer containing 2 % FITC-labeled collagen monomers. Cells suspensions has been copolymerized with Matrigel and FITC-labeled collagen and degradation has been allowed for 40 h. Solid-phase collagen containing the cells will be pelleted, whereas FITC released into the supernatant will be analyzed by spectrofluorometry. One hundred percent values have been obtained by complete collagenase (1mg/ml) digestion of cell-free collagen lattices. Background fluorescence has been obtained by pelletting non-digested cell-free lattices. These experiments have been performed with control cells and with EPCs treated with the physiologic protease inhibitor cocktail or with cancer cells treated with the chemical protease inhibitor cocktail.

Cell migration in 3D-collagen matrices

To visualize the efficacy of the protease inhibitor cocktails to induce an amoeboid migration style we used reconstruction by time-lapse video microscopy and confocal microscopy, using HT1080 cells as a model for a clear visualization of fiber breakdown in the process of proteolytic migration and shift to the amoeboid style. Subconfluent cells were detached by EDTA (2 mmol/L), washed, incorporated into three-dimensional collagen lattice (1.67 mg/mL; native dermal bovine type I collagen; RD Systems), and monitored by time-lapse video microscopy. We used HT1080 cells as model for a clear visualization of fiber breakdown in the process of proteolytic migration. To observe amoeboid condition, the protease inhibitor cocktail was added to the lattice before polymerization as well as to the supernatant. For three-dimensional time-lapse confocal microscopy (Leica-SP5 system), cells within the lattice were labeled by calcein-AM (1 μmol/L), scanned at 3-min time intervals for

simultaneous fluorescence and back scatter signal (reflection), and reconstructed. Three-dimensional motility of cells is shown by time lapse of xyzt analysis (three-dimensional analysis during time). Movies are a two-dimensional projection (xy) of all stacks during a time course. xy two-dimensional migration of cells has been excluded by analysis of zx axis movements during the same time course (see supplementary movie 1 and 2 on line publication of this work [138]).

RhoA and Rac1 activity assay

Cells from different experimental conditions (control, protease inhibitor cocktail, anti-uPAR aODN and anti-uPAR aODN + protease inhibitor cocktail) were directly lysed in RIPA buffer, the lysates were clarified by centrifugation, and RhoA-GTP or Rac-GTP was quantified. Briefly, lysates were incubated with 10 µg Rhotekin-glutathione *S*-transferase (GST) fusion protein (Upstate) or p21 activated kinase-GST fusion protein, both absorbed on glutathione-Sepharose beads for 1 h at 4°C. Immunoreactive RhoA or Rac1 was then quantified by Western blot analysis. Lysates were normalized for RhoA or Rac1 content by immunoblot.

Immunofluorescence analysis

Immunofluorescence was performed on cancer cells and EPC grown on coverslips in their culture conditions. Once at confluence, cells were treated with protease inhibitor cocktail respective and two hours later fixed in 4% paraformaldehyde. TRITC-labelled phalloidin (P1951, Sigma) was applied to the cells to visualize cell morphology and the arrangement of actin cytoskeleton. Nuclei were stained with the fluorescent Hoechst 33342 dye (DAPI) (10µg/ ml) (Invitrogen) for 15 min at rt. To display uPAR and integrins in cancer cells the anti-human primary antibodies used were rabbit polyclonal antibody anti-uPAR FL-290 (1:100) (SANTA CRUZ BIOTECHNOLOGY, INC) mouse anti–β1 integrin subunit MAB 1969 (1:100), and mouse anti–β3 integrin subunit (1:100) (Chemicon International). The secondary antibodies used for immunostainings were Alexa 488–conjugated goat anti-mouse IgG (1:200) (Molecular Probes, Eugene, OR), and Texas Red–conjugated goat anti-rabbit IgG (1:200) (Molecular Probes).

The coverslips containing the immunolabeled cells were observed under a Bio-Rad MRC 1024 ES confocal laser scanning microscope (Bio-Rad, Hercules, CA) equipped with a 15-

mW krypton/Argon laser source for fluorescence measurements, using an excitation wavelength appropriate for Alexa 488 (495 nm) and Texas Red (595 nm). Series of optical sections (X- and Y-steps: 512 _ 512 pixels) were then obtained through the depth of the cells, with a thickness of 1 _m at intervals of 0.8 _m (Z-step). A single composite image was obtained by superimposition of twenty optical sections for each sample observed. The collected images were analysed by ImageJ software to evaluate co-localization.

uPAR down-regulation with antisense oligodeoxinucleotide (u-PAR aODN)

uPAR gene expression was inhibited with an 18-mer phosphorothioate aODN (ISIS Pharmaceuticals, Carlsbad Research Center, CA, USA, product designation: ISIS 17916) . The sequence of ISIS 17916 is 50-CGG CGG GTG ACC CAT GTC-30. As negative control, we used a completely degenerated 18-mer ODN (scrambleODN): such ODN is a mixture of all the possible combinations of the bases, which compose the aODN. ODN uptake and stability were enhanced by combining ODNs (10 mmol/l) with a cationic liposome (13 mmol/l), namely DOTAP (Boehringer Mannheim, Mannheim, Germany). Cell cultures were treated daily with ODNs for 4 days, on the basis of preliminary experiments indicating a steady-state reduction of uPAR number and of uPAR mRNA after 3 days of aODN treatment. Since the half-life of cationic lipidcombined ODNs in the culture medium was about 24 h, the initial treatment with 10 mM cationic lipid-combined ODN was followed by a second addition of 5 mM after 24 h in order to restore the initial concentration. On the fourth day, cells were subjected to invasivity assays , to evaluate the role of the uPAR on amoeboid migration. In all the experiments performed with ODNs, we have supplemented cells with heat-inactivated serum (15 min at 651C) in order to inactivate serum nucleases able to degrade the added compounds.

Treatment of cells with M25 peptide

Disruption of uPAR-integrin interaction was obtained with the M25 peptide, previously identified in a phage display library [143-145], able to uncouple uPAR interaction with integrin α-chain. The peptide was produced in collaboration with PRIMM srl, Milan, Italy. In the β-propeller model of α-chain folding, the sequence of this peptide (STYHHLSLGYMYTLN) spans an exposed loop on the ligand-binding surface of α-chain,

thus impairing integrin-uPAR interaction. In cell culture both M25 and scramble-M25 (sM25) were used at 50 μM for 2h at 37°C.

Statistical analysis

Results are expressed as means ± SD. Multiple comparisons were performed by the Student test. Statistical significances were accepted at $p<0.05$.

CHAPTER 4:
RESULTS

Function of uPAR in mesenchymal invasion of tumor cells

uPAR is expressed by cells that move in a mesenchymal fashion, since uPAR-bound uPA promotes plasminogen activation to plasmin and subsequent MMPs and proteases activation-dependent ECM degradation.

In order to correlate uPAR espression level to invasive property of cancer cell lines, we performed Boyden Chambre-Matrigel invasion assay. We found a correlation between uPAR expression levels and the number of invasive cells. First of all we evaluated the expression levels of uPAR in melanoma and prostatic carcinoma cell lines (figure 5A and 5B), than we assayed the invasion property (figure 5C). Quantitative Real-Time PCR and Western Blotting analysis showing that uPAR expression was proportional to the number of invasive cells in the Boyden chamber assay.

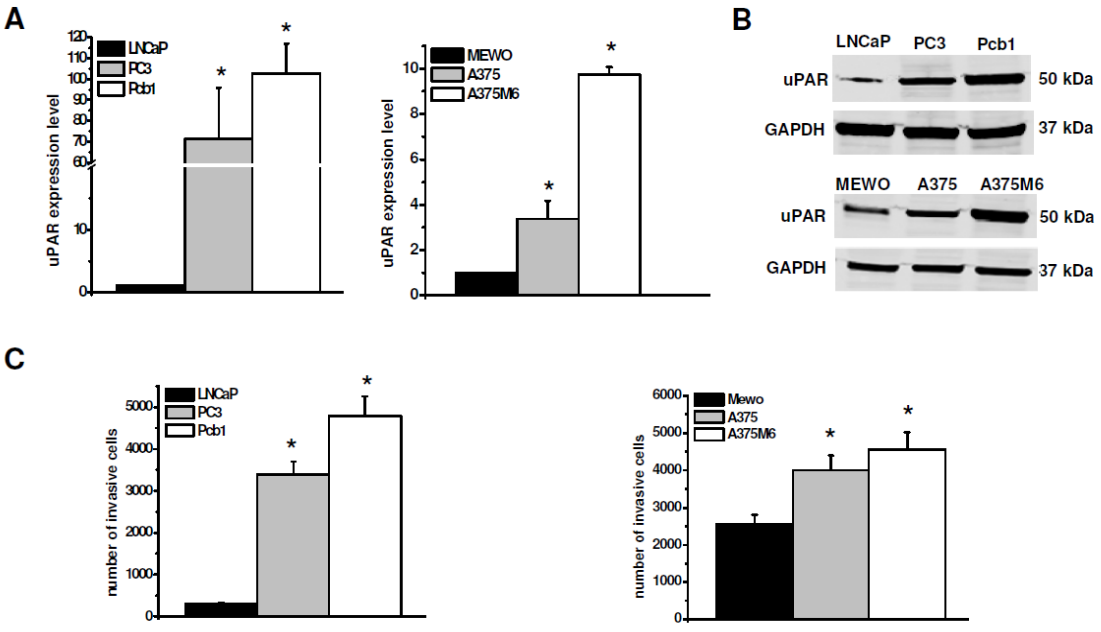

Figure 5: uPAR expression and function in mesenchymal invasion of prostate cancer and melanoma cells. Panel A: Quantitative Real-Time PCR of uPAR in melanoma and prostate cancer cell lines. Results are the mean of three different experiments ± SD. * : $p<0.05$ with respect to LNCaP and MEWO cells, respectively. Panel B: Western Blotting analysis of uPAR in prostate cancer and melanoma cell lines. Numbers on the right refer to molecular weights expressed in kDa. GAPDH used as a reference loading control. Panel C: invasion of porous filters coated with a 3D Matrigel layer, showing the differential total number of invading cells/filter for each one of the used cell lines.

Blocking uPAR mesenchymal function with an antibody (R3) against uPAR domain-1, thereby masking the uPA binding site, resulted into a decrease of invasion which was similar in all the examined cancer cell lines (figure 6). The use of the blocking antibody blunted the uPAR-dependent proteolytic cascade without using protease inhibitors.

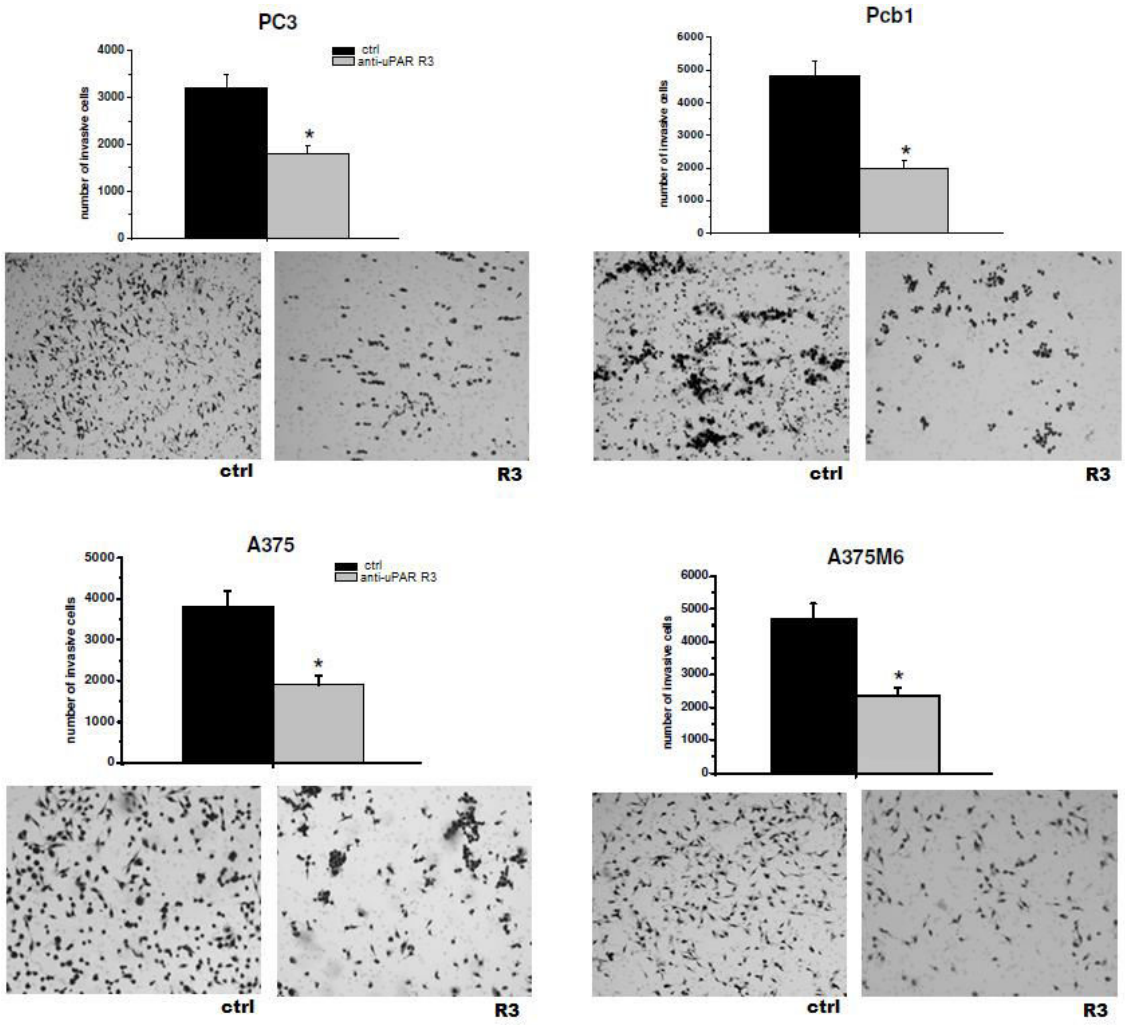

Figure 6: uPAR function in mesenchymal invasion of prostate cancer and melanoma cells. Activity of the R3 uPAR-blocking antibody on Matrigel invasion. The pictures show the typical appearance of filters in the absence and in the presence of the R3 antibody for each cell line. Results are the mean of three different experiments ± SD. * : $p<0.05$ with respect to LNCaP and MEWO cells (Figure 5B), or with respect to control (Figure 5C), respectively.

Induction of the amoeboid phenotype

To appraise the acquisition of the amoeboid phenotype performed Matrigel invasion, collagenase activity assay, Rac1/RhoA activation and cell morphology, in the presence of the inhibitor cocktail added to the cell suspension and to Matrigel solution before polymerization. To evaluate whether exposure to a protease inhibitor cocktail induced a protease-independent invasion, we subjected cancer cell lines to a Boyden chamber migration assay through a thick

Matrigel coating,. In figure 7A we show the percent amoeboid response of each cell line. Respect to the mesenchymal control was not comparable in terms of invasive cells, ranging from 30% to 72% depending on the cancer cell line, indicating that plasticity of cell migration upon variation of microenvironment conditions is greatly variable among cancer cells.

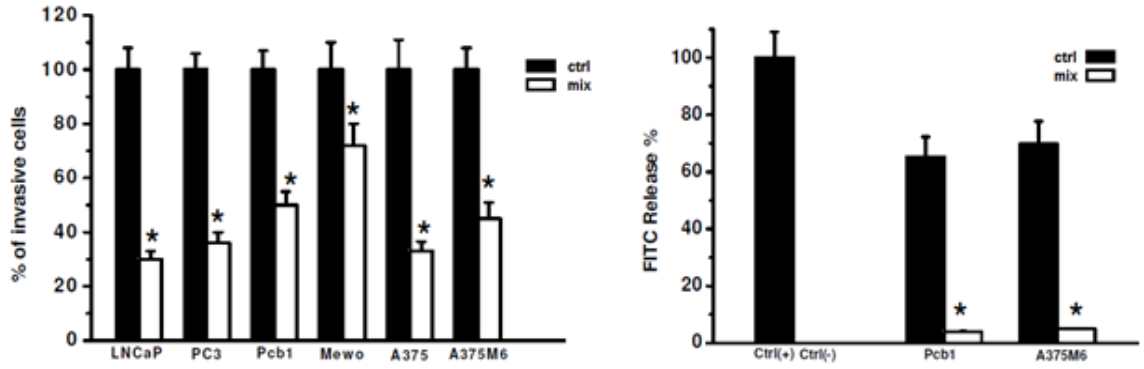

Figure 7: Induction of the amoeboid movement in prostate cancer and melanoma cells. Panel A: the histogram on the left shows invasion of porous filters coated with a 3D Matrigel layer, expressed as % cells moving under amoeboid conditions for each one of the cell lines. Refer to figure 5C for the absolute number of invading cells under mesenchymal conditions. Mix: presence of the protease inhibitors cocktail. Results are the mean of five different experiments performed in triplicate on each cell line ± SD. * : $p<0.05$. Panel B: The histogram shows the collagenolytic activity of Pcb1 and A375M6 cells under mesenchymal and amoeboid conditions; Ctrl-: collagenolytic activity in the absence of cells and of added exogenous collagen; Ctrl+: collagenolytic activity in the absence of cells but in the presence of exogenous collagenase. Results are the mean of two different experiments performed in triplicate on each cell line ± SD. * : $p<0.05$.

We performed collagenase activity assay of two different cancer cell lines sharing an high invasive potential (see figure 5C). To prove the proteases inhibition we have carried out collagen degradation assay, where the cells are plunged in FITC-labelled collagene. When proteases degrades FITC-collagene, it gives off fluorescence (more flourescence = more proteases activity). The panel B istogram in figure 7, shows the collagenolytic activity of Pcb1 and A375M6 cells under mesenchymal and amoeboid conditions expressed as % collagen degradation with respect to the positive control obtained by addition of exogenous collagenase. The experimental conditions here referred to as "amoeboid" were characterized by a residual proteolytic activity that did not account for the size of the invasive cell population (Figure 7B). To characterize the motility shift we also analyzed the activation of two recognized regulators of the cytoskeleton, the small GPTases RhoA and Rac1. Mesenchymal motility has been recognized to be causally linked to activation of Rac, which drives motility by promoting lamellipodia and filopodia, and inhibition of Rho GTPases, whereas an opposite phenotype has been associated with amoeboid motility. Western blotting data for the activated forms of RhoA and Rac1, compared to total RhoA and Rac1, provided

univocal results for all the examined cell lines, showing a decrease of activated Rac1 and an increase of activated RhoA upon shifting of cells to the amoeboid movement (Figure 8). The overall morphology of the cell and its dependency on actin cytoskeleton assembly is characteristic of the movement style. Mesenchymal motility is connoted by an elongated, fibroblast-like, cell morphology with established cell polarity, dependent on the small GTPase Rac which, in turn, organizes actin polymerization to form filopodia and lamellipodia , giving origin to actin-rich protrusions. These features were exhibited by cancer cells under control conditions. Under the stimulus of proteases inhibition all the cell lines acquired a round morphology and a sub-membranous cortical actin localization, features connoting the amoeboid movement (figure 9).

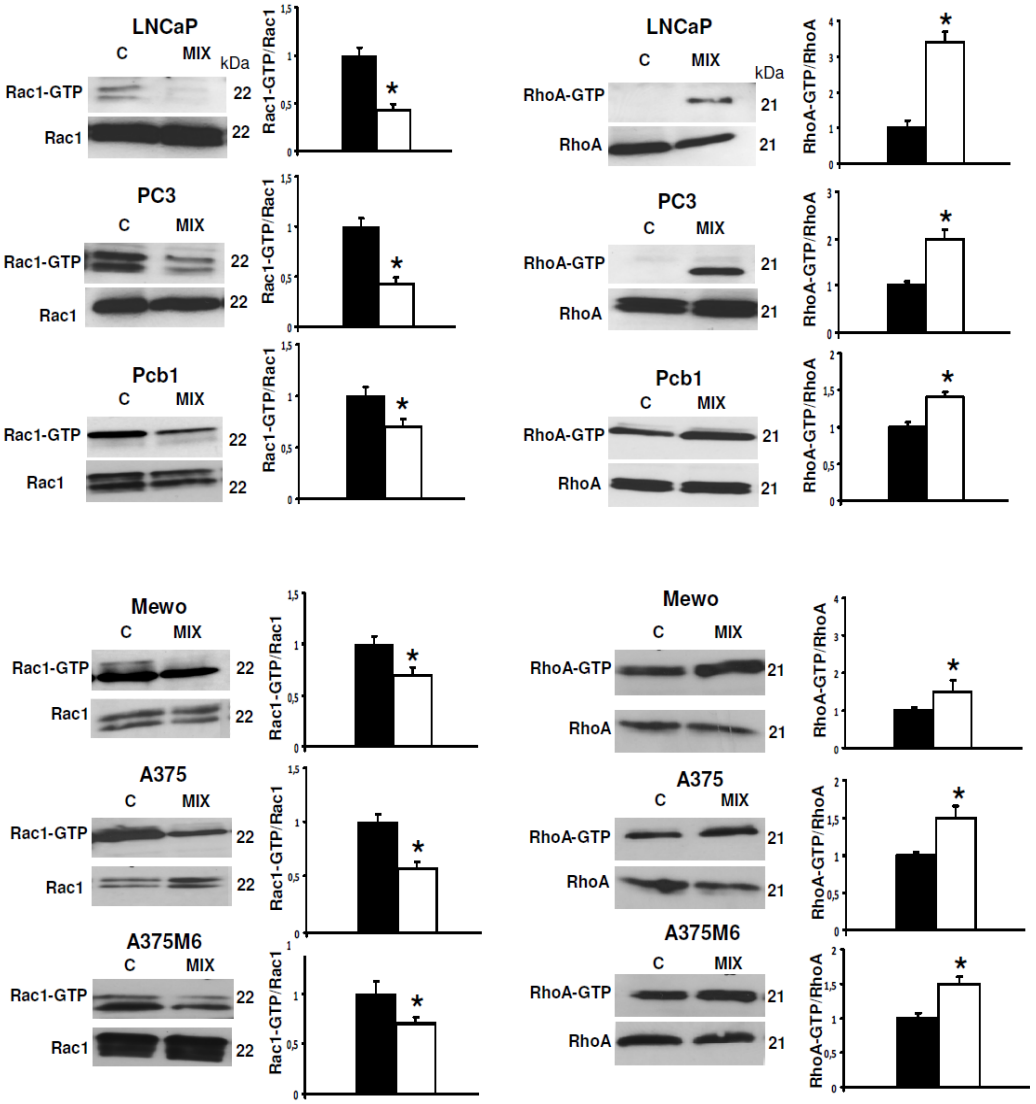

Figure 8: Biochemical features evaluation of the amoeboid movement in prostate cancer and melanoma cells. Western blotting of total and GTP-loaded forms of small Rho-GTPases RhoA and Rac1 under mesenchymal and amoeboid conditions for each prostate cancer and melanoma cell line. Three experiments were performed for each cell line in each condition. Histograms report band densitometry; * indicates statistical significance at $p<0.05$. Numbers on the right refer to molecular weights expressed in kDa. Rac1- GTP and

RhoA-GTP, GTP-loaded forms of small Rho GTP-ases; Rac1 and RhoA, total un-loaded forms of small Rho GTP-ases, used as a reference loading control.

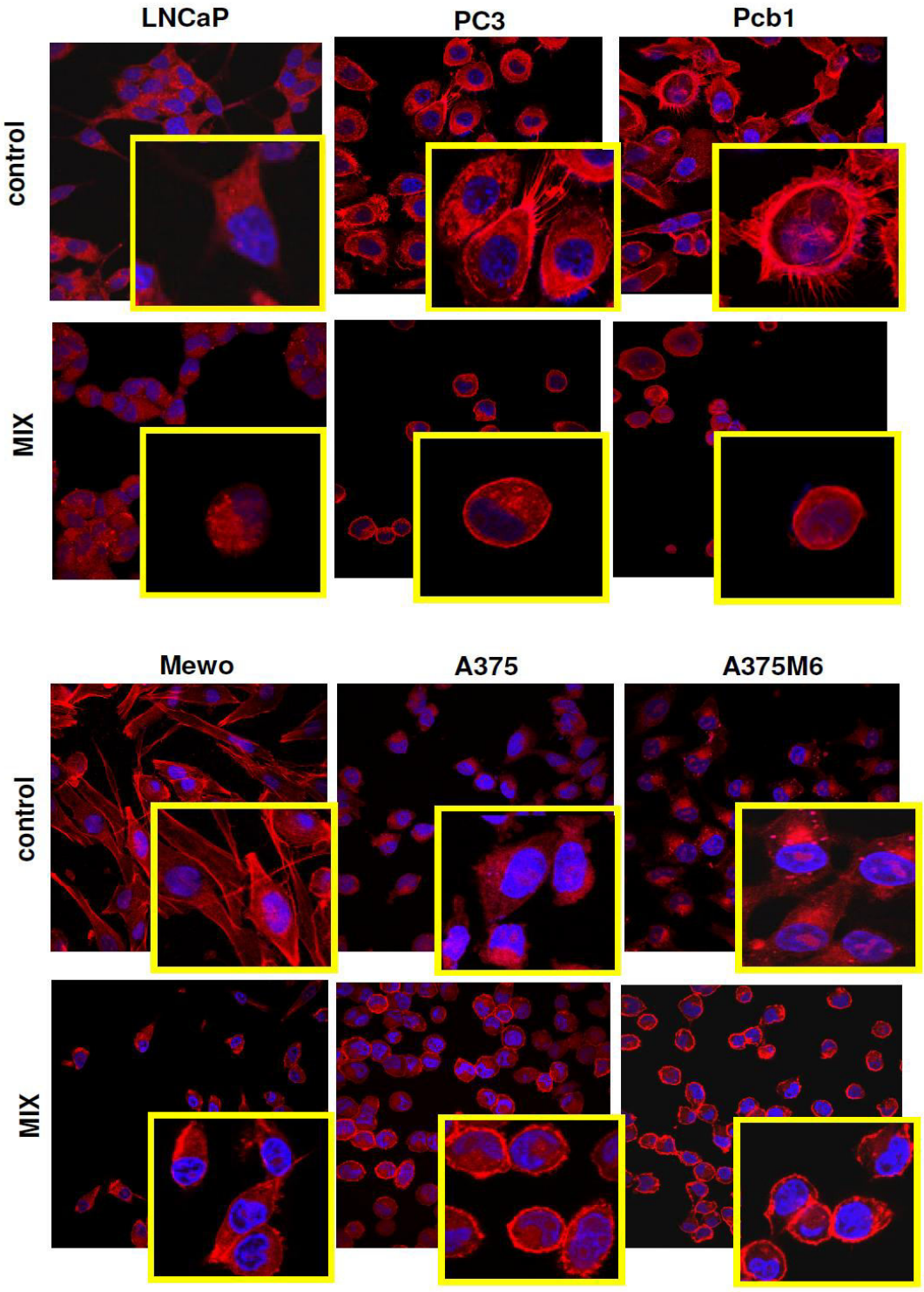

Figure 9: Morphological features of the mesenchymal (elongated) to amoeboid (roundish) transition (MAT) of prostate cancer and melanoma cells. Each picture shows the general pattern and related magnification of a small field for each cell line. Red: phalloidin staining of the actin cytoskeleton. Blue: nuclear staining with DAPI. Magnification 40 X for reference pictures and 100 X for enlarged insets. Results shown are representative of two different preparations of each cell line under mesenchymal and amoeboid conditions. Round cells, perinuclear cortical actin localization and the loss of actin-rich filopodia are evident in amoeboid conditions.

The WST-1 assay showed that viable cells were more that 95% under both control and protease inhibitors treatment. Moreover, once re-incubated with an inhibitor cocktail-free medium, treated cells completely recovered their functional and morphological mesenchymal features (data not shown).

Requirement of uPAR in amoeboid migration

Genetic uPAR knockdown has demonstrated robust antitumor activity both *in vitro* and in pre-clinical studies. To induce the loss of uPAR function we used the uPAR-aODN previously used in other studies of our laboratory [140]. uPAR-aODN produced an evident reduction of uPAR expression inducing a strong decrease of mesenchymal and amoeboid movements (figure 10A and 10B).

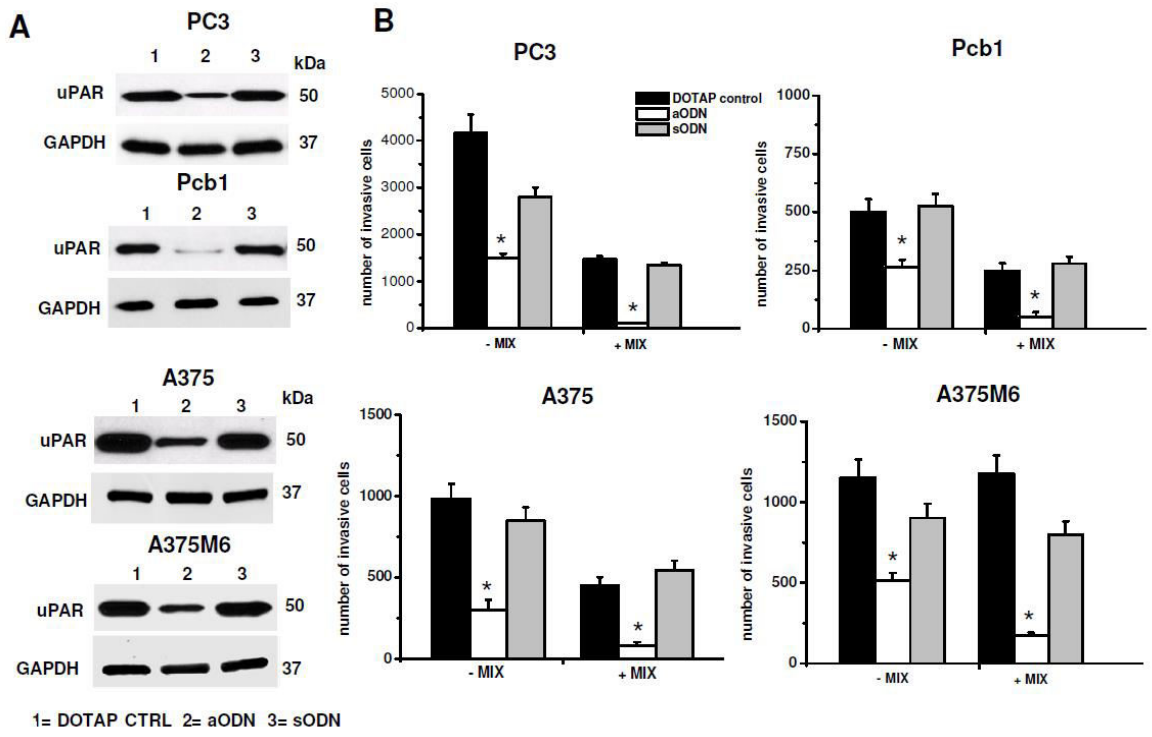

Figure 10: Effects of uPAR silencing with uPAR-aODN on invasion in mesenchymal and amoeboid conditions of prostate and melanoma cancer cells. Panel A: Western Blotting analysis of uPAR for each prostate cancer and melanoma cell line after uPAR-aODN treatment. DOTAP: treatment of cells with the cationic liposome alone; aODN: treatment of cells with DOTAP liposomes-delivered uPAR-antisense oligodeoxynucleotide; sODN: treatment of cells with DOTAP liposomes-delivered scramble oligodeoxynucleotide. Numbers on the right of each Western blotting refer to molecular weights expressed in kDa. GAPDH used as a reference loding control. Panel B: Matrigel invasion under mesenchymal (-MIX) and amoeboid (+MIX) conditions. Results are the mean of three experiments performed in triplicate on each cell line ± SD. * : $p<0.05$ with respect to controls.

Both in control and in the presence of protease inhibitors all the cell lines showed a reduced active Rac1 paralleled by an increased RhoA activation, while uPAR-aODN treatment resulted into reduced Rac1 activation either in the absence or in the presence of the inhibitor cocktail. The RhoA/Rac1 ratio in the presence of aODN and aODN + inhibitor cocktail conformed to the classical amoeboid pattern indicating a prevalence of RhoA activity in prostate cancer cell lines, while it showed smaller variations with respect to controls in melanoma cell lines (figure 11). Therefore, under amoeboid conditions and in the presence of uPAR knockdown, cancer cells still activate ameoboid-related transductions but are unable to invade 3D matrices, indicating that the loss of uPAR is detrimental for both movement styles. The residual movement observed in the absence of protease inhibitors in control cells treated with uPAR-aODN must be ascribed to proteases of different families.

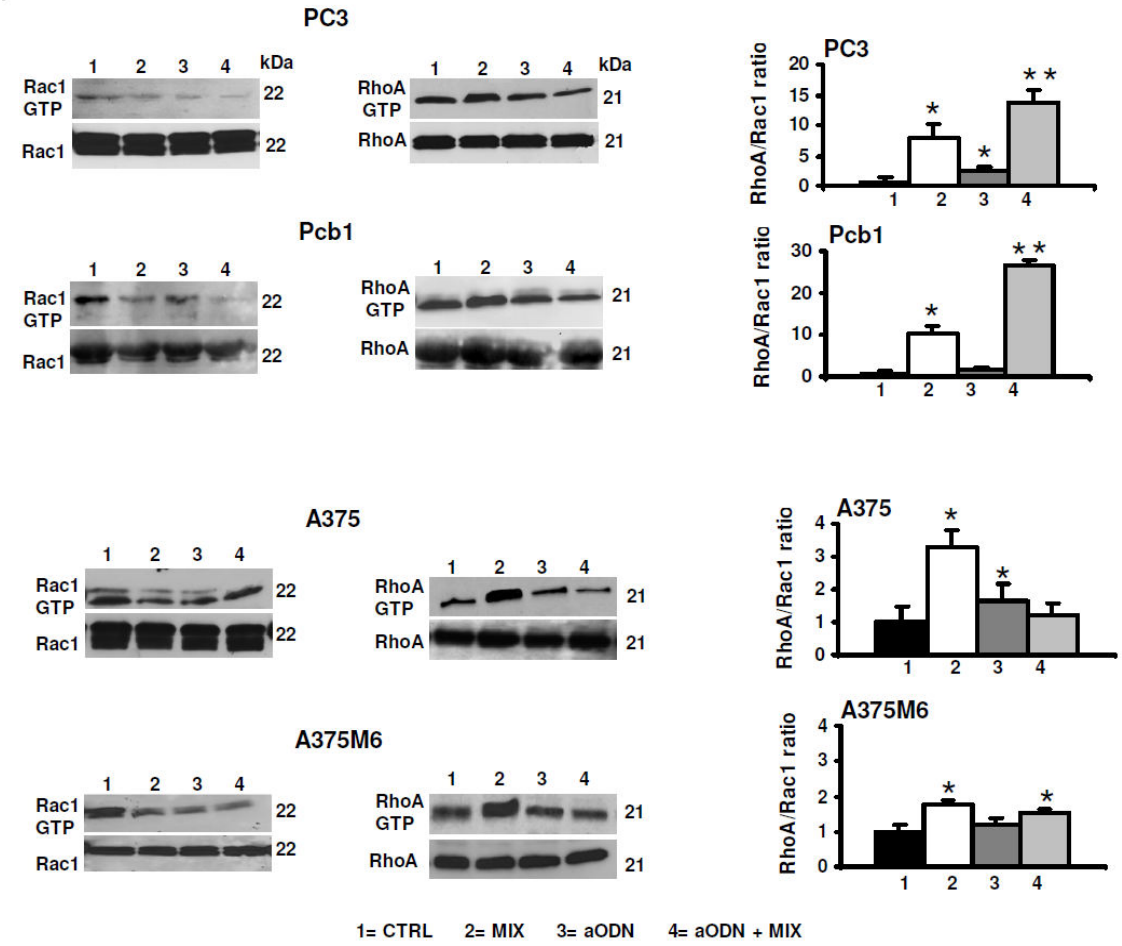

Figure 11: Effects of uPAR silencing with uPAR-aODN on i small Rho-GTPases activation in mesenchymal and amoeboid conditions of prostate and melanoma cancer cells. Western blotting of total and GTP-loaded forms of small Rho-GTPases RhoA and Rac1 under mesenchymal and amoeboid conditions for each prostate cancer and melanoma cell line, untreated and treated with aODN/sODN, respectively. Histograms report RhoA/Rac1 ratio obtained by band densitometry quantification. *: statistical significance at $p<0.05$ with respect to control; **: statistical significance at $p<0.01$ with respect to controls. Numbers on the right of each Western blotting refer to molecular weights expressed in kDa. For other symbols, refer to the legend of figure 5.

The full-length D1D2D3 form of uPAR is required to induce amoeboid migration

Native uPAR is organized in three differently folded homologous domains of about 90 amino acids each (D1, D2 and D3 from the N-terminus), stabilized by intra- molecular disulphide bonds. The X-ray structure shows that uPAR binds uPA by directly interacting with D1, in a pocket built by all three domains. These structural features suggest the necessity for cooperation of all three uPAR domains for high-affinity binding of uPA. uPAR may be anchored to the cell surface either in its native form (D1D2D3) or in a truncated form (D2D3), as a result of a cleavage of the D1-D2 linker region. The uPAR-negative human embrional kidney-293 (HEK- 293) cells transfected with cDNA of intact uPAR (uPAR-D1D2D3), with cDNAs corresponding to the truncated form of uPAR (uPAR-D2D3) and with pcDNA3 empty vector (no-uPAR) [146] were used to evaluate whether the native D1D2D3 or the cleaved D2D3 form of uPAR was involved in uPAR-dependent amoeboid movement style. The three differentially transfected cell lines were capable of invading Matrigel-coated filters, while only the uPAR-D1D2D3 cell line showed invasion capabilities upon exposure to a protease inhibitor-rich environment (figure 12).

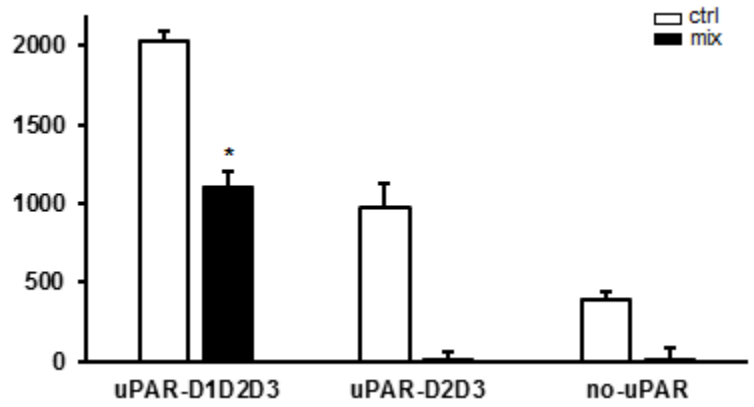

Figure 12: Migration features in HEK-293 cells transfected with intact uPAR (D1D2D3) and truncated uPAR (D2D3). Invasion of porous filters coated with a 3D Matrigel layer, showing the differential total number of invading cells/ filter under mesenchymal and amoeboid conditions, as reported in the text. +/-Mix: presence or absence of the protease inhibitor cocktail. Results are the mean of three different experiments performed in triplicate on each cell line ± SD. *: $p<0.05$ with respect to each control.

This indicates that the presence of full length uPAR is strictly required in order to shift from the mesenchymal to amoeboid movement style. Also in these cells collagenolysis was inhibited by the protease inhibitor mixture (data not shown). Experiments aimed to evaluate small GTPases Rac1 and RhoA activation showed a decrease of activated Rac1 in the presence of protease inhibitors in all the transfectants, while a significant increase of RhoA activation was observed only in uPAR-D1D2D3 cells (figure 13 A).

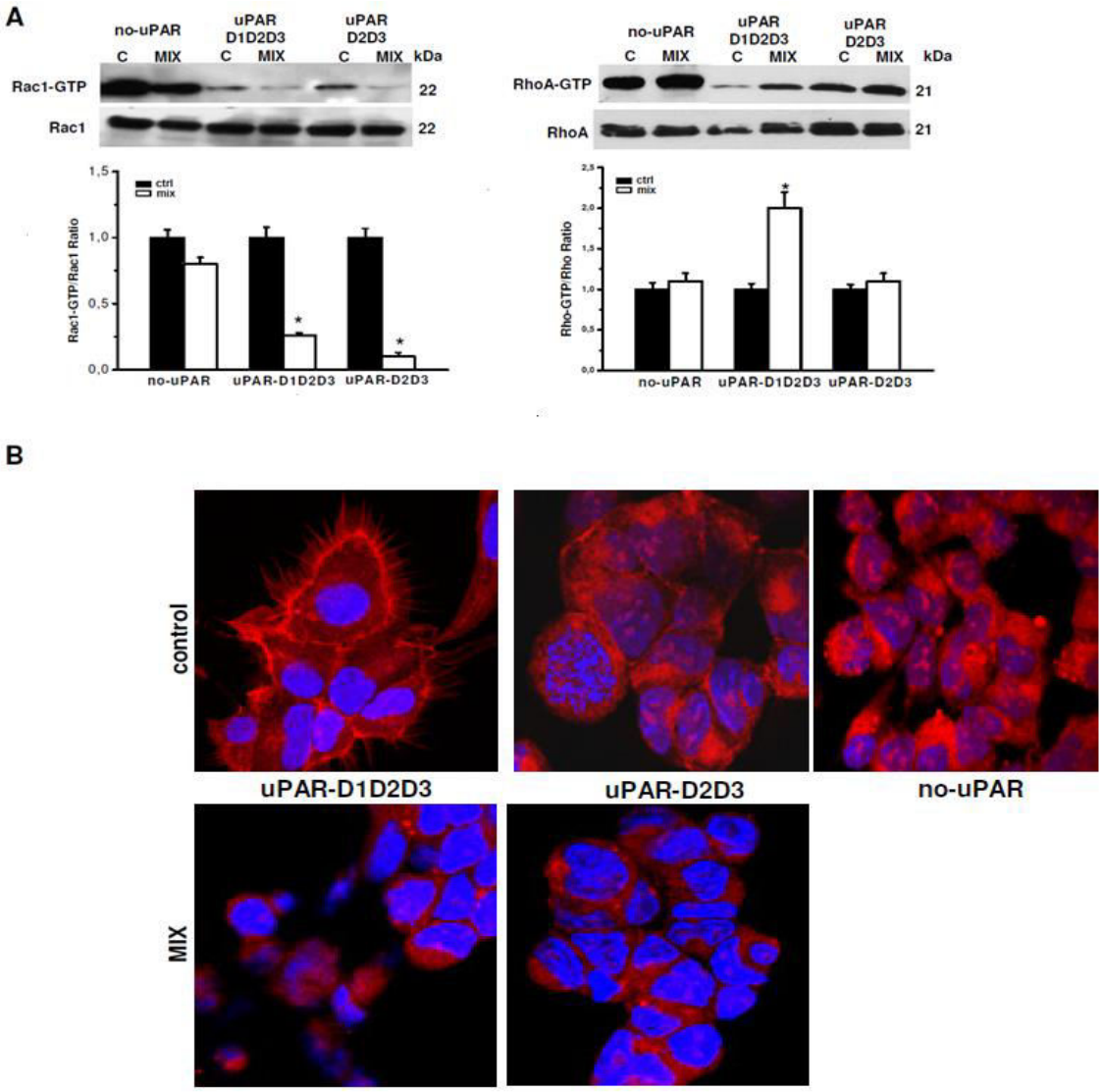

Figure 13: Mesenchymal and amoeboid features in HEK-293 cells transfected with intact uPAR (D1D2D3) and truncated uPAR (D2D3). Panel A: Western blotting of total and GTP-loaded forms of small Rho-GTPases RhoA and Rac1 under mesenchymal and amoeboid conditions for each HEK-293 transfectant. Three experiments were performed for each transfectant in each condition. Histograms report band densitometry, assuming 1 as the reference value of controls in each condition. * shows statistical significance at $p<0.05$. Panel B: Morphological features of the mesenchymal (elongated) to amoeboid (roundish) transition (MAT) of each HEK-293 transfectant. Red: phalloidin staining of the actin cytoskeleton. Blue: nuclear staining with DAPI. Magnification: 200 X. Results shown are representative of two different preparations of each cell line under mesenchymal and amoeboid conditions. No-uPAR cells did not adhere under amoeboid conditions.

Morphological study of actin assembly of the three cell lines plated on VN-enriched Matrigel-coated surfaces showed the presence of actin protrusions and an overall spindle-like morphology only in full-length uPAR-expressing cells, while an overall feature of round cells was similarly exhibited by no-uPAR and uPAR-D3D3-expressing cells, which did not show actin protrusions (figure 13 B). In a protease inhibitor-rich milieu no-uPAR cells were unable to adhere, while the totality of uPAR-D1D2D3 and uPAR-D2D3 cells assumed a round shape, lost actin filament protrusions and exhibited a rim of perinuclear cortical actin. Taken together, these data show that uPAR supports mesenchymal and amoeboid movement style only when expressed in its full-length native form.

Integrins bridge uPAR and actin cytoskeleton.

Already established uPAR-mediated pathways include uPAR association with integrins, the key molecules that promote rearrangement of the actin cytoskeleton and cell movement.10 PCb1 cells, M6 melanoma cells and the three HEK-293 clones show an integrin pattern in line with previous observations (figure 14) .

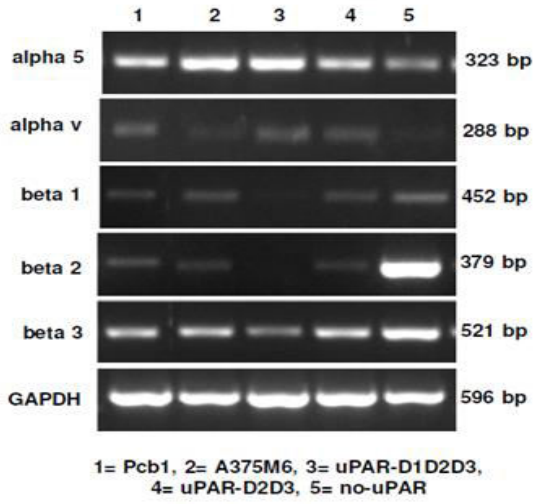

Figure 14: Integrin pattern. Semiquantitative RT-PCR of the shown integrin α and β chains in cell lines used in this study. GAPDH was used as a reference control. Product size, espressed in bp, are reported on the right.

Confocal immuno-fluorescence analysis of integrin β1 and uPAR in PCb1 and of integrin β3 and uPAR in A375M6 cells is shown in figure 15. These data show that uPAR-integrins interactions persist under both mesenchymal and amoeboid conditions. Treatment of cells with 50 μM peptide M25 for 2h at 37°C uncoupled uPAR from integrins, in the absence (data

not shown) and in the presence of the inhibitor cocktail (figure 15). In presence of scramble M25 the cells share uPAR-integrin interaction comparable to controls.

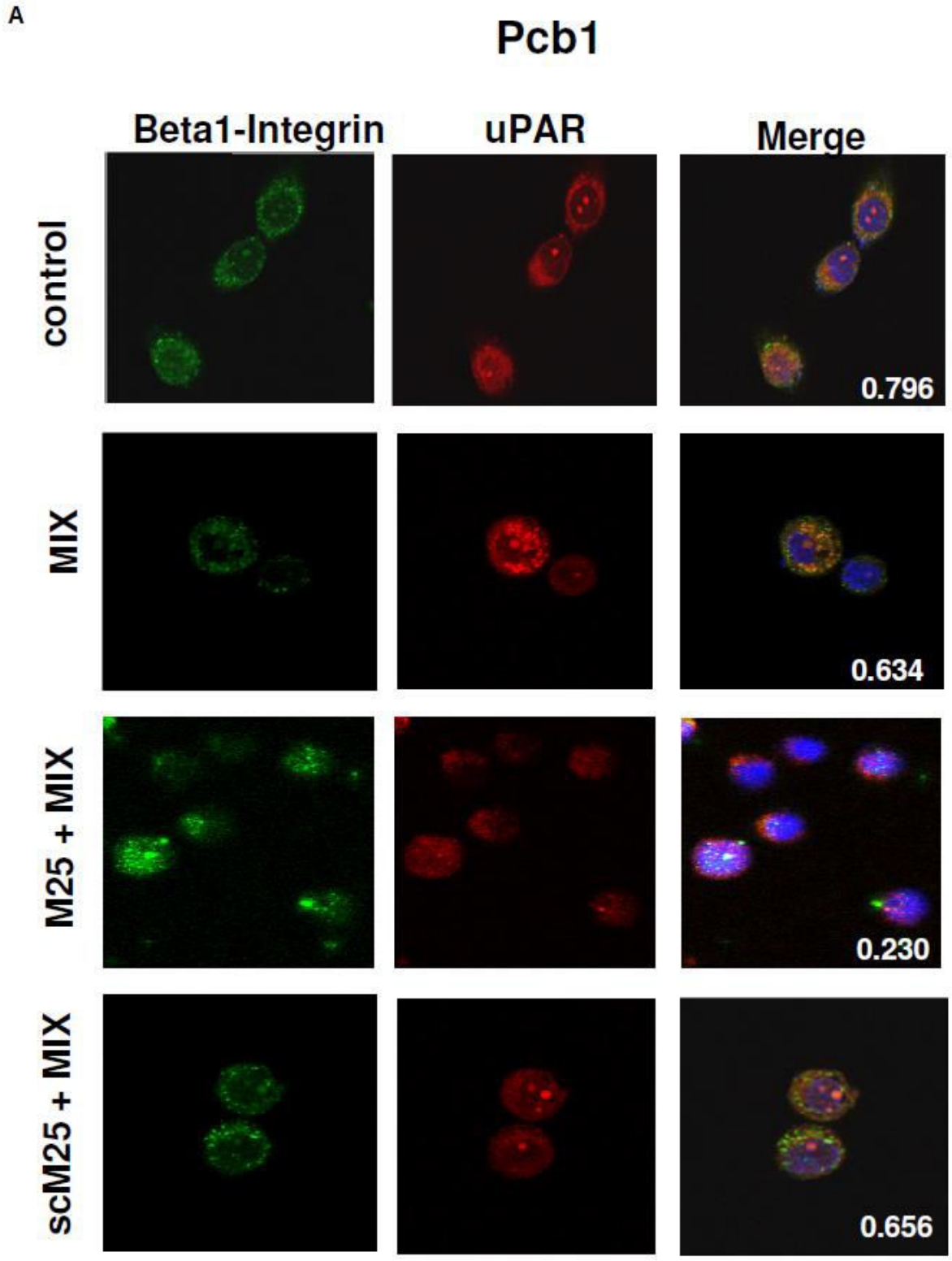

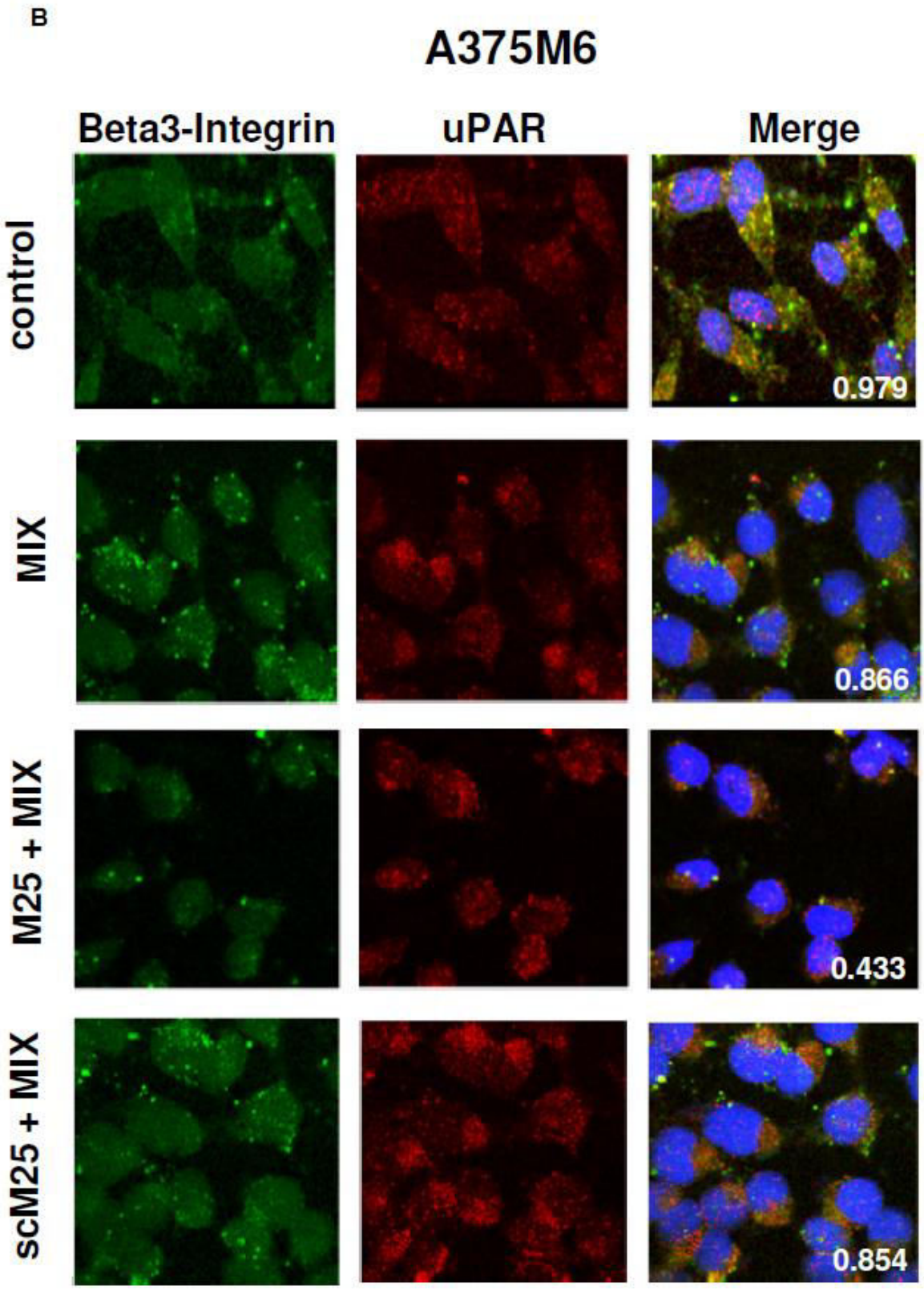

Figure 15: Integrin-upar interaction. Confocal microscopy for uPAR (red fluorescence)-β1-integrins (green fluorescence) co-localization in Pcb1 prostate carcinoma cells (panel A) and for uPAR (red fluorescence)- β3-integrins (green fluorescence) co-localization in A375M6 melanoma cells (panel B) under mesenchymal (control) and amoeboid (+MIX) conditions, in the absence and in the presence of M25 peptide and of scramble M25 peptide (sM25). Nuclear staining: DAPI (blue). The co-localization score is reported within each picture. Refer also to table 1 for a complete view of co-localization scores in all the examined cell lines. Magnification: 40 X. The shown pictures are representative of 50 different pictures for each experimental condition that were studied by Image J analysis.

Immunoprecipitation experiments with lysates of Pcb1 and A375M6 cells demonstrated the activity of M25 peptide in uncoupling uPAR-integrin β1 or β3 interaction (figure 16). The statistical analysis of uPAR-integrin co-localization for the cell lines considered in this study is reported in table 3.

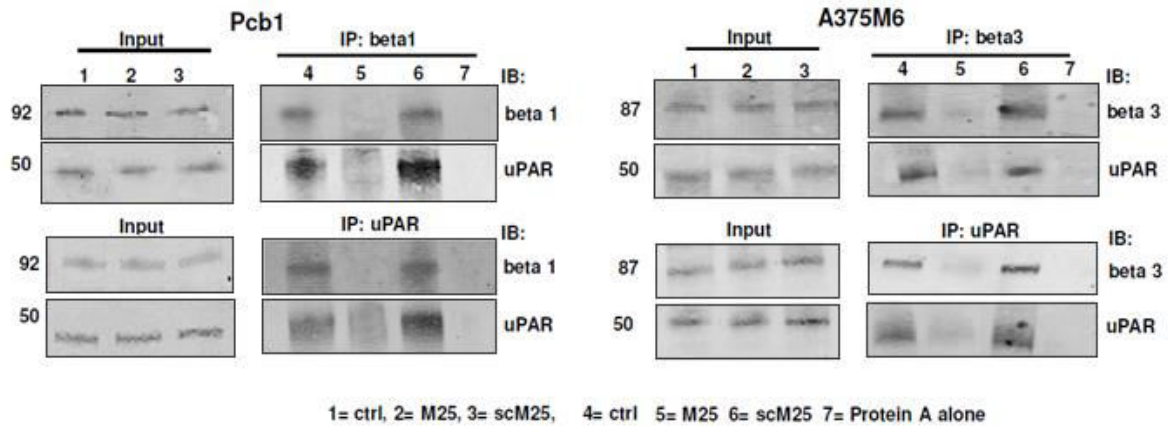

Figure 16: Integrin-uPAR interaction. Immunoprecipitation of uPAR and β1-integrins in Pcb1 prostate carcinoma cells and of uPAR and β3-integrins in A375M6 melanoma cells. Input: Western blotting of aliquots of cell lysates before immunoprecipitation, used as a reference loading control. IP beta 1: immunoprecipitate obtained with anti-beta 1 antibodies; IB beta 1: immunoblotting with anti-beta 1 antibodies; IP beta 3: immunoprecipitate obtained with anti-beta 3 antibodies; IB beta 3: immunoblotting with anti-beta 3 antibodies; IB uPAR: immunoblotting with anti-uPAR antibody; IP uPAR: immunoprecipitate obtained with anti-uPAR antibodies. Molecular weights, expressed in kDa, are reported on the left.

Parallel experiments aimed to evaluate uPAR-actin and integrins-actin colocalization showed that both uPAR and integrins co-localize with actin also in amoeboid conditions, where the thick ring of cortical actin/uPAR and cortical actin/integrin overlap (figure 17A). The use of peptide M25 uncoupled all the observed co-localizations (uPAR, integrins, actin) and produced structural alteration of actin which lost the stress fibres organization and acquired a granular feature under both mesenchymal and amoeboid conditions (figure 17B). The statistical analysis of uPAR-actin and integrin-actin co-localization for all the cell lines is reported in table 3

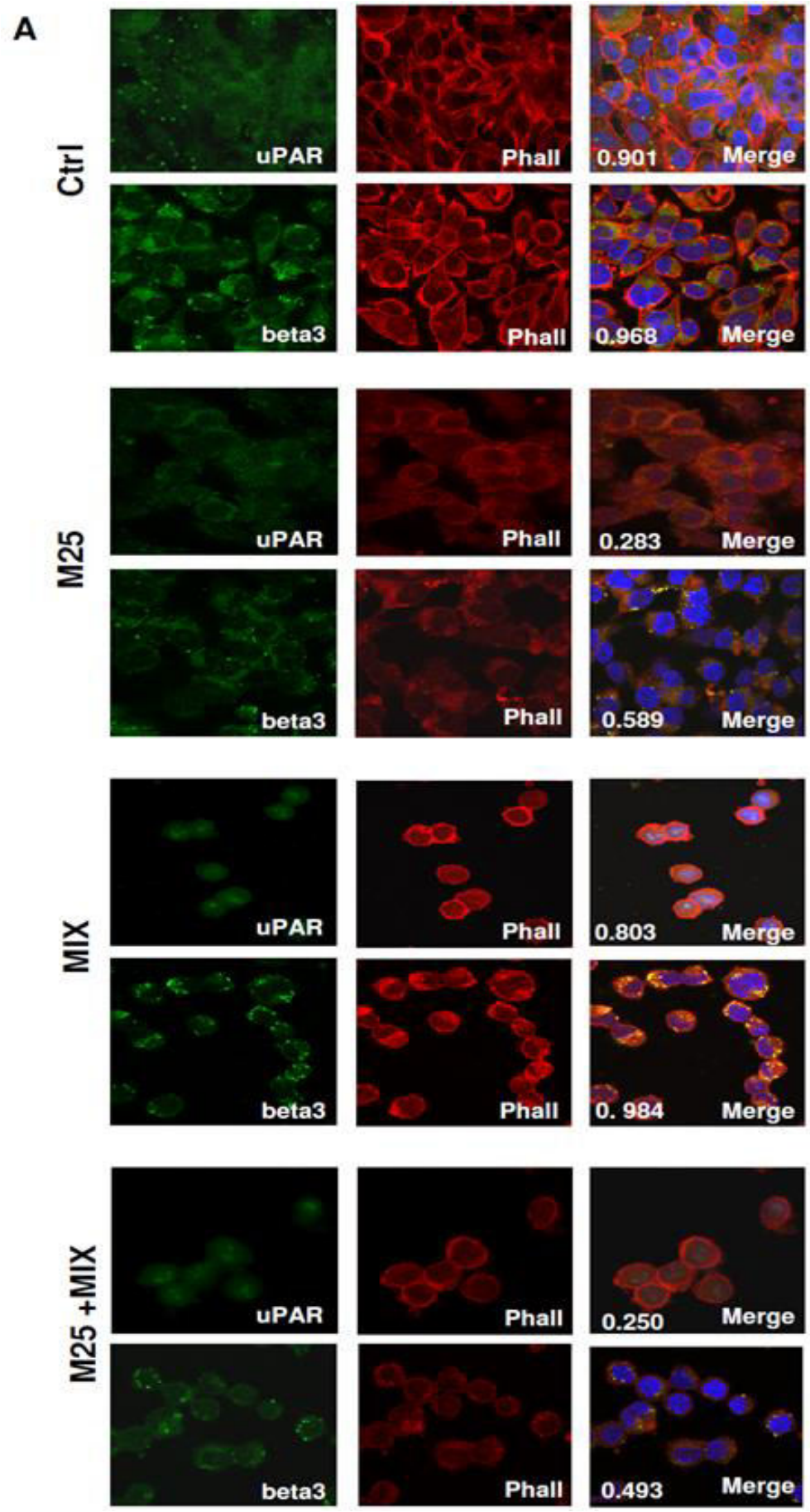
A
Ctrl
uPAR
Phall
0.901
Merge
beta3
Phall
0.968
Merge
M25
uPAR
Phall
0.283
Merge
beta3
Phall
0.589
Merge
MIX
uPAR
Phall
0.803
Merge
beta3
Phall
0. 984
Merge
M25 +MIX
uPAR
Phall
0.250
Merge
beta3
Phall
0.493
Merge

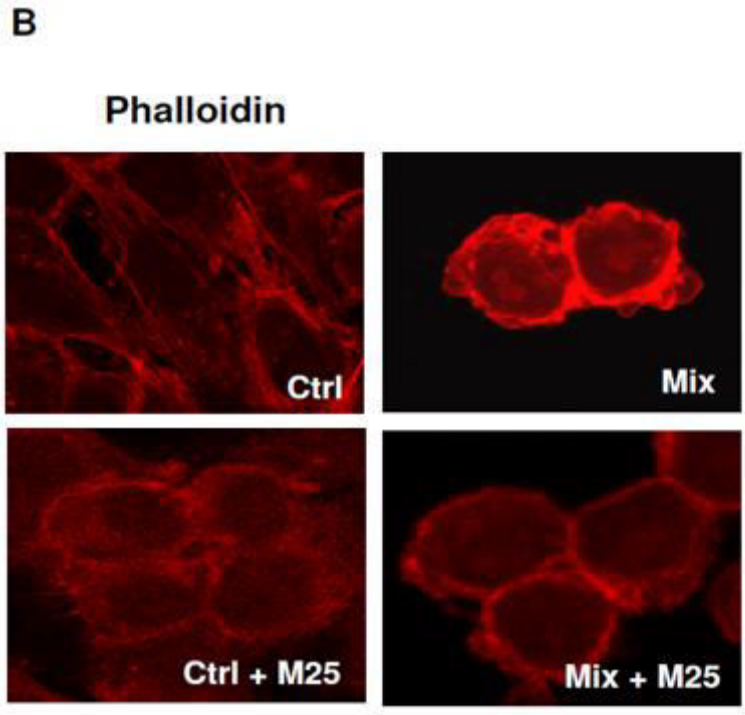

Figure 17: uPAR-actin co-localization. Panel A: confocal microscopy for uPAR (green fluorescence) and falloidin (red fluorescence), in A375-M6 melanoma cells under mesenchymal (control) and amoeboid (+MIX) conditions, in the absence of M25 peptide, and in the presence of M25 peptide or of its scramble counterpart (sM25). The co-localization score is reported within each figure, as well as in table 1. Nuclear staining: DAPI (blue). Magnification: 40 X. The shown pictures are representative of 50 different pictures for each experimental condition that were studied by Image J analysis, as reported in the legend to table 1. Panel B: Magnification (200 X) of selected sections of panel A to show actin cytoskeleton (revealed by red falloidin staining) derangement as an effect of M25 peptide treatment.

Antibody	Cells line & treatment	Colocalization coefficient (M2)
Anti-uPAR+Phalloidin	M6 ctrl	0,901
Anti-uPAR+Phalloidin	M6 + M25	0,283
Anti-uPAR+Phalloidin	M6 + mix	0,803
Anti-uPAR+Phalloidin	M6 + M25 + mix	0,250
Anti-uPAR+Phalloidin	Pcb1 ctrl	0,853
Anti-uPAR+Phalloidin	Pcb1 + M25	0,265
Anti-uPAR+Phalloidin	Pcb1 + mix	0,745
Anti-uPAR+Phalloidin	Pcb1 + M25 + mix	0,293
Anti-uPAR+Anti-Integrin β3	M6 ctrl	0,798
Anti-uPAR+Anti-Integrin β3	M6 + mix	0,713
Anti-uPAR+Anti-Integrin β1	Pcb1 ctrl	0,848
Anti-uPAR+Anti-Integrin β1	Pcb1 + mix	0,732
Anti-uPAR+Anti-Integrin β3	M6 ctrl	0,979
Anti-uPAR+Anti-Integrin β3	M6 + M25	0,542
Anti-uPAR+Anti-Integrin β3	M6 + mix	0,866
Anti-uPAR+Anti-Integrin β3	M6 + M25 + mix	0,433
Anti-uPAR+Anti-Integrin β1	Pcb1 ctrl	0,796
Anti-uPAR+Anti-Integrin β1	Pcb1 + M25	0,152
Anti-uPAR+Anti-Integrin β1	Pcb1 + mix	0,634
Anti-uPAR+Anti-Integrin β1	Pcb1 + M25 + mix	0,230
Anti-uPAR+Phalloidin	HEK uPAR 293	0,771
Anti-uPAR+Phalloidin	HEK uPAR 293 + mix	0,893
Anti-uPAR+Anti-Integrin β1	HEK uPAR 293	0,731
Anti-uPAR+Anti-Integrin β1	HEK uPAR 293 + mix	0,762
Anti-Integrin β3+Phalloidin	M6 ctrl	0,968
Anti-Integrin β3+Phalloidin	M6 + M25	0,589
Anti-Integrin β3+Phalloidin	M6 + mix	0,984
Anti-Integrin β3+Phalloidin	M6 + M25 + mix	0,493

M25 concentration = 50uM

Table 3. Colocalization analysis. M25 concentration is 50 µM.

Activity of the M25 peptide on mesenchymal and amoeboid migration styles and related transductions.

On the basis of these results we reasoned that the property of M25 peptide to uncouple uPAR from integrins, and hence from actin under both mesenchymal and amoeboid conditions, could produce functional effects similar to those obtained with uPAR aODN on mesenchymal and amoeboid migration styles. Therefore we studied Matrigel invasion and Rac-1/RhoA modulation under each relevant experimental condition. Similarly to genetic uPAR knockdown, results of Matrigel invasion obtained on PCb1, A375 M6 and Hek-293 cells clearly show that M25 peptide exerts a very intense inhibition of the amoeboid movement of cells treated with the inhibitor cocktail and partially inhibits the movement of control cells that move with a pre-specified mesenchymal migration style (figure 18).

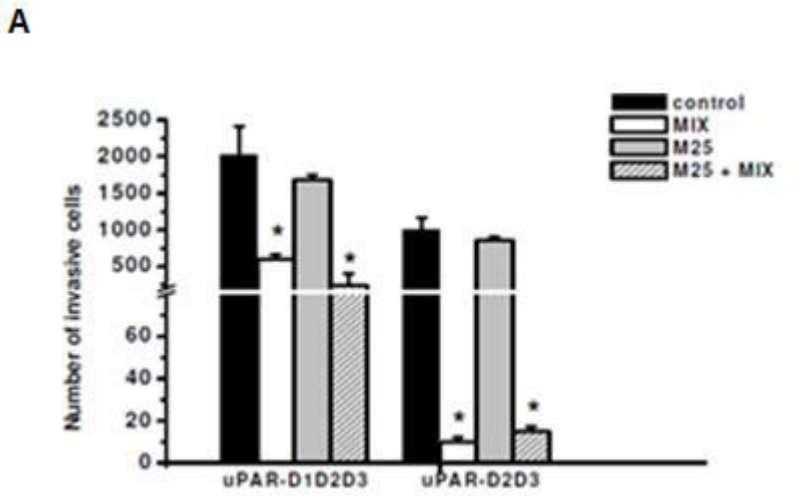

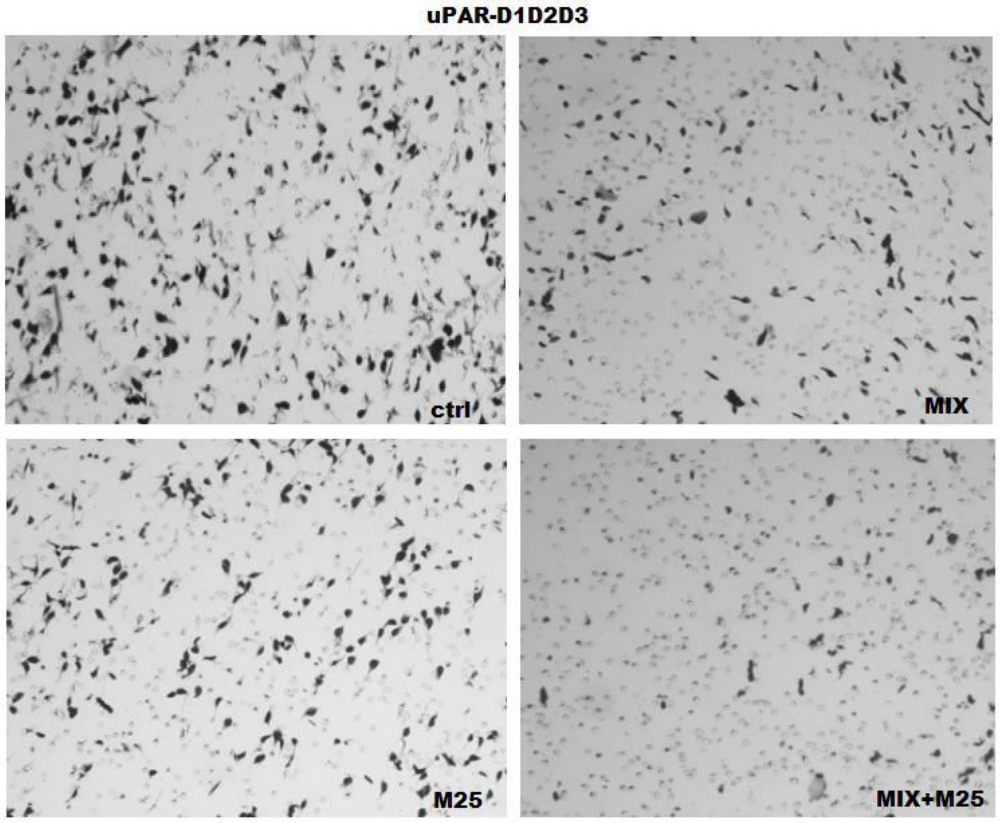
uPAR-D1D2D3
ctrl
MIX
M25
MIX+M25

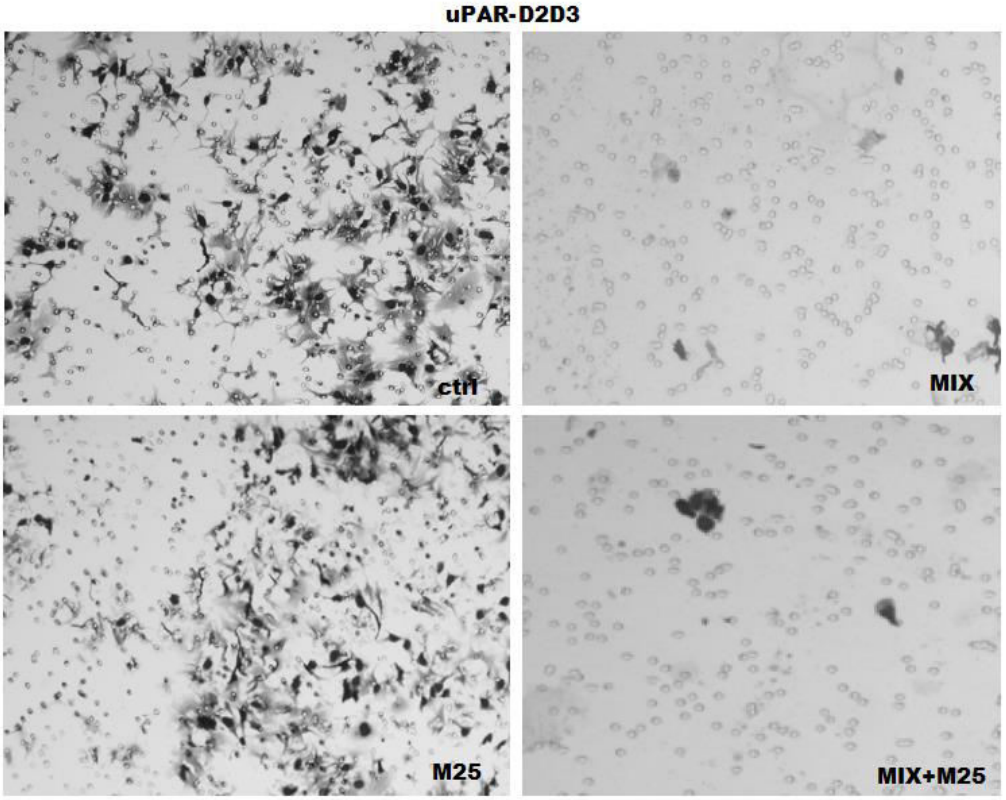
uPAR-D2D3
ctrl
MIX
M25
MIX+M25

B

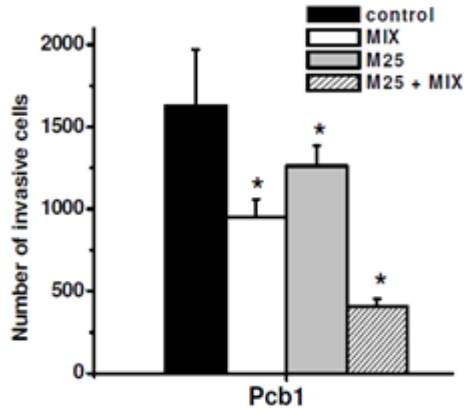
control
MIX
M25
M25 + MIX
Number of invasive cells
2000
1500
1000
500
0
*
*
*
Pcb1

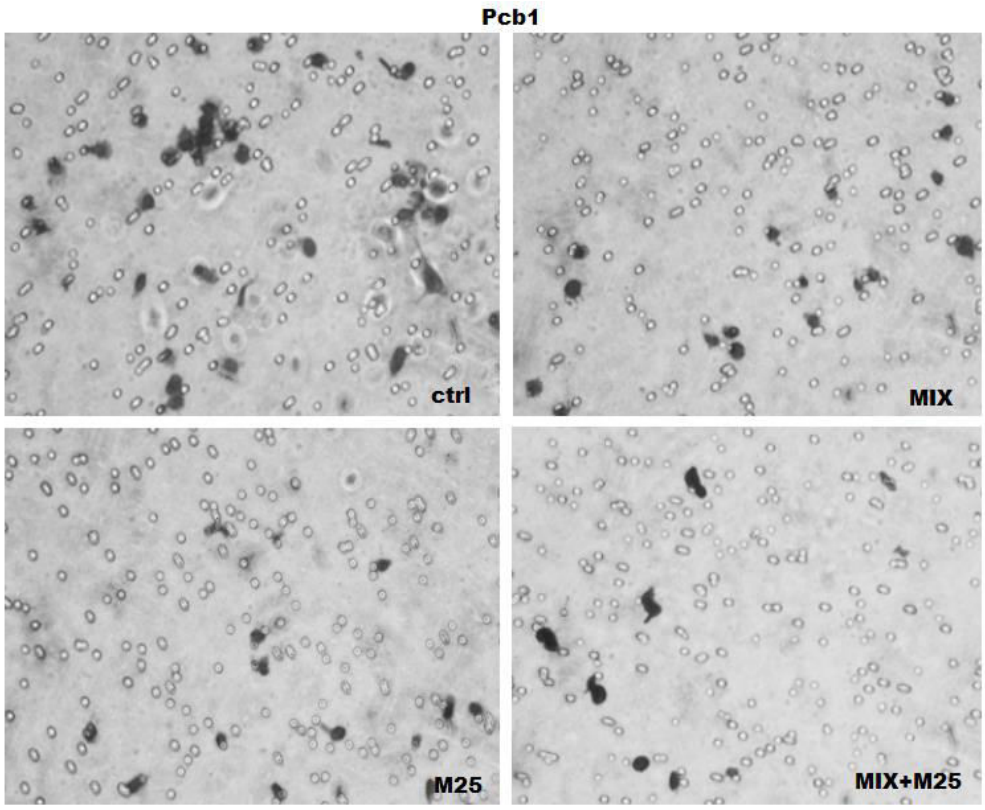
Pcb1
ctrl
MIX
M25
MIX+M25

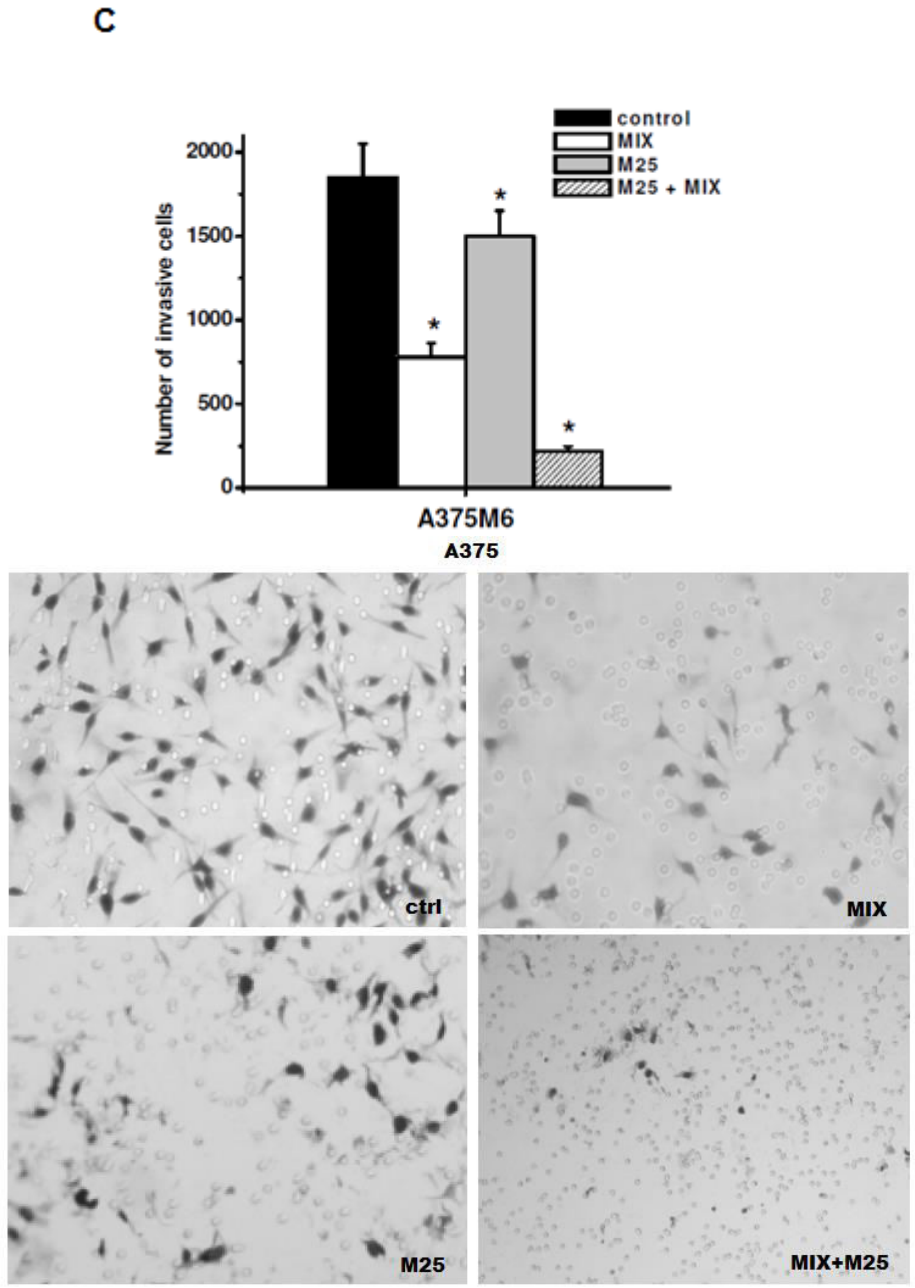

Figure 18: M25 treatment effect on invasivity. Invasion of porous filters coated with a 3D Matrigel layer, by HEK-293 transfectants (panel A), Pcb1 (panel B) and M6 cells (panel C) under amoeboid and mesenchymal conditions, in the absence and in the presence of M25 peptide. Results are the mean of three different experiments performed in triplicate on each cell line ± SD. *: $p<0.05$. The pictures show the typical appearance of filters in each experimental condition.

Results obtained on small Rho-GTPases show that the shift from mesenchymal to amoeboid movement increases the RhoA/Rac1 ratio, even in the presence of M25 peptide (figure 19), but such a Rho over-activation does not support amoeboid movement owing to the M25-dependent weakening of actin cytoskeleton-integrins-uPAR functional axis. Overall, the phenotypic effects obtained with the M25 peptide are similar to those obtained with uPAR-aODNs, allowing us to conclude that uPAR regulates plasticity of cell movement in both the

mesenchymal and amoeboid migration styles by an integrin-mediated coupling of the cell membrane to the actin cytoskeleton.

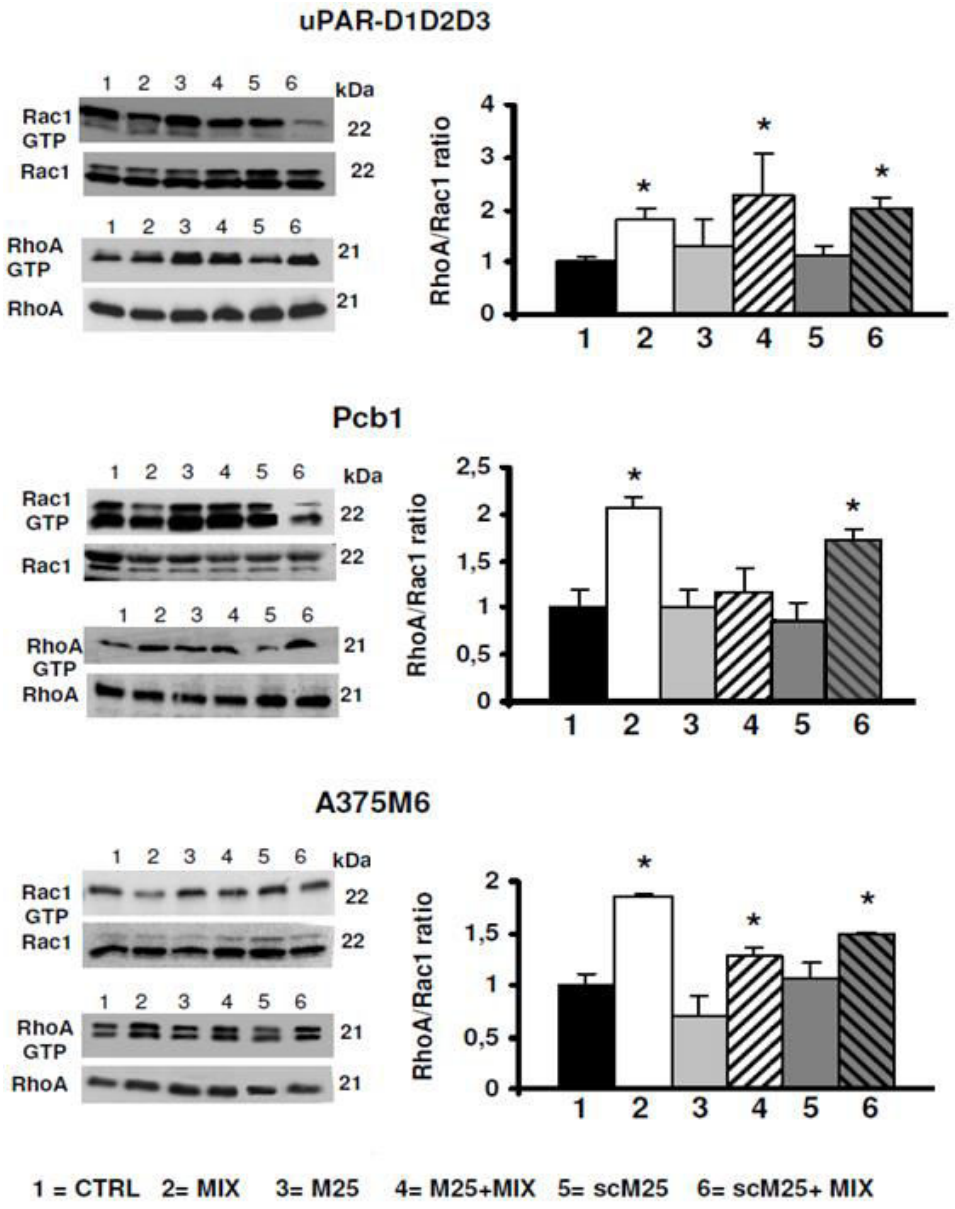

Figure 19: Biochemical effects of M25 treatment. Western blotting of total and GTP-loaded forms of small Rho-GTPases Rac1 and RhoA under mesenchymal and amoeboid conditionsconditions ± M25 peptide for each prostate cancer and melanoma cell line. Three experiments were performed for each cell line in different conditions. Histograms report RhoA/Rac1 ratio obtained by band densitometry quantification and * shows statistical significance at $p<0.05$. Numbers on the right of each Western blotting refer to molecular weights expressed in kDa.

Evaluation of protease inibitors toxicity in EPC

In the end we evaluated the amoeboid phenotype of EPC since they are recruited in the tumoral microenvironment to form new blood vessels to provide nutrients to the cancer. To re-create a condition most similar to tumoral microenvironment we tested a physiological protease inhibitor cocktail. In order to compare the effects of the physiological protease inhibitor mixture with the former chemical mix, we performed WST1 (data not shown) Trypan Blue viability assay (figure 20). Taking in to account of the toxicity of chemical mixture, we performed the following EPC experiments with the physiologic mix.

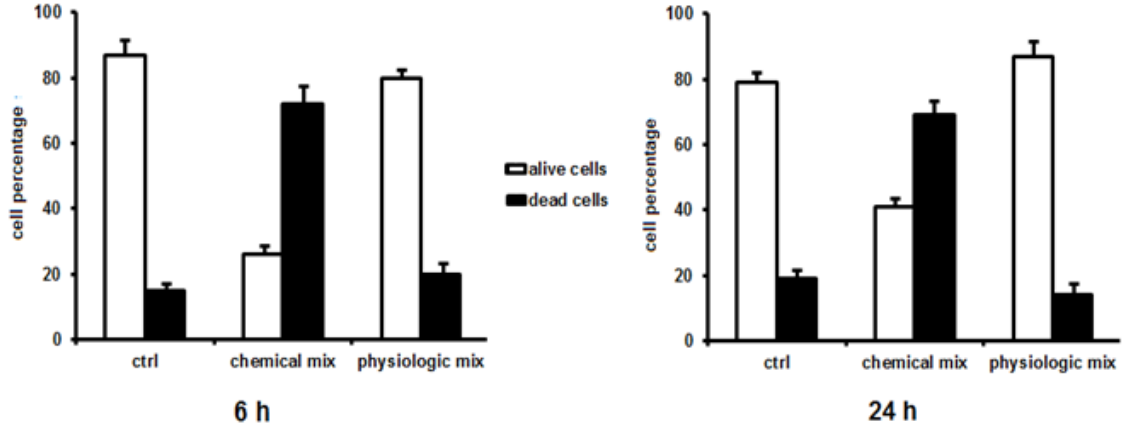

Figure 20: Trypan Blue viability assay. In histograms are reported the results of Trypan blue exclusion test to assess the cell viability. A viable cell have a clear cytoplasm whereas a nonviable cell have a blue cytoplasm. The percentage was obtained from cell counts using Burker chamber. We have choosen to test the physiological protease inhibitor mix at 6 and 24 hours because they are respectively the invasivity assay and morphogenesis endpoint.

Evaluation of angiogenetic properties of EPC *in vitro*

After isolation and cytofluorimetric characterization, we have evaluated EPC angiogenetic properties using capillary morphogenesis. Treated with physiological mix EPC M2 clone maintained their angiogenetic capability (figure 21).

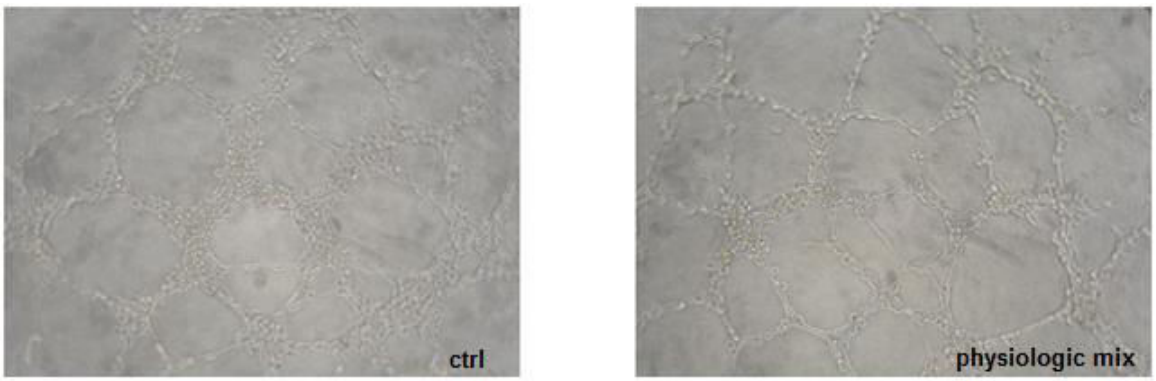

Figure 21: Capillary morphogenesis. Evaluation of capability to form capillary-like tubes in vitro, measuring the percentage of the photographic field occupied by cells engaged in capillary-like cord formation by image analysis.. Panel A: control EPC, Panel B: EPCs treated with physiologic protease inhibitor mix.

Induction of amoeboid phenotype in EPC

Matrigel invasion, and cell morphology. To evaluate whether exposure to a protease inhibitor cocktail induced a protease-independent invasion, we subjected EPcells to a Boyden chamber migration assay through a thick Matrigel coating, in the presence of the physiologic inhibitor cocktail added to Matrigel solution before polymerization. As shown in figure 22, where we have reported invasivity assay histogram, the physiologic mix increases the number of invasive cells. To prove the proteases inhibition we have carried out collagen degradation assay, where the cells are plunged in FITC-labelled collagene. When proteases degrades FITC-collagene, it gives off fluorescence (more flourescence = more proteases activity). We observed that in the presence of the mix fluorescence percentage is drastically reduced compared to control (figure 23). These data suggest that invasive EPCs use amoeboid migration in 3D Matrigel matrices.

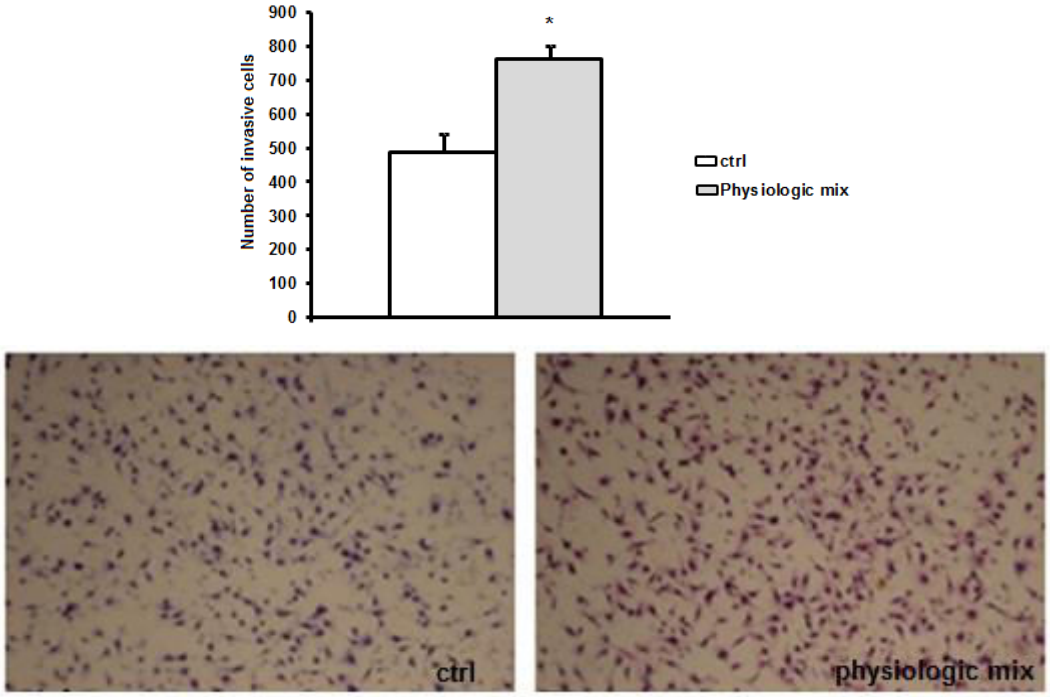

Figure 22: Invasivity assay after physiological protease inhibitors treatment. EPCs invasion performed by Boyden chambers method, it has been expressed as number of cells which cross the filter. Physiologic mix: presence of the protease inhibitor cocktail. Results are the mean of five different experiments performed in triplicate on each cell line ± SD. * : $p<0.05$.

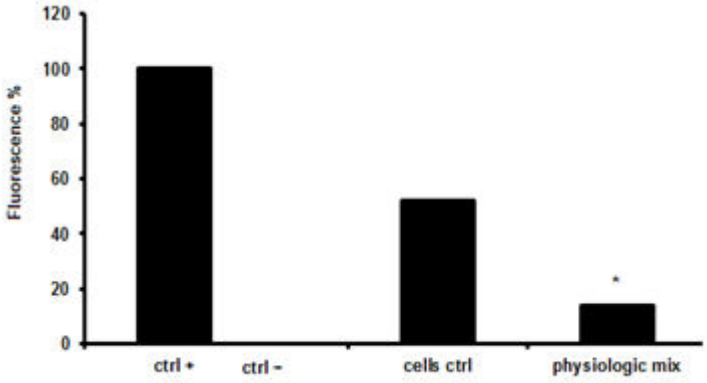

Figure 23: Collagene degradation assay. The histogram shows the collagenolitic activity of EPCs under mesenchymal and amoeboid conditions, expressed as % collagen degradation with respect to the positive control obtained by addition of exogenous collagenase. Ctrl-: collagenolytic activity in the absence of cells and in the presence of exogenous collagen; Ctrl+: collagenolytic activity in the absence of cells but in the presence collagenase 1mg/ml; cells ctlr: control EPCs in the presence of exogenous collagen; physiologic mix: EPCs trated with protease inhibitor cocktail in the presence of exogenous collagen.

Also in this section of the project we characterized the motility shift by mesuring the activation level of small GPTases RhoA and Rac1. From western blotting experiments we have seen that EPCs treated with physiologic protease inhibitor cocktail express decreased activated Rac1 and an increased activated RhoA (figure 24).

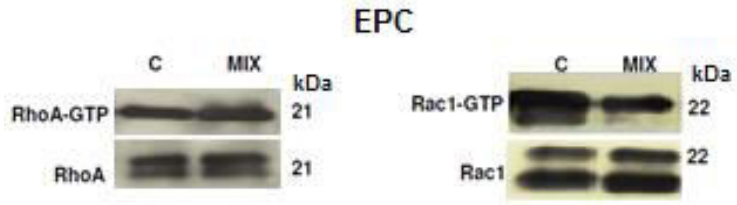

Figure 24: Biochemical features evaluation of the amoeboid movement in prostate cancer and melanoma cells. Western blotting of total and GTP-loaded forms of small Rho-GTPases RhoA and Rac1 under mesenchymal and amoeboid conditions for EPCs.

We performed a morphological analysis of EPCs compared with the respective control. Figure 25 shows that physiological inhibitors combination induces a change in the morphology of EPCs including the loss of stress fibers, clearly visible in cells undergoing mesenchymal migration.

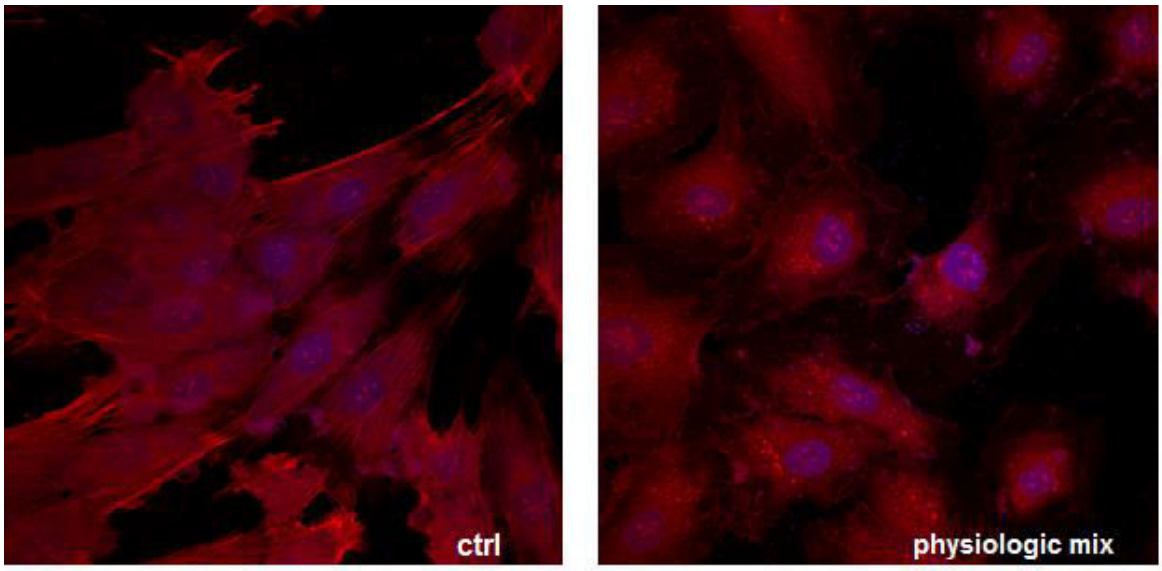

Figure 25: Morphological features of the mesenchymal to amoeboid transition (MAT) of EPCs. Each picture shows the general pattern of a small field for both control and treated cells. Red: phalloidin staining of the actin cytoskeleton. Blue: nuclear staining with DAPI. Magnification 40 X for reference pictures and 100 X for enlarged insets. Results shown are representative of two different preparations under mesenchymal and amoeboid conditions.

CHAPTER 5:
DISCUSSION

A ten years analysis of the prospective multicentre Chemo-N0 (node negative) trial has identified the uPA/ uPAR system as the only level-of-evidence-1 cancer biomarker system for prognosis and/or prediction in node-negative breast cancer [31]. uPAR contributes to multiple features of the malignant character, including high metastatic potential [32], angiogenesis [33], epithelial-to-mesenchymal-transition (EMT) [34] and cancer cell stemness [35]. Our data show that uPAR has a role in sustaining both mesenchymal and amoeboid migration style of cancer cells by controlling the state of the actin cytoskeleton assembly via its integrin-mediated interaction with cytoskeleton.

Far-off and recent studies have underlined the key role of multiple proteases and their receptors in mesenchymal migration style of cancer cell during the invasion process so that the property of cancer cells to proteolytically degrade anatomical barriers has attained the role of a marker of cancer cell malignancy. Amoeboid motility has been originally described in the amoeba *Dictyostelium discoideum*, but it is also exploited by eukaryotic cells under particular environmental cues, such as the need to rapidly slide through lose interstitial tissues with gaps that accommodate the cell body using flexible and weak adhesion sites, producing a movement that depends on dynamic cytoplasmic protrusions due to intracellular compartmentalization of cytoplasm between an intact cortical actin cytoskeleton and the locally expanded cell membrane (blebs). Pioneer studies enlightened the possibility of cancer cells to move within tissues according to amoeboid features, leading to the so-called “cortical expansion model for amoeboid chemotaxis” of malignant cells [39]. Cancer cell amoeboid motility has now become an issue, accounting for rapid movement of invading cells within the primary and the metastatic site.

Herein we have shown that malignant cells derived from human melanoma and prostate cancer exhibit a uPAR-dependent mesenchymal invasion across a 3D Matrigel substrate, that is proportional to uPAR expression and that may be strongly reduced by preventing uPAR interaction with its ligand uPA. We confirm the main role of uPAR in mesenchymal migration also in human embrional kidney 293 cells (HEK-293) transfected with the full-length form (D1D2D3) of the human uPAR. We observed a residual mesenchymal Matrigel invasion that could be surely ascribable to the activity of multiple proteases. Our results indicate that the uPAR-driven proteolytic activity accounts for more than 50% of single migrating cells in all the studied cancer cell lines. The residual cell invasion has to be related to many other proteases such as members of the MMP and cathepsin families. Due to the high number of involved molecules it was not possible to use blocking antibodies, while the use of

specific protease inhibitors could induce the shift to an amoeboid movement style. The same cells shifted toward an amoeboid migration style (MAT) upon exposure to a protease inhibitor cocktail. Our observation that not the whole cancer cell populations undergo MAT and that the percentage of shifting cells varies among the different cell lines independently of their origin (primary tumor or metastasis) indicates that this feature is independent of cancer progression. Also small Rho-GTPases activation and cell morphology were consistent with MAT. Although under mesenchymal conditions not all the studied cell lines showed an unambiguously elongated cell shape, the acquisition of amoeboid features in the presence of the inhibitor cocktail, such as the attainment of a round shape and reorganization of actin according to a strictly sub-cortical location were evident.

The results obtained with uPAR-aODN on mesenchymal and amoeboid movement clearly show uPAR requirement in both styles of cancer cell migration. Moreover, the data obtained with HEK-293 cells transfected with the truncated or with the native form of uPAR show that only the full-length form supports amoeboid movement. Many proteases cleave the receptor (cleaved uPAR, c-uPAR) [40]. c-uPAR, devoid of D1, is unable to bind extracellular uPAR ligands, uPA and VN, as well as to interact with integrins, indicating that uPAR cleavage is a mechanism that negatively regulates uPAR activities associated with a migratory and invasive phenotype: in fact the full-length uPAR and uPA are up-regulated and are negative prognostic factors in several tumors [31]. In order to elucidate the mechanism whereby native uPAR regulates amoeboid movement, we decided to explore the in-ward uPAR activities by studying its property to regulate the actin cytoskeleton [92,26,41]. Interaction of uPAR with integrins is the foundation stone of the cell migration signalosome [116]. In our cancer cells we have confirmed uPAR interaction with β1 and β3 integrins by confocal microscopy and immunoprecipitation, showing that such interactions are present under both mesenchymal and amoeboid conditions. Integrins, which lack actin-binding domains, are indirectly connected to the actin cytoskeleton through different protein complexes that contain over a hundred different types of proteins, talin, α-actinin, filamin, tensin, parvin and myosin-X being the most studied, that transmit the mechanical force from the cell membrane to the actin cytoskeleton for cytoplasm contraction during cell movement [139]. We have shown herein that uPAR co-localizes with actin cytoskeleton in all the examined conditions, including the amoeboid one, where the thick ring of cortical actin and uPAR overlap. In the β-propeller model of α-chain folding, the sequence of the M25 peptide spans an exposed loop on the uPAR-binding surface of α-chain, thus impairing integrin-uPAR interaction [143]. M25 peptide not only uncoupled uPAR from integrins in all the cells and experimental conditions

studied in this work, but it also produced a structural alteration of actin which lost the stress fibres and cortical organization under the mesenchymal and amoeboid conditions, and acquired a granular feature. It is therefore evident that M25 peptide uncouples uPAR from integrins, and hence from actin, thereby producing functional effects similar to those obtained with uPAR aODN on mesenchymal and amoeboid migration styles. The final effects of both treatments, that lead to an alteration of actin assembly, which is no longer efficiently bound to integrins modified by the loss of interaction with uPAR, result into a weakening of actin-membrane coupling and in the loss of the tensile force that determines translocations of the cell body [139]. Actin disorganization impaired both mesenchymal and amoeboid migration of cancer cells. Also the activity of small Rho- GTPases was deranged by the use of M25 peptide as well as by uPAR-aODN, thus partially inhibiting mesenchymal migration and totally inhibiting the amoeboid one. As the M25 peptide is specific for inhibition of uPAR-integrin α-chain interaction, its limited effects on mesenchymal migration may be accounted for by the failure of the peptide to inhibit integrin-MMPs interactions that also regulate mesenchymal motility [144,145].

Available data indicate that a successful strategy to combat invasion and metastatic diffusion of aggressive cancer cells is the identification of molecular targets that control the ability of cancer cells to adapt to the environment by regulating plasticity of cancer cells. Taken together, the results obtained in the present study show that uPAR, a recognized marker of cancer cell progression is a molecular mediator of plasticity in cancer cell motility by regulating contractile forces in tumor cell migration through the functional axis uPAR-integrins-actin. Together with the many so far reported pro-tumoral activities of uPAR, our observations make the uPA/uPAR system an attractive target for the treatment of cancer that has not yet been extensively explored in the clinic.

To better understand the molecular mechanisms of amoeboid migration during angiogenesis, we have decided to study the amoeboid angiogenesis, as a possible form of EPC migration to cancer to form new blood vessels EPCs are recruited into circulation in response to growth factors secreted from tumors, such as VEGF, that promote mobilization of endothelial cells to sites of vasculogenesis.

Endothelial cells contribute at least in two ways to tumor progression: first, recruitment of EPCs stimulates the sprouting of new tumor blood vessels to feed primary growth; second, changes in the structure of the existing vascular endothelium create an escape route for cancer cells to generate distant metastases. Furthermore, to allow successful metastases in distant organs, cancer cells interact with endothelial cells activating trans-endothelial migration

(TEM). This process resembles the leukocyte extravasation during the inflammatory response where the activated endothelium supports adhesion and diapedesis of the leukocyte through the vasculature.

In this section of the study, after demonstration of EPC angiogenesis properties, we tested on this cell line the toxicity of protease inhibitor mixtures used to prevent mesenchymal movement.

The results obtained showed that EPCs are critically susceptible to chemical mix, but this effect has not been observed after treatment with physiological protease inhibitor mixture.

After invasion assay we have shown that the number of invasive EPCs, in presence of physiologic mix increases respect to the control. Furthermore, we confirm the mesenchymal migration inhibition using a collagenolysis assay, where the treated EPCs with inhibitor mix showed a reduced collagenolytic activity respect to the control.

From GTPase assays on EPCs, it is emerged that in protease inhibitors-treated EPCs RhoA activation level increases and Rac1 activation level decreases respect to control. This result allows us to confirm that EPCs are able to perform amoeboid migration.

Furthermore this fact has been confirmed by confocal morphologic analysis, where we observed that treated EPCs have a reduced cytoplasm and loose stress fibers, typical of mesenchymal movement.

The future prospectives of this project is to investigate the role of uPAR during MAT by controlling the receptor expression and to perform in vivo assays to study the effects of control EPCs, amoeboid EPCs and uPAR-silenced EPCs on human melanoma development and metastasis.

CHAPTER 6:
REFERENCES

1. Yokota j, Tumor progression and metastasis, Carcinogenesis, 2000 Mar;21(3):497-503. Review.
2. Ishimaru G, Ookawa K, Yamaguchi N, Sakamoto M, Hirohashi S, Muto T, Yokota J. Allelic losses associated with the metastatic potential of colorectal-carcinoma. Int J Oncol. 1994 Aug;5(2):267-73.
3. Thorstensen L, Qvist H, Nesland JM, Giercksky KE, Lothe RA. Allelotype profiles of local recurrences and distant metastases from colorectal-cancer patients. Int J Cancer. 1996 Dec 20;69(6):452-6.
4. Kerbel RS, Viloria-Petit A, Okada F, Rak J. Establishing a link between oncogenes and tumor angiogenesis. Mol Med. 1998 May;4(5):286-95. Review.
5. Corn PG. The tumor microenvironment in prostate cancer: elucidating molecular pathways for therapy development.Cancer Manag. Res.2012 4:183–93.
6. Alphonso A, Alahari SK. Stromal cells and Integrins: conforming to the needs of the tumor microenvironment. Neoplasia, 2009;11(12):1264–71.
7. Olumi AF, Grossfeld GD, Hayward SW, Carroll PR, Tlsty TD, Cunha GR. Carcinoma-associated fibroblasts direct tumor progression of initiated human prostatic epithelium. Cancer Res.1999;59(19):5002–11.
8. Vella LJ. The emerging role of exosomes in epithelial-mesenchymal-transition in cancer. Front Oncol. 2014 Dec; 19;4:361. Review.
9. Parri M, Chiarugi P. Rac and Rho GTPases in cancer cell motility control. Cell Commun Signal. 2010; 8: 23.
10. Campellone KG, Welch MD. A nucleator arms race: cellular control of actin assembly. Nat Rev Mol Cell Biol. 2010;11:237–251.
11. Chesarone MA, Goode BL. Actin nucleation and elongation factors: mechanisms and interplay.Curr Opin Cell Biol. 2009;21:28–37.
12. Miki H, Yamaguchi H, Suetsugu S, Takenawa T. IRSp53 is an essential intermediate between Rac and WAVE in the regulation of membrane ruffling. Nature. 2000;408:732–735.
13. Knight B, Laukaitis C, Akhtar N, Hotchin NA, Edlund M, Horwitz AR. Visualizing muscle cell migration in situ. Curr Biol. 2000;10:576–585.
14. Mermall V, Post PL, Mooseker MS: Unconventional myosins in cell movement, membrane traffic, and signal transduction. Science 1998, 279:527-533.
15. van Leeuwen FN, van DS, Kain HE, van der Kammen RA, Collard JG: Rac regulates phosphorylation of the myosin-II heavy chain, actinomyosin disassembly and cell spreading. Nat Cell Biol 1999, 1:242-248.
16. Rottner K, Hall A, Small JV: Interplay between Rac and Rho in the control of substrate contact dynamics. Curr Biol. 1999, 9:640-648.
17. Price LS, Leng J, Schwartz MA, Bokoch GM: Activation of Rac and Cdc42 by integrins mediates cell spreading. Mol Biol Cell. 1998, 9:1863-1871.
18. Jin G, Sah RL, Li YS, Lotz M, Shyy JY, Chien S. Biomechanical regulation of matrix metalloproteinase-9 in cultured chondrocytes. J Orthop Res. 2000;18:899–908.
19. Kheradmand F, Werner E, Tremble P, Symons M, Werb Z. Role of Rac1 and oxygen radicals in collagenase-1 expression induced by cell shape change. Science. 1998;280:898–902.
20. Westermarck J, Kahari VM. Regulation of matrix metalloproteinase expression in tumor invasion.FASEB J. 1999;13:781–792.
21. Zhuge Y, Xu J. Rac1 mediates type I collagen-dependent MMP-2 activation. role in cell invasion across collagen barrier. J Biol Chem. 2001;276:16248–16256.

22. Fukata Y, Amano M, Kaibuchi K. Rho-Rho-kinase pathway in smooth muscle contraction and cytoskeletal reorganization of non-muscle cells. Trends Pharmacol Sci. 2001;22:32–39.
23. Totsukawa G, Yamakita Y, Yamashiro S, Hartshorne DJ, Sasaki Y, Matsumura F. Distinct roles of ROCK (Rho-kinase) and MLCK in spatial regulation of MLC phosphorylation for assembly of stress fibers and focal adhesions in 3T3 fibroblasts. J Cell Biol. 2000;150:797–806.
24. Potter DA, Tirnauer JS, Janssen R, Croall DE, Hughes CN, Fiacco KA, Mier JW, Maki M, Herman IM: Calpain regulates actin remodeling during cell spreading. J Cell Biol 1998, 141:647-662. 53.
25. Cox EA, Huttenlocher A: Regulation of integrin-mediated adhesion during cell migration. Microsc Res Tech 1998, 43:412-419.
26. Nabeshima K, Inoue T, Shimao Y, Okada Y, Itoh Y, Seiki M, Koono M: Front-cell-specific expression of membrane-type 1 matrix metalloproteinase and gelatinase A during cohort migration of colon carcinoma cells induced by hepatocyte growth factor/scatter factor. Cancer Res 2000, 60:3364-3369.
27. Bach TL, Barsigian C, Chalupowicz DG, Busler D, Yaen CH, Grant DS, Martinez J: VE-cadherin mediates endothelial cell capillary tube formation in fibrin and collagen gels. Exp Cell Res 1998, 238:324-334.;
28. Carmeliet P, Lampugnani MG, Moons L, Breviario F, Compernolle V, Bono F, Balconi G, Spagnuolo R, Oostuyse B, Dewerchin M, Zanetti A, Angellilo A, Mattot V, Nuyens D, Lutgens E, Clotman F, de Ruiter MC, Gittenberger-de Groot A,Poelmann R, Lupu F, Herbert JM, Collen D, Dejana E. Targeted deficiency or cytosolic truncation of the VE-cadherin gene in mice impairs VEGF-mediated endothelial survival and angiogenesis. Cell 1999, 98:147-157.
29. van Kempen LC, van den Oord JJ, van Muijen GN, Weidle UH, Bloemers HP, Swart GW: Activated leukocyte cell adhesion molecule/CD166, a marker of tumor progression in primary malignant melanoma of the skin. Am J Pathol 2000, 156:769-774.
30. Graeber SH, Hulser DF: Connexin transfection induces invasive properties in HeLa cells. Exp Cell Res 1998, 243:142-149.
31. Hsu M, Andl T, Li G, Meinkoth JL, Herlyn M: Cadherin repertoire determines partner-specific gap junctional communication during melanoma progression. J Cell Sci 2000, 113:1535-1542.
32. Friedl P, Noble PB, Walton PA, Laird DE, Chauvin PJ, Tabah RJ, Black M, Za¨ nker KS: Migration of coordinated cell clusters in mesenchymal and epithelial cancer explants in vitro. Cancer Res 1995, 55:4557-4560.
33. Bach TL, Barsigian C, Chalupowicz DG, Busler D, Yaen CH, Grant DS, Martinez J: VE-cadherin mediates endothelial cell capillary tube formation in fibrin and collagen gels. Exp Cell Res 1998, 238:324-334.
34. Hegerfeldt Y, Tusch M, Brocker EB, Friedl P: Collective cell movement in primary melanoma explants: plasticity of cell–cell interaction, b1-integrin function, and migration strategies. Cancer Res 2002, 62:2125-2130.
35. Sweeney SM, DiLullo G, Slater SJ, Martinez J, Iozzo RV, Lauer-Fields JL, Fields GB, San Antonio JD: Angiogenesis in collagen I requires a2b1 ligation of a GFP]GER sequence and possibly p38 MAPK activation and focal adhesion disassembly. J Biol Chem. 2003, 278:30516-30524.
36. Davis GE, Camarillo CW: Regulation of endothelial cell morphogenesis by integrins, mechanical forces, and matrix guidance pathways. Exp Cell Res. 1995, 216:113-123.

37. O'Brien LE, Jou TS, Pollack AL, Zhang Q, Hansen SH, Yurchenco P, Mostov KE: Rac1 orientates epithelial apical polarity through effects on basolateral laminin assembly. Nat Cell Biol. 2001, 3:831-838.
38. Gerhardt H, Wolburg H, Redies C: N-cadherin mediates pericytic-endothelial interaction during brain angiogenesis in the chicken. Dev Dyn. 2000, 218:472-479.
39. Friedl P. Prespecification and plasticity: shifting mechanisms of cell migration. Curr Opin. 2004; 16: 14-23.
40. Grinnell F: Fibroblasts, myofibroblasts, and wound contraction. J Cell Biol 1994, 124:401-404.
41. Tamariz E, Grinnell F: Modulation of fibroblast morphology and adhesion during collagen matrix remodeling. Mol Biol Cell 2002, 13:3915-3929.
42. Ballestrem C, Hinz B, Imhof BA, Wehrle-Haller B: Marching at the front and dragging behind: differential aVb3-integrin turnover regulates focal adhesion behavior. J Cell Biol 2001, 155:1319-1332.
43. Maaser K, Wolf K, Klein CE, Niggemann B, Zanker KS, Brocker EB, Friedl P: Functional hierarchy of simultaneously expressed adhesion receptors: integrin a2b1 but not CD44 mediates MV3 melanoma cell migration and matrix reorganization within three-dimensional hyaluronan-containing collagen matrices. Mol Biol Cell 1999, 10:3067-3079.
44. Wolf K, Mazo I, Leung H, Engelke K, von Andrian UH, Deryugina EI, Strongin AY, Bröcker EB, Friedl P. Compensation mechanism in tumor cell migration: mesenchymal-amoeboid transition after blocking of pericellular proteolysis. J Cell Biol. 2003; 160: 267-277.
45. Deryugina EI, Ratnikov B, Monosov E, Postnova TI, DiScipio R, Smith JW, Strongin AY: MT1-MMP initiates activation of pro-MMP-2 and integrin aVb3 promotes maturation of MMP-2 in breast carcinoma cells. Exp Cell Res 2001, 263:209-223.
46. Friedl P, Zanker KS, Bro¨ cker E-B: Cell migration strategies in 3D extracellular matrix: differences in morphology, cell matrix interactions, and integrin function. Microsc Res Tech 1998,43:369-378.
47. Ballestrem C, Hinz B, Imhof BA, Wehrle-Haller B: Marching at the front and dragging behind: differential aVb3-integrin turnover regulates focal adhesion behavior. J Cell Biol 2001, 155:1319-1332.
48. Zamir E, Katz M, Posen Y, Erez N, Yamada KM, Katz BZ, Lin S, Lin DC, Bershadsky A, Kam Z : Dynamics and segregation of cell-matrix adhesions in cultured fibroblasts. Nat Cell Biol 2000,2:191-196.
49. Petroll WM, Ma L: Direct, dynamic assessment of cell-matrix interactions inside fibrillar collagen lattices. Cell Motil Cytoskeleton 2003, 55:254-264. 26. Keely PJ, Westwick JK, Whitehead IP, Der CJ, Parise LV: Cdc42 and Rac1 induce integrin-mediated cell motility and invasiveness through PI(3)K. Nature 1997, 390:632-636.
50. Keely PJ, Westwick JK, Whitehead IP, Der CJ, Parise LV: Cdc42 and Rac1 induce integrin-mediated cell motility and invasiveness through PI(3)K. Nature 1997, 390:632-636.
51. Clark EA, King WG, Brugge JS, Symons M, Hynes RO: Integrinmediated signals regulated by members of the rho family of GTPases. J Cell Biol 1998, 142:573-586.
52. Nobes CD, Hall A: Rho GTPases control polarity, protrusion, and adhesion during cell movement. J Cell Biol 1999, 144:1235-1244.
53. Friedl P, Borgmann S, Brocker EB: Leukocyte crawling through extracellular matrix and the dictyostelium paradigm of movement—lessons from a social amoeba. J Leukoc Biol 2001, 70:491-509.

54. Francis K, Palsson B, Donahue J, Fong S, Carrier E: Murine Sca-1R/LinS cells and human KG1a cells exhibit multiple pseudopod morphologies during migration. Exp Hematol 2002, 30:460-463.
55. Wang W, Wyckoff JB, Frohlich VC, Oleynikov Y, Huttelmaier S, Zavadil J, Cermak L, Bottinger EP, Singer RH, White JG, Cermak L, Bottinger EP, Singer RH, White JG, Segall JE, Condeelis JS. Single cell behavior in metastatic primary mammary tumors correlated with gene expression patterns revealed by molecular profiling. Cancer Res 2002, 62:6278-6288.
56. Friedl P, Entschladen F, Conrad C, Niggemann B, Zanker KS: CD4R T lymphocytesmigrating in three-dimensional collagen lattices lack focal adhesions and utilize b1-integrin-independent strategies for polarization, interaction with collagen fibers and locomotion. Eur J Immunol 1998, 28:2331-2343.
57. Wolf K, Muller R, Borgmann S, Brocker EB, Friedl P: Amoeboid shape change and contact guidance: T cell migration mechanisms in fibrillar collagen independent of matrix remodeling by MMPs and other proteases. Blood 2003, 102:3262-3269.
58. Mandeville JT, Lawson MA, Maxfield FR: Dynamic imaging of neutrophil migration in three dimensions: mechanical interactions between cells and matrix. J Leukoc Biol 1997,61:188-200.
59. Friedl P, Wolf K: Proteolytic and non-proteolytic migration in tumor cells and leukocytes. Biochem Soc Symp 2003, 70:277-285.
60. Worthylake RA, Lemoine S, Watson JM, Burridge K: RhoA is required for monocyte tail retraction during transendothelial migration. J Cell Biol 2001, 154:147-160.
61. Smith A, Bracke M, Leitinger B, Porter JC, Hogg N: LFA-1-induced T cell migration on ICAM-1 involves regulation of MLCKmediated attachment and ROCK-dependent detachment.J Cell Sci 2003, 116:3123-3133.
62. Cartier-Michaud A, Malo M, Charriere-Bertrand C, Gadea G, Anguille C, Supiramaniam A Lesne A, Delaplace F, Hutzler G, Roux P, Lawrence DA, Barlovatz-Meimon G. Matrix-bound PAI-1 supports cell blebbing via RhoA/ ROCK1 signaling. PLoS One. 2012; 7: e32204.
63. Sahai E, Marshall CJ: Differing modes of tumour cell invasion have distinct requirements for Rho/ROCK signalling and extracellular proteolysis. Nat Cell Biol 2003, 5:711-719.
64. Nobes CD, Hall A: Rho GTPases control polarity, protrusion, and adhesion during cell movement. J Cell Biol 1999, 144:1235-1244.
65. Fukata Y, Amano M, Kaibuchi K: Rho–Rho-kinase pathway in smooth muscle contraction and cytoskeletal reorganization of non-muscle cells. Trends Pharmacol Sci 2001, 22:32-39.
66. Maddox AS, Burridge K: RhoA is required for cortical retraction and rigidity during mitotic cell rounding. J Cell Biol 2003, 160:255-265.
67. Tran Quang C, Gautreau A, Arpin M, Treisman R: Ezrin function is required for ROCK-mediated fibroblast transformation by the Net and Dbl oncogenes. EMBO J 2000, 19:4565-4576.
68. Worthylake RA, Burridge K: RhoA and ROCK promote migration by limiting membrane protrusions. J Biol Chem 2003, 278:13578-13584.
69. Etienne-Manneville S, Hall A: Rho GTPases in cell biology. Nature 2002, 420:629-635.
70. Ridley AJ: Rho GTPases and actin dynamics in membrane protrusions and vesicle trafficking. Trends Cell Biol 2006, 16:522-529.

71. Valencia A, Chardin P, Wittinghofer A, Sander C: The ras protein family: evolutionary tree and role of conserved amino acids. Biochemistry 1991, 30:4637-4648.
72. Bosco EE, Mulloy JC, Zheng Y: Rac1 GTPase: a “Rac” of all trades. Cell Mol Life Sci 2009, 66:370-374.
73. Cote JF, Vuori K: GEF what? Dock180 and related proteins help Rac to polarize cells in new ways. Trends Cell Biol 2007, 17:383-393.
74. Schmidt A, Hall A: Guanine nucleotide exchange factors for Rho GTPases: turning on the switch. Genes Dev 2002, 16:1587-1609.
75. Pechlivanis M, Kuhlmann J: Hydrophobic modifications of Ras proteins by isoprenoid groups and fatty acids–More than just membrane anchoring. Biochim Biophys Acta 2006, 1764:1914-1931.
76. Ellerbroek SM, Wennerberg K, Burridge K: Serine phosphorylation negatively regulates RhoA in vivo. J Biol Chem 2003, 278:19023-19031.
77. Chardin P: Function and regulation of Rnd proteins. Nat Rev Mol Cell Biol 2006, 7:54-62.
78. Li X, Bu X, Lu B, Avraham H, Flavell RA, Lim B: The hematopoiesis-specific GTP-binding protein RhoH is GTPase deficient and modulates activities of other Rho GTPases by an inhibitory function. Mol Cell Biol 2002, 22:1158-1171.
79. Schmidt-Mende J, Geering B, Yousefi S, Simon HU: Lysosomal degradation of RhoH protein upon antigen receptor activation in T but not B cells. Eur J Immunol 2010, 40:525-529.
80. DerMardirossian C, Bokoch GM: GDIs: central regulatory molecules in Rho GTPase activation. Trends Cell Biol 2005, 15:356-363.
81. Moon SY, Zheng Y: Rho GTPase-activating proteins in cell regulation. Trends Cell Biol 2003, 13:13-22.
82. Fiegen D, Haeusler LC, Blumenstein L, Herbrand U, Dvorsky R, Vetter IR, Ahmadian MR: Alternative splicing of Rac1 generates Rac1b, a selfactivating GTPase. J Biol Chem 2004, 279:4743-4749.
83. Matos P, Collard JG, Jordan P: Tumor-related alternatively spliced Rac1b is not regulated by Rho-GDP dissociation inhibitors and exhibits selective downstream signaling. J Biol Chem 2003, 278:50442-50448.
84. Kwon T, Kwon DY, Chun J, Kim JH, Kang SS: Akt protein kinase inhibits Rac1-GTP binding through phosphorylation at serine 71 of Rac1. J Biol Chem 2000, 275:423-428.
85. Didsbury J, Weber RF, Bokoch GM, Evans T, Snyderman R: rac, a novel rasrelated family of proteins that are botulinum toxin substrates. J Biol Chem 1989, 264:16378-16382.
86. Ambruso DR, Knall C, Abell AN, Panepinto J, Kurkchubasche A, Thurman G, Gonzalez-Aller C, Hiester A, deBoer M, Harbeck RJ, Oyer R, Johnson GL, Roos D: Human neutrophil immunodeficiency syndrome is associated with an inhibitory Rac2 mutation. Proc Natl Acad Sci USA 2000,97:4654-4659.
87. Werner E: GTPases and reactive oxygen species: switches for killing and signaling. J Cell Sci 2004, 117:143-153.
88. Haataja L, Groffen J, Heisterkamp N: Characterization of RAC3, a novel member of the Rho family. J Biol Chem 1997, 272:20384-20388.
89. Mira JP, Benard V, Groffen J, Sanders LC, Knaus UG: Endogenous, hyperactive Rac3 controls proliferation of breast cancer cells by a p21- activated kinase-dependent pathway. Proc Natl Acad Sci USA 2000,97:185-189.
90. Wheeler AP, Ridley AJ: Why three Rho proteins? RhoA, RhoB, RhoC, and cell motility. Exp Cell Res 2004, 301:43-49.

91. Del Rosso M, Margheri F, Serrati S, Chilla A, Laurenzana A, Fibbi G. The urokinase receptor system, a key regulator at the intersection between inflammation, immunity, and coagulation. Curr Pharm Des. 2011; 17: 1924-1943.
92. Kjoller L. The urokinase plasminogen activator receptor in the regulation of the actin cytoskeleton and cell motility. Biol Chem. 2002; 383: 5-19.
93. Margheri F, Manetti M, Serrati S, Nosi D, Pucci M, Matucci-Cerinic M Kahaleh B, Bazzichi L, Fibbi G, Ibba- Manneschi L, Del Rosso M. Domain 1 of the urokinase-type plasminogen activator receptor is required for its morphologic and functional, beta2 integrin-mediated connection with actin cytoskeleton in human microvascular endothelial cells: failure of association in systemic sclerosis endothelial cells. Arthritis Rheum. 2006; 54: 3926-3938.
94. Shetty S, Idell S. Urokinase induces expression of its own receptor in Beas2B lung epithelial cells. J Biol Chem. 2001 Jul 6;276(27):24549-56.
95. Heymans S, Luttun A, Nuyens D, Theilmeier G, Creemers E, Moons L, Dyspersin GD, Cleutjens JP, Shipley M, Angellilo A, Levi M, Nübe O, Baker A, Keshet E, Lupu F, Herbert JM, Smits JF, Shapiro SD, Baes M, Borgers M, Collen D, Daemen MJ, Carmeliet P. Inhibition of plasminogen activators or matrix metalloproteinases prevents cardiac rupture but impairs therapeutic angiogenesis and causes cardiac failure. Nat Med. 1999 Oct;5(10):1135-42.
96. Ploug M, Ronne E, Behrendt N, Jensen AL, Blasi F, Dano K. Cellular receptor for urokinase plasminogen activator. Carboxyl-terminal processing and membrane anchoring by glycosyl-phosphatidylinositol. J Biol Chem.1991; 266: 1926-1933.
97. Xue W, Mizukami I, Todd RF, 3rd, Petty HR. Urokinase-type plasminogen activator receptors associate with beta1 and beta3 integrins of fibrosarcoma cells: dependence on extracellular matrix components. Cancer Res. 1997; 57: 1682-1689.
98. Liu D, Aguirre Ghiso J, Estrada Y, Ossowski L. EGFR is a transducer of the urokinase receptor initiated signal that is required for in vivo growth of a human carcinoma. Cancer Cell. 2002 Jun;1(5):445-57.
99. Bohuslav J, Horejsí V, Hansmann C, Stöckl J, Weidle UH, Majdic O, Bartke I, Knapp W, Stockinger H. Urokinase plasminogen activator receptor, beta2-integrins, and Src-kinases within single a receptor complex of human monocytes. J Exp Med. 1995 Apr;181(4):1381-90.
100. Dass K, Ahmad A, Azmi AS, Sarkar SH and Sarkar FH. Evolving role of uPA/uPAR system in human cancers. Cancer Treat Rev 2008; 34: 122-136.
101. Ge Y and Elghetany MT. Urokinase plasminogen activator receptor (CD87): something old, something new. Lab Hematol 2003; 9: 67-71.
102. de Bock CE and Wang Y. Clinical significance of urokinase-type plasminogen activator receptor (uPAR) expression in cancer. Med Res Rev 2004; 24: 13-39
103. J.L. Fisher, P.S. Mackie, M.L. Howard, H. Zhou, P.F. Choong The expression of the urokinase plasminogen activator system in metastatic murine osteosarcoma: an in vivo mouse model; Clin Cancer Res, 7 (6) (2001), pp. 1654–1660
104. Migita T, Sato E, Saito K, Mizoi T, Shiiba K, Matsuno S, Nagura H, Ohtani H. Differing expression of MMPs-1 and -9 and urokinase receptor between diffuse- and intestinal-type gastric carcinoma. Int J Cancer 1999; 84: 74–9.;19
105. Kawasaki K, Hayashi Y, Wang Y, Suzuki S, Morita Y, Nakamura T, Narita K, Doe W, Itoh H, Kuroda Y. Expression of urokinase-type plasminogen activator receptor and plasminogen activator inhibitor-1 in gastric cancer. J Gastroenterol Hepatol 1998; 13: 936–44.
106. Heiss MM, Babic R, Allgayer H, Gruetzner KU, Jauch KW, Loehrs U, Schildberg FW. Tumor-associated proteolysis and prognosis: new functional risk factors in

gastric cancer defined by the urokinase-type plasminogen activator system. J Clin Oncol 1995; 13:2084–93.
107. Heiss MM, Allgayer H, Gruetzner KU, Babic R, Jauch KW, Schildberg FW. Clinical value of extended biologic staging by bone marrow micrometastases and tumor-associated proteases in gastric cancer. Ann Surg 1997; 226: 736–44.
108. Allgayer H, Babic R, Grutzner KU, Beyer BC, Tarabichi A, Schildberg FW, Heiss MM. Tumor-associated proteases and inhibitors in gastric cancer: analysis of prognostic impact and individual risk protease patterns. Clin Exp Metastasis 1998; 16: 62–73.
109. Kaneko T, Konno H, Baba M, Tanaka T, Nakamura S. Urokinase-type plasminogen activator expression correlates with tumor angiogenesis and poor outcome in gastric cancer. Cancer Sci 2003; 94: 43–9.
110. Allgayer H, Heiss MM, Riesenberg R, Grutzner KU, Tarabichi A, Babic R, Schildberg FW. Urokinase plasminogen activator receptor (uPA-R): one potential characteristic of metastatic phenotypes in minimal residual tumor disease. Cancer Res 1997; 57:1394–9.
111. Heiss MM, Simon EH, Beyer BC, Gruetzner KU, Tarabichi A, Babic R, Schildberg FW, Allgayer H. Minimal residual disease in gastric cancer: evidence of an independent prognostic relevance of urokinase receptor expression by disseminated tumor cells in the bone marrow. J Clin Oncol 2002; 20: 2005–16.
112. Verdegem D, Moens S, Stapor P, Carmeliet P. Endothelial cell metabolism: parallels and divergences with cancer cell metabolism. Cancer Metab. 2014 Sep15;2:19. doi: 10.1186/2049-3002-2-19. eCollection 2014. Review.
113. Potente M, Gerhardt H, Carmeliet P: Basic and therapeutic aspects of angiogenesis. Cell 2011, 146:873–887.
114. Phng LK, Gerhardt H. Angiogenesis: a team effort coordinated by notch. Dev Cell 2009, 16:196–208.
115. Jakobsson L, Franco CA, Bentley K, Collins RT, Ponsioen B, Aspalter IM, Rosewell I, Busse M, Thurston G, Medvinsky A, Schulte-Merker S, Gerhardt H. Endothelial cells dynamically compete for the tip cell position during angiogenic sprouting. Nat Cell Biol 2010, 12:943–953.
116. Margheri F, Schiavone N, Papucci L, Magnelli L, Serrati S, Chilla A Laurenzana A, Bianchini F, Calorini L, Torre E, Dotor J, Feijoo E, Fibbi G, Del Rosso M. GDF5 regulates TGFβ-dependent angiogenesis in breast carcinoma MCF-7 cells: in vitro and in vivo control by anti-TGFβ peptides. PLoS One. 2012 7: e50342.
117. Armulik A, Genove G, Betsholtz C. Pericytes: developmental, physiological, and pathological perspectives, problems, and promises. Dev Cell 2011, 21:193–215.
118. Welti J, Loges S, Dimmeler S, Carmeliet P. Recent molecular discoveries in angiogenesis and antiangiogenic therapies in cancer. J Clin Invest 2013, 123:3190–3200.
119. Asahara T, Murohara T, Sullivan A, Silver M, van der Zee R, Li T, Witzenbichler B, Schatteman G, Isner JM. Isolation of putative progenitor endothelial cells for angiogenesis. Science. 1997 Feb 14;275(5302):964-7.
120. Ingram DA, Mead LE, Tanaka H, Meade V, Fenoglio A, Mortell K, Pollok K, Ferkowicz MJ, Gilley D, Yoder MC. Identification of a novel hierarchy of endothelial progenitor cells using human peripheral and umbilical cord blood. Blood. 2004;104:2752-2760.
121. Timmermans F, Plum J, Yoder MC, Ingram DA, Vandekerckhove B, Case J. Endothelial progenitor cells: identity defined? J Cell Mol Med. 2009;13:87-102.

122. Yoder MC, Mead LE, Prater D, Krier TR, Mroueh KN, Li F, Krasich R, Temm CJ, Prchal JT, Ingram DA. Redefining endothelial progenitor cells via clonal analysis and hematopoietic stem/progenitor cell principals. Blood. 2007;109:1801-1809.
123. Orimo A, Gupta PB, Sgroi DC, Arenzana-Seisdedos F, Delaunay T, Naeem R, Carey VJ, Richardson AL, Weinberg RA. Stromal fibroblasts present in invasive human breast carcinomas promote tumor growth and angiogenesis through elevated SDF-1/CXCL12 secretion. Cell 2005;121:335-348.
124. Peichev M, Naiyer AJ, Pereira D, Zhu Z, Lane WJ, Williams M, Oz MC, Hicklin DJ, Witte L, Moore MA, Rafii S. Expression of VEGFR-2 and AC133 by circulating human CD34+ cells identifies a population of functional endothelial precursors. Blood. 2000;95:952–958.
125. Gehling UM, Ergün S, Schumacher U, Wagener C, Pantel K, Otte M, Schuch G, Schafhausen P, Mende T, Kilic N, Kluge K, Schafer B, Hossfeld DK, Fiedler W. In vitro differentiation of endothelial cells from AC133-positive progenitor cells. Blood. 2000;95:3106–3112.
126. Yin AH, Miraglia S, Zanjani ED, Almeida-Porada G, Ogawa M, Leary AG, Olweus J, Kearney J, Buck DW. AC133, a novel marker for human hematopoietic stem and progenitor cells. Blood. 1997;90:5002–5012.
127. Harraz M, Jiao C, Hanlon HD, Hartley RS, Schatteman GC. CD34-blood-derived human endothelial cell progenitors. Stem Cells. 2001;19: 304–312.
128. Zhao Y, Glesne D, Huberman E. A human peripheral blood monocytederived subset acts as pluripotent stem cells. Proc Natl Acad Sci U S A. 2003;100:2426–2431.
129. Hirschi KK, Ingram DA, Yoder MC. Assessing identity, phenotype, and fate of endothelial progenitor cells. Arteriosclerosis, thrombosis, and vascular biology 2008; 28: 1584.
130. Rohde E, Malischnik C, Thaler D, Maierhofer T, Linkesch W, Lanzer G, Guelly C, Strunk D. Blood monocytes mimic endothelial progenitor cells. Stem cells (Dayton, Ohio) 2006; 24:357.
131. Yoon CH, Hur J, Park KW, Kim JH, Lee CS, Oh IY, Kim TY, Cho HJ, Kang HJ, Chae IH, Yang HK, Oh BH, Park YB, Kim HS. Synergistic neovascularisation by mixed transplantation of early endothelial progenitor cells and late outgrowth endothelial cells: the role of angiogenic cytokines and matrix metalloproteinases. Circulation 2005; 112: 1618.
132. Robert E. Verloop, Pieter Koolwijk, Anton Jan van Zonneveld, Victor W.M. van Hinsbergh. Proteases and receptors in the recruitment of endothelial progenitor cells in neovascularisation. Eur. Cytokine Netw.2009; 20: 207-19.
133. Nakahata, T, Ogawa, M. Hemopoietic colony-forming cells in umbilical cord blood with extensive capability to generate mono- and multipotential hemopoietic progenitors. J Clin Invest 1982. 70:1324-1328.
134. Mayani, H, Lansdorp, PM. Thy-1 expression is linked to functional properties of primitive hematopoietic progenitor cells from human umbilical cord blood. Blood 1994. 83:2410-2417.
135. Vaziri H, Dragowska W, Allsopp RC, Thomas TE, Harley CB, Lansdorp PM. Evidence for a mitotic clock in human hematopoietic stem cells: loss of telomeric DNA with age. Proc Natl Acad Sci USA 1994. 91:9857-9860.
136. De La Selle V, Gluckman E, Bruley-Rosset M. Newborn blood can engraft adult mice without inducing graft-versus-host disease across non H-2 antigens. Blood 1996. 87:3977-3983.
137. Kumar, Vinay; Abbas, Abul K; Fausto, Nelson; Robbins, Stanley L; Cotran, Ramzi S (2005). Robbins and Cotran pathologic basis of disease (7th ed.). Philadelphia: Elsevier Saunders.

138. Margheri F, Luciani C, Taddei ML, Giannoni E, Laurenzana A, Biagioni A, Chillà A, Chiarugi P, Fibbi G, Del Rosso M. The receptor for urokinase-plasminogen activator (uPAR) controls plasticity of cancer cell movement in mesenchymal and amoeboid migration style. Oncotarget. 2014 Mar 30;5(6):1538-53.
139. Roca-Cusachs P, Iskratsch T, Sheetz MP. Finding the weakest link: exploring integrin-mediated mechanical molecular pathways. J Cell Sci, 2012; 125: 3025-3038.
140. Margheri F, Chilla A, Laurenzana A, Serrati S, Mazzanti B, Saccardi R Santosuosso M, Danza G, Sturli N, Rosati F, Magnelli L, Papucci L, Calorini L, Bianchini F,Del Rosso M, Fibbi G. Endothelial progenitor cell-dependent angiogenesis requires localization of the full-length form of uPAR in caveolae. Blood 2011; 118: 3743-3755.
141. Gleghorn JP, Pratt ED, Denning D, Liu H, Bander NH, Tagawa ST, Nanus DM, Giannakakou PA, Kirby BJ. Capture of circulating tumor cells from whole blood of prostate cancer patients using geometrically enhanced differential immunocapture (GEDI) and a prostate-specific antibody. Lab Chip. 2010; 10: 27-29.
142. Parri M, Taddei ML, Bianchini F, Calorini L, Chiarugi P. EphA2 reexpression prompts invasion of melanoma cells shifting from mesenchymal to amoeboid-like motility style. Cancer Res. 2009; 69: 2072-2081.
143. Simon DI, Wei Y, Zhang L, Rao NK, Xu H, Chen Z, Liu Q, Rosenberg S, Chapman HA. Identification of a urokinase receptor-integrin interaction site. Promiscuous regulator of integrin function. J Biol Chem. 2000; 275: 10228-10234.
144. Stefanidakis M, Koivunen E. Cell-surface association between matrix metalloproteinases and integrins: role of the complexes in leukocyte migration and cancer progression. Blood. 2006; 108: 1441-1450.
145. Yue J, Zhang K, Chen J. Role of integrins in regulating proteases to mediate extracellular matrix remodeling. Cancer Microenviron. 2012; 5: 275-283.
146. Montuori N, Carriero MV, Salzano S, Rossi G, Ragno P. The cleavage of the urokinase receptor regulates its multiple functions. J Biol Chem. 2002; 277: 46932-46939.